01 Feb 1997

Strength of flexural members using structural grade 80 of A653 steel (web crippling tests)

Shaojie Wu

Wei-wen Yu
Missouri University of Science and Technology, wwy4@mst.edu

Roger A. LaBoube
Missouri University of Science and Technology, laboube@mst.edu

Civil Engineering Study 97-3
Cold-Formed Steel Series

Third Progress Report

STRENGTH OF FLEXURAL MEMBERS USING STRUCTURAL GRADE 80 OF A653 STEEL (WEB CRIPPLING TESTS)

by

Shaojie Wu
Research Associate

Wei-Wen Yu
Roger A. LaBoube
Project Directors

A Research Project Sponsored by
the American Iron and Steel Institute

February, 1997

Department of Civil Engineering
University of Missouri-Rolla
Rolla, Missouri

ABSTRACT

This Third Progress Report summarizes the web crippling tests of 148 specimens and evaluates the test results along with an additional 114 web crippling tests which were reported in 1986 as part of a project on Design of Automotive Structural Components Using High-Strength Sheet Steels. The 148 web crippling tests conducted in this program are the part of the overall project on Strength of Flexural Members Using the Structural Grade 80 of ASTM A653 Steel (former ASTM A446 Grade E Steel). The objectives of the ongoing project are to study the strength and structural performance of flexural members as affected by using the high-strength, low-ductility Structural Grade 80 Steel and to develop appropriate design criteria based on the test programs.

Four loading conditions, namely End-One-Flange (EOF), Interior-One-Flange (IOF), End-Two-Flange (ETF), and Interior-Two-Flange (ITF) conditions, were considered in the web crippling tests in this program and in those reported in 1986. The web crippling test program for this study included 136 single-rib and double-rib specimens having a hat-shaped section and sloped webs and 12 single-rib specimens having a hat-shaped section and vertical webs. The previous 114 specimens reported in 1986 had a single-rib hat-shaped section with vertical webs. For the specimens tested in this program, the yield strength of the steel ranged from 103.9 to 112.5 ksi, h/t ratio from 25.99 to 208.19, R/t ratio from 2.16 to 5.51, N/t ratio from 34.48 to 88.24, N/h ratio from 0.22 to 2.02, thickness of steel sheet ranged from 0.017 to 0.029 inches, and the angle between the plane of the web and the plane of bearing surface ranged from 59.5 to 90 degrees. All specimens were loaded to failure.

Both the web crippling tests in this program and those reported in 1986 indicated that the tested ultimate loads for the four loading conditions were higher than the predicted loads using the AISI Specification, and modified kC_1 and kC_3 factors (1.691 for kC_1 when F_y exceeds 91.5 ksi and 1.34 for kC_3 when F_y exceeds 66.5 ksi), for the yield strength of the steels exceeding 80 ksi. The ratio of the tested ultimate load to the calculated load

tends to increase with increase in the yield strength of the steels beyond 80 ksi. Therefore, it is conservative to use the kC_1 and kC_3 factors in Section 3.4 of the current AISI Specification for predicting web crippling strength of structural members with yield strength exceeding 80 ksi. It appears that the low ductility of the Structural Grade 80 steel does not reduce the web crippling strength of the members made of such steels.

As a result, new modified kC_1 and kC_3 factors were developed based on the 262 web crippling tests which included the following parameters: the yield strength F_y ranged from 58.2 ksi to 165.1 ksi, h/t ratio from 25.99 to 208.19, R/t ratio from 1.496 to 5.696, N/t ratio from 22.70 to 88.24, N/h ratio from 0.17 to 2.02, thickness of steel sheets ranged from 0.017 in. to 0.088 in., and the angle between the plane of the web and the plane of bearing surface ranged from 59.5 to 90 degrees. Reasonable agreement was found between the tested ultimate loads and the predicted loads using the newly modified kC_1 and kC_3 factors. It is also recommended that in order to simplify designs, the current kC_1 in Section 3.4 of the AISI Specification can be used for all the IOF, ITF, EOF, and ETF loading conditions, resulting in a simple but conservative solution.

TABLE OF CONTENT

LIST OF TABLES

LIST OF FIGURES

1. INTRODUCTION

1.1 BACKGROUND

Cold-formed steel decks have been widely used in buildings as load-carrying structural elements, such as floor and roof decks (Yu 1991, SDI 1992, USD 1994). One of the main structural functions for the steel decks is to carry live and dead loads and transfer the loads to beams or girders. As a result, the decks work as flexural members. The steel decks usually consist of several hat-shaped ribs formed together in their cross section. When such decks, either in single-span or multi-span, are subject to uniform or concentrated loads, the overall stability of the decks, such as lateral torsional buckling, often does not control the moment capacity of the members.

In the United States, it is a common practice that steel decks are made of the Structural Grade 80 of ASTM A653 steel (formerly ASTM A446 Grade E steel). The unique property of the Structural Grade 80 steel, as compared to the conventional steels used for cold-formed members, is that it has a high specified yield strength (F_y=80 ksi (551.6 MPa) and a low tensile-to-yield strength ratio (F_u/F_y=1.03). The ductility of the steel is unspecified (ASTM A446) and was reported to be smaller than the ductility requirements for the conventional steels (Dhalla and Winter 1971).

Due to the lack of ductility and low tensile-to-yield strength ratio of the Structural Grade 80 steel and considering the required ductility for adequate structural performance, Section A3.3.2 of the specifications for the design of cold-formed steel structural members (AISI 1986, AISI 1991) permits the use of the steel for particular configurations provided that (1) the yield strength, F_y, used for the design of members, is taken as 75% of the specified minimum yield point or 60 ksi (413.7 MPa), whichever is less, and (2) the tensile strength, F_u, used for the design of connections and joints, is taken as 75% of the specified minimum tensile strength or 62 ksi (427.5 MPa), whichever is less.

In the past, studies on the strength and performance of structural components made of the Structural Grade 80 steel were limited (Wu, Yu, and LaBoube 1995). The reduction of the specified material properties by 25% for design purposes is based on the fact that the structural performance of cold-formed members and connections made of such a steel has not been fully investigated and understood. Therefore, an in-depth investigation on structural performance of flexural members made of the Structural Grade 80 steel as affected by high yield and tensile strengths, low ductility, and low F_u/F_y ratio of the steel is needed.

1.2 OBJECTIVE AND SCOPE

In September 1994, a research project entitled "Strength of Flexural Members Using Structural Grade 80 of A653 and Grade E of A611 Steels" was initiated at the University of Missouri-Rolla under the sponsorship of American Iron and Steel Institute. The objective of the overall research is to study the structural performance and strength of the cold-formed steel members and connections made of ASTM A653 Structural Grade 80 steel. In addition, appropriate design criteria will be developed for consideration in the AISI Specifications.

The overall research consists of three phases: preliminary study (first phase); experimental investigation (second phase); and development of design recommendations (third phase). The preliminary study has been completed, which included literature review, evaluation of earlier existing test data, and material tests. The results of the first phase of the study were reported in the First Progress Report (Wu, Yu, and LaBoube 1995). The experimental investigation includes several tasks: (1) Design and prepare test specimens for beam tests and connection tests; (2) Conduct beam tests for determining section strength (effective yield moment); (3) Conduct beam tests for determining web crippling strength; (4) Conduct a preliminary study of screw and welded connections; (5) Evaluate all available test results. The beam tests for flexural strength have been completed and the results of the beam tests were evaluated and presented in the Second Progress Report (Wu, Yu, and LaBoube 1996). This Third Progress Report reviews previous web crippling tests using high-strength

steels in Section 2; describes the specimens for web crippling tests and test setup in Section 3; presents the test results on the web crippling strength of the panels with EOF, IOF, ETF, and ITF loading conditions in Section 4; evaluates the results along with additional web crippling test data reported in 1986 in Section 5; and discusses the development of new design criteria in Section 6. A summary is included in Section 7. The connection tests are planned for further study and the results of the tests will be included in the Fourth Progress Report.

2. LITERATURE REVIEW

PREVIOUS WEB CRIPPLING TESTS USING HIGH-STRENGTH SHEET STEELS

In 1986, a research on web crippling strength of cold-formed steel beams using high-strength sheet steels was completed at the University of Missouri-Rolla as a part of an overall project on ``Design of Automotive Structural Components Using High-Strength Sheet Steels (Santaputra and Yu 1986)." The purpose of the research was to study the structural behavior and strength of cold-formed steel beams made of high-strength steels and subjected primarily to web crippling load and a combination of web crippling load and bending moment. It was intended to use the research findings for a possible development of new and/or modified design criteria and to extend the use of materials having yield strengths exceeding the limitations included in the AISI design specifications at the time.

In the 1986 UMR study, a total of 150 hat sections and 96 I-beams were tested for four basic loading conditions, namely EOF, IOF, ETF, and ITF conditions. An additional 18 tests were also performed for the transition ranges between the basic loading conditions. For all the specimens, the yield strength of the steels ranged from 58.2 to 165.1 ksi, h/t ratio from 31.90 to 108.70, R/t ratio from 1.496 to 5.696, N/t ratio from 22.70 to 43.50, N/h ratio from 0.395 to 0.738, and thickness of steel sheet from 0.046 to 0.088 inches. The tests were conducted in a load control mode and all specimens were loaded to failure.

Two fundamental failure modes were recognized during the tests. One was called overstressing or bearing failure, and another was called web buckling failure. In the overstressing mode, the webs underneath the bearing plate slowly crushed and the bearing plate penetrated down into the webs when a peak load was reached. Afterward, the load could be maintained at the peak load level while the bearing plate continued to penetrate down. The out-of-plane deformation of the webs underneath the bearing plate tended to be relatively small. This mode of failure usually occurred in the specimens made of a yield strength less than or

around 80 ksi. However, for the specimens made of a yield strength exceeding 100 ksi, the situation was different. The webs underneath the bearing plate became unstable when a peak load was reached. Then the webs suddenly crushed underneath the bearing plate, following a quick drop of applied load. A relatively large out-of-plane deformation of the webs was accompanied with the failure. The deformation was even apparent before the peak load was reached.

It was found that the kC_1 and kC_3 factors, stated in Section 3.4 of the AISI Specifications for predicting the web crippling strength of structural members, represent two parabolic curves with respect to yield strength of steel, F_y, as shown in Fig. 2.1. The values of the factors reach a peak at the F_y equal to 91.5 ksi for kC_1 and 66.5 ksi for kC_3 and then decrease with further increases in yield strength. Apparently, it may not be rational to use the descending branch of the curves for predicting web crippling strength with higher yield strength of steels since the factors were mainly developed based on the materials with yield strength less than 60 ksi (Herakul and Yu, 1978). Considering this situation, Santaputra and Yu made a modification for the kC_1 and kC_3 factors in order for them to be used for predicting web crippling strength of the specimens. They removed the descending branches of the curves and replaced them with horizontal lines at the peak of the curves. The peak value for kC_1 was taken as 1.691 at the yield strength of 91.5 ksi and this value was also used for the yield strength larger than 91.5 ksi. Similarly, the peak value for kC_3 was taken as 1.34 at the yield strength of 66.5 ksi and it was used for the yield strength larger than 66.5 ksi as well.

With the use of the modified kC_1 and kC_3 factors, the tested ultimate loads were compared with the calculated loads using the 1986 edition of the AISI Specification. For the specimens with hat-shaped section, it was found that the tested ultimate loads for the four basic loading conditions were usually larger than the calculated loads, especially for the yield strength larger than 80 ksi, and the ratio of the tested ultimate load to the calculated load tended to increase with the increases in the yield strength.

Based on the observation of the two fundamental failure modes and the differences between the tested and

predicted values, a set of new equations were developed to be used for predicting web crippling strength of automotive structural members made of high-strength steels. These equations have completely different formats from those presently included in Section 3.4 of the AISI Specifications. Additional web crippling test data from three other sources were also considered in the development of the equations. Using the available test data, a set of parameters were used for deriving the equations. These parameters ranged as follows: the yield strength from 27.5 to 165.1 ksi, h/t ratio from 22.4 to 259.8, R/t ratio from 0.94 to 9.77, N/t ratio from 6.77 to 79.05, N/h ratio from 0.080 to 2.406, and the thickness of steel sheets from 0.0253 to 1.148 inches. The comparisons between the tested failure loads and predicted loads indicated good agreements between the proposed equations and the available test data.

3. DESIGN OF SPECIMENS FOR WEB CRIPPLING TESTS

In the present investigation reported herein, the specimens for web crippling tests were designed by using the Structural Grade 80 of ASTM A653 steel. The h/t ratios of the specimens were selected based on the current deck panel products from the steel deck industry. Special consideration was taken to ensure specific failure mode corresponding to each of four basic loading conditions (EOF, IOF, ETF, and ITF). Section 3.1 describes different cross-sections of the specimens. Section 3.2 presents actual dimensions of the specimens.

3.1 CROSS-SECTIONS AND THICKNESSES OF TEST SPECIMENS

Nineteen sections were selected for studying the web crippling strength. Of the nineteen sections, sixteen sections had single rib or double ribs with sloped webs, while three sections had only single rib and vertical webs (90 degree angle with respect to bearing surface). The main section parameters include: web flat-depth-to-thickness ratio (h/t), inside bend radius (R), and the angle between plane of web and plane of bearing surface (θ).

Two types of steel sheets, namely 22 and 26 gage sheets, were used for the specimens with the sloped webs, while only 22 gage sheet was used for the specimens with the vertical webs. The selected h/t ratio ranged from 25.86 to 206.90 and the w/t ratios from 34.48 to 117.64 for the specimens with the sloped webs. For the specimens with the vertical webs, the h/t ratio ranged from 51.72 to 155.17 and the w/t ratio from 68.97 to 155.17. The h/t ratios were determined based on the current cold-formed steel deck products (USD 1994, SDI 1992) and considering the limit on maximum h/t ratio in the AISI Specification. The designed inside bend radius, R, was taken as 1/16 and 1/8 inches, resulting in a R/t ratio ranging from 2.16 to 7.35 for the specimens with the sloped webs, while the designed inside bend radius for the specimens with the vertical webs was 1/8 inches. The designed angle between the plane of the web and the plane of the bearing surface, θ, was taken as 60 degrees for the specimens with the sloped webs and 90 degrees for the specimens with the vertical webs.

For the sections with the sloped webs, the specimens with the h/t ratio of less than 100 consisted of two ribs, while the specimens with the h/t ratio of over 100 had a single rib. All specimens with the vertical webs had a single rib.

Table 3.1.1 illustrates the variation of the h/t and w/t ratios used for the nineteen sections, and Figure 3.1.1 shows the shape of the sections. In Table 3.1.1, each combination of h/t, w/t, and R/t ratios corresponds to one section.

The material properties of the Structural Grade 80 steel were determined based on a total of seventy-six tensile coupon tests (Wu, Yu, and LaBoube 1995). The tensile coupons were made of 22, 24, 26, and 28 gage steel sheets and cut from the sheets with the orientation both parallel and perpendicular to the rolling direction of the sheets. The results of the tensile coupon tests are presented in Table 3.1.2. It is noted in the table that with decreases in thickness of the steel sheets, the yield and tensile strengths tend to increase, but the ductility tends to decrease. In the direction perpendicular to the rolling direction, the 0.2% offset yield strength and the tensile strength of the sheets are much higher than those in the rolling direction, while the ductility is much lower than that in the rolling direction.

3.2 MEASURED DIMENSIONS OF TEST SPECIMENS

For each of the nineteen sections, the members were manufactured from long sheets. A segment was cut from the members representing each section. The dimensions of each segment were carefully measured using a calliper with an accuracy of 0.001 inches (0.025 mm). The angle between planes of the web and adjacent flanges was measured twice using an angular ruler, one with respect to the compression flange and the other with respect to the tension flange. The measured dimensions of all elements and the angles of all webs are given in Table 3.2.1, and the shape of the sections is shown in Figure 3.1.1. In these tables, each section is designated as: t**h**R**θ*, where "t**" represents gage number (thickness), such as t22 (22 gage); "h**"

represents the flat depth of the web, such as h1 (h=1.0 inch); "R**" indicates the inside bend radius; and "θ" represents the angle of the web, such as θ60 (60 degree angle).

The length of the specimens was determined based on the width of the bearing plates, the minimum distance between two adjacent bearing plates (1.5h), and the minimum distance between a bearing plate and the end of a specimen (1.5h) as required for the EOF, IOF, ETF, and ITF loading conditions in the AISI Specifications. It was intended to exceed the required minimum distance in the actual specimens as to ensure the validity of each one-flange loading condition. For the EOF loading condition, the length of the specimens was designed to exceed the minimum distance requirement, but was short enough to avoid flexural failure in the middle of the specimen. The length of the specimens for the IOF loading condition was short enough to reduce the effect of moment on the interaction between the moment and the web crippling load. This would allow the web crippling load to be the control factor in the combined moment-web crippling failure. Due to the use of the shorter length for the specimens with the IOF loading condition, the shear lag effect was considered in determining the effective section flexural strength. Once the lengths of the specimens were determined, the specimens were very carefully cut from the members representing each section.

For all the specimens, the actual h/t ratio ranged from 25.99 to 208.19, the actual w/t ratios from 35.19 to 156.03, the actual R/t ratio from 2.16 to 5.51, the actual N/t ratio from 34.48 to 88.24, the actual N/h ratio from 0.22 to 2.02, the actual angle between the plane of web and plane of bearing surface from 59.5 to 90 degree, the actual thickness of steel sheet from 0.017 to 0.029 inches, and the actual yield strength of the steel from 103.9 to 112.5 ksi. The actual values are listed in Table 3.2.2 for all the sections.

4. WEB CRIPPLING TESTS

A total of 148 specimens were tested to study the web crippling strength of the specimens using the Structural Grade 80 steel. Among the 148 specimens, 39 specimens were tested in EOF loading condition, 38 specimens in IOF loading condition, 36 specimens in ETF loading condition, and 35 specimens in ITF loading condition. All the tests were conducted through a displacement control program and all the panels were tested to failure. Section 4.1 describes the test setup. Section 4.2 deals with the test procedure. Sections 4.3 through 4.6 present the test results for the EOF, IOF, ETF, and ITF loading conditions, respectively.

4.1 TEST SETUP

The MTS 880 Test System located at the Engineering Research Laboratory of the University of Missouri-Rolla, as shown in Fig. 4.1.1, was used to carry out the deck panel tests. It consists of a loading frame with top and bottom platens (on the right of the picture), various control panels (in the middle of the picture), and a data acquisition system (on the left in the picture) with a real time computer monitor (not shown in the picture). The System uses the close-loop control scheme with three main control modes, namely load, strain, and displacement controls which are automatically operated in the System. During a test, the top platen is stationary, while the bottom platen is controlled by the System to move up and down as to apply load.

In the EOF loading condition, the specimen was placed on two simple supports (one was a roller condition and the other was a pin condition) which were fastened on a wide flange support beam 84 inches long. The support beam was firmly connected to the bottom platen of the MTS 880 loading frame. The width of the end bearing plates was taken as 1 inch at the two supports. A 4-inch wide bearing plate together with a fixed roller was placed at the center of the specimen. Load was applied to the central fixed roller which was against the unmovable top platen of the loading frame while moving the bottom platen upwards. Bracing was attached to the tension flange of the specimen using C-clamps at a distance of at least 1.5h away form the edge of the end

bearing plates and at three locations near the central bearing plate to prevent the section from changing its shape as shown in Fig. 4.1.2. For the specimens having a single rib with sloped webs, and a h/t ratio exceeding 100, the bracing was fastened to the tension flange at a distance of 1/4 inch away from the edge of the end bearing plates. Wooden blocks or an overlapping segment of the same section were used under the central bearing plate to avoid premature failure of the webs near the center of the specimen as shown in Fig. 4.1.3. The test setup for the EOF loading condition is illustrated in Figures 4.1.2.

In the IOF loading condition, the test setup was similar to that in the EOF loading condition, except that the width of the end bearing plates was taken as 3 inches, while the width of the central bearing plate was taken as 1.5 inches. Wooden blocks were placed at the supports instead of under the central bearing plate. The test setup is shown in Fig. 4.1.4.

In the ETF loading condition, one end of the specimen was placed on a support which was fastened on the wide flange supporting beam. At this end of the specimen, a 1-inch wide bearing plate was laid underneath the bottom flange of the specimen as well as on the top flange of the specimen as shown in Fig. 4.1.5. A fixed roller was then placed on the top of the top bearing plate. A wooden block was used to support the other end of the specimen prior to testing. Load was applied to the fixed roller which was against the unmovable top platen of the loading frame while moving the bottom platen upwards. After the load was applied, the wooden block at the other end was removed away. Bracing was attached to the tension flange of the specimen using C-clamps at a distance of at least 1.5h away from the edge of the end bearing plate and at two locations near the other end of the specimen to prevent the section from changing its shape as shown in Fig. 4.1.5. For the specimens having a single rib with sloped webs, and h/t ratio exceeding 100, bracing was fastened to the tension flange at a distance of 1/4 inch away from the edge of the end bearing plate. The test setup in the ETF loading condition is illustrated in Figures 4.1.6.

In the ITF loading condition, the test setup was similar to that for the ETF loading condition, except that the

top and the bottom bearing plates were placed at the center of the specimen. For all the specimens tested in this loading condition, bracing was attached to the tension flange at a distance of at least 1.5h away from the edge of the central bearing plate. The test setup in the ITF loading condition is illustrated in Figures 4.1.7.

4.2 TEST PROCEDURE

Prior to testing, lines were drawn on specimens to indicate locations of loading and centers of support. The specimen was then put on the support beam on the MTS loading frame along with the bearing plates. The bearing plates were carefully aligned with the existing lines on the specimen. The load conditioner in the MTS system was zeroed.

The displacement control mode of the MTS system was then started immediately after continuous data recording was initiated. The bottom platen of the MTS loading frame moved upwards to push the top fixed roller against the top platen, resulting in an applied load at the center of the fixed roller. The displacement mode continued throughout testing with a displacement rate of 0.00014 inches per second. After the specimen had failed, the displacement control mode was terminated while the data recording continued until the top fixed roller was automatically and gradually released away from the top platen in order to obtain the descending branch in the load-displacement relationship.

4.3 TEST RESULTS FOR EOF LOADING CONDITION

A total of 39 specimens were tested for the EOF loading condition, which involved 19 sections as shown in Table 3.2.1. Of the 39 specimens, 33 specimens had the sloped webs, while 6 specimens had the vertical webs. For each section, two specimens were tested. If the two tested loads differed from each other for about 10%, a third test was conducted for the same section. Under the displacement control mode, all the specimens experienced gradual failure. The out-of-plane deformation of webs for the specimens with larger h/t ratios

occurred gradually at the early stage of loading and continued to increase until failure. A sudden drop of applied load due to buckling of the web was not observed during tests. The tested ultimate loads for all the specimens are listed in Table 5.1.1.

For the specimens with two ribs and sloped webs (h/t ratio less than 100), shortly after the load was applied, the outer tips of the unstiffened flanges and the middle portion of the stiffened flange at the end bearing plates started to deform upward as shown in Fig. 4.3.1. This upward deformation continued to increase with further increases in applied load. The outer tips of the unstiffened flanges also tended to deform laterally during the loading process, while the corners of the stiffened flange at the end bearing plate did not have much freedom to move laterally. This may cause the two inner webs to carry more load than the two outer webs. Both the inner and the outer webs were bent with concave curvature. As a result, the two inner webs failed by forming an inclined yield line in the lower portion of the webs as shown in Figures 4.3.1 and 4.3.2. In Fig. 4.3.2 the outer webs tended to remain straight, and a residual deformation existed in the inner webs.

For the specimens with single rib and sloped webs (h/t ratio larger than 100), the outer tips of the unstiffened flanges at the end bearing plates also tended to deform upward and laterally shortly after the load was applied. However, due to the use of the bracing near the edge of the end bearing plate, the upward and lateral deformations of the unstiffened flanges could not develop considerably with further increase in applied load. The lower portion of the webs at the end bearing plates tended to bend with concave curvature. Eventually an inclined yield line was formed in the lower portion of the webs, resulting in the failure of the specimen. The residual deformation of the webs after test can be seen in Fig. 4.3.2.

The specimens with single rib and vertical webs performed in the similar way as the specimens with single rib and sloped webs. The slight difference was that the outer tips of the unstiffened flanges at the end bearing plates tended to deform largely upward due to the fact that the bracing was placed at a distance of at least 1.5h away from the edge of the end bearing plate as shown in Fig. 4.3.3. The specimens failed also by forming an

inclined yield line in webs, similar to the failure observed in the specimens with single rib and sloped webs. The residual deformation after test could be seen in the webs as well, as indicated in Fig. 4.3.4 (three specimens in the lower portion of the picture).

For the similar h/t and w/t ratios, the specimens with smaller R/t ratio tended to develop slightly higher loads than the specimens with larger R/t ratio. Since the actual two R/t ratios did not differ significantly, the R/t ratio seemed not to be a controlling parameter to affect the web crippling strength.

4.4 TEST RESULTS FOR IOF LOADING CONDITION

A total of 38 specimens were tested for the IOF loading condition, which involved 19 sections as shown in Table 3.2.1. Of the 38 specimens, 32 specimens had the sloped webs, while 6 specimens had the vertical webs. For each section, two specimens were tested and the results of the two specimens were fairly consistent. Under the displacement control mode, all the specimens experienced gradual failure. The out-of-plane deformation of webs for the specimens with larger h/t ratios occurred gradually at the early stage of loading and continued to increase until failure. A sudden drop of applied load due to buckling of the webs was not observed during tests. The tested ultimate loads for all the specimens are listed in Table 5.2.1.

For the specimens with two ribs and sloped webs (h/t ratio less than 100), shortly after the load was applied, the compression flange underneath the central bearing plate started to bend downward. The upper portion of the webs under the central plate tended to deform outward near the two transverse edges of the plate at the early stage of loading. This outward deformation of the web continued to increase with further increases in applied load, while the web-flange corners underneath the central plate were pushed down by the plate with respect to adjacent corners outside the central plate. When a peak load was reached, the two local outward deformation of the web near the two transverse edges of the central plate joined together to form an outward bulged web as shown in Figure 4.4.1 and 4.4.2. Shortly after the peak was reached, a yield line was formed in

the upper portion of each web underneath the central bearing plate as shown in Fig. 4.4.3. The web-flange corners underneath the central plate continued to be pushed downward, while the outward bulged deformation of the web further increased until the outer edge of the bulged deformation was about 1h to 1.5h away from the edge of the central plate. The peak load decreased slowly. The residual deformation of the specimens after test can be seen in Figures 4.4.4, 4.4.5, and 4.4.6.

The behavior of the specimens with single rib and sloped webs and the specimens with single rib and vertical webs was similar to that of the specimens with two ribs and sloped webs as shown in Figure 4.4.7. The residual deformation of the specimens after test can be seen in Figures 4.4.6 and 4.4.7. For the similar h/t and w/t ratios, the specimens with smaller R/t ratio tended to develop slightly higher loads than the specimens with larger R/t ratio.

4.5 TEST RESULTS FOR ETF LOADING CONDITION

A total of 36 specimens were tested for the ETF loading condition, which involved 16 sections as shown in Table 3.2.1. All of the 36 specimens had the sloped webs. For each section, two specimens were tested. If the two tested loads differed from each other by 10%, a third test was conducted for the same section. Under the displacement control mode, all the specimens experienced gradual failure. The out-of-plane deformation of webs for the specimens with larger h/t ratios occurred gradually at the early stage of loading and continued to increase until failure. A sudden drop of applied load due to buckling of the webs was not observed during tests. The tested ultimate loads for all the specimens are listed in Table 5.3.1. For the similar h/t and w/t ratios, the specimens with smaller R/t ratio tended to develop slightly higher loads than the specimens with larger R/t ratio.

For the specimens with two ribs and sloped webs (h/t ratio less than 100), similar to those specimens in the EOF loading condition, the outer tips of the unstiffened flanges and the middle portion of the stiffened flange

at the end bearing plates started to deform upward shortly after the load was applied. This upward deformation continued to increase with further increases in applied load as shown in Fig. 4.5.1. The outer tips of the unstiffened flanges also tended to deform laterally during the loading process, while the corners of the stiffened flange at the end bearing plate did not have much movement laterally. This could cause the two inner webs to carry more load than the two outer webs. Both the inner and the outer webs were bent with concave curvature for most of the specimens as shown in Fig. 4.5.1, while few specimens experienced convex curvature of the inner and outer webs as shown in Fig. 4.1.5. As a result, the two inner webs failed by forming an inclined yield line in the lower or upper portion of the web as shown in Figures 4.5.1. and 4.1.5. Figure 4.5.2 indicates that the outer webs tended to remain after the tests, and the residual deofrmation existed in the inner webs.

For the specimens with single rib and sloped webs (h/t ratio larger than 100), the outer tips of the unstiffened flanges at the end bearing plates also tended to deform upward and laterally shortly after the load was applied. However, due to the use of the bracing near the edge of the end bearing plate, the upward and lateral deformations of the unstiffened flanges could not develop considerably with further increase in applied load. Two different deformed shapes of the webs were observed during tests, namely asymmetric curvature and symmetric convex curvature of the webs as shown in Figures 4.5.3 and 4.5.4. Most of the specimens tended to form the symmetric shape with convex curvature. It was found that the specimens with the asymmetrically deformed shape resulted in a larger load than its counterpart with symmetrically deformed shape for the same section. Eventually an inclined yield line was formed in the lower or upper portion of the web, resulting in the failure of the specimen. The residual deformation of the web after test can be seen in Figure 4.5.5.

4.6 TEST RESULTS FOR ITF LOADING CONDITION

A total of 35 specimens were tested for the ITF loading condition, which involved 16 sections as shown in Table 3.2.1. All of the 35 specimens had the sloped webs. For each section, two specimens were tested. If the

two tested loads differed from each other by 10%, a third test was conducted for the section. Under the displacement control mode, all the specimens experienced gradual failure. The out-of-plane deformation of webs for the specimens with larger h/t ratios occurred gradually at the early stage of loading and continued to increase until failure. A sudden drop of applied load due to buckling of the webs was not observed during tests. The tested ultimate loads for all the specimens are listed in Table 5.4.1. For the similar h/t and w/t ratios, the specimens with smaller R/t ratio tended to develop slightly higher loads than the specimens with larger R/t ratio.

For all the specimens with single rib or two ribs, the out edges of unstiffened flanges and the middle portion of the stiffened flange above the bottom central bearing plate tended to deform upward shortly after load was applied, but with further increases in applied load, the development of the upward deformation seemed to be very slow. The bottom portion of the web above the bottom central bearing plate started to bend with concave curvature, while the top portion of the web underneath the top central bearing plate tended to bend with convex curvature, forming a double curvature in webs. As the load increased, a small bottom portion of the web above the bottom bearing plate was flattened out and the web-flange corner underneath the top bearing plate was pushed downward as compared to the corners outside the top bearing plate as shown in Figures 4.6.1 and 4.6.2. This caused the sloped webs to become vertical and resulted in the formation of the yield lines in the bottom portion of the web above the bottom bearing plate and in the top portion of the web underneath the top bearing plate as shown in Figure 4.6.3. A peak load was reached shortly before the yield lines were formed. After the webs between the top and bottom bearing plates became vertical, the applied load decreased very slowly, and for some specimens, the load started to increase slightly again. The residual deformation in the specimens after tests can be seen in Figure 4.6.4.

5. EVALUATION OF TEST RESULTS

The results of the 148 web crippling tests with the EOF, IOF, ETF, and ITF loading conditions were evaluated using the AISI Specification (AISI 1986), actual and specified material properties, and the measured dimensions. Also evaluated are the 114 web crippling tests that were reported by Santaputra and Yu (1986). The sectional properties of the 114 specimens can be found in Santaputra and Yu (1986). This section presents the results of the evaluation. In the following discussion, Sections 5.1 through 5.4 evaluate the test results with the EOF, IOF, ETF, and ITF loading conditions, respectively.

5.1 EVALUATION OF TEST RESULTS WITH EOF LOADING CONDITION

As discussed in Section 2, the present kC_1 and kC_3 factors stated in Section 3.4 of the AISI Specifications for predicting the web crippling strength of cold-formed structural members may not be rational for the members made of high-strength steels (yield strength larger than 80 ksi). For all the specimens tested in this research program, the yield strength of the steel ranged from 103.9 to 112.5 ksi, which will result in both kC_1 and kC_3 factors being on the descending branches of the kC_1 vs. F_y and kC_3 vs. F_y curves shown in Fig. 2.1. Thus, a modification on the kC_1 and kC_3 factors, as used by Santaputra and Yu (1986), was employed again to predict the web crippling strength of the specimens tested in this program. The modification was to remove the descending branches of the kC_1 vs. F_y and kC_3 vs. F_y curves and replace them with horizontal lines at the peak of the curves. The peak value for kC_1 was taken as 1.691 at the yield strength of 91.5 ksi and this value was also used for the yield strength larger than 91.5 ksi. Similarly, the peak value for kC_3 was taken as 1.34 at the yield strength of 66.5 ksi and it was used for the yield strength larger than 66.5 ksi as well. Prior to the peak values, the present kC_1 and kC_3 factors stated in the AISI Specifications are used.

The tested ultimate loads of the 39 specimens with the EOF loading condition were compared with the calculated loads using the modified kC_3 factor as discussed above. The ratio of the tested ultimate load to the

calculated load is plotted with respect to the yield strength, F_y, for the 39 specimens tested in this program and 30 specimens reported by Santaputra and Yu as shown in Fig. 5.1.1. The load ratios are also listed in Table 5.1.1. It is shown in the figure that the ratio of the tested ultimate load to the calculated load tends to increase with increases in the yield strength of steel, especially when the yield strength is larger than 80 ksi. It is noted that the load ratios are all larger than 1.0, ranging from 1.25 to 2.91. This indicates that using the modified kC_3 for predicting the web crippling strength of the specimens made of high-strength steels is conservative for the EOF loading condition and the conservatism increases with increases in the yield strength.

The ratio of the tested ultimate load to the calculated load is also plotted with respect to the h/t ratio of the specimens as shown in Figure 5.1.2. It is noted that the trend between the load ratio and the h/t ratio does not appear to follow the same trend as observed in Fig. 5.1.1. It implies that the h/t ratio may not be a significant factor to affect the web crippling strength of the specimens made of high-strength steels on the basis of using the present equations in the AISI Specifications for the web crippling strength calculation, that is, using the factor (179-0.33(h/t)) for stiffened flanges and the factor (117-0.15(h/t)) for unstiffened flanges in Section 3.4 of the AISI Specifications. Relatively large scatter of the data can be seen in Fig. 5.1.2 for the specimens with the h/t ratio less than 100. It has to be addressed that for the specimens with the h/t ratio larger than 100 and having the sloped webs, bracing was attached to the tension flanges of the specimens at a distance of 1/4" away from the edge of the end bearing plate to prevent the section from changing its shape. By doing so, the tested loads of these single-rib specimens with sloped webs were consistent with those of the specimens with vertical webs and braced at least 1.5h away from the end bearing plate.

5.2 EVALUATION OF TEST RESULTS WITH IOF LOADING CONDITION

Similar to the modified kC_3 factor used for predicting the web crippling strength for the EOF loading condition as discussed in Section 5.1, the modified kC_1 factor was used for predicting the web crippling strength of the 38 specimens tested in this research program for the IOF loading condition. The flexural

strength of the specimens was determined by using the AISI Specification and a yield strength reduction factor obtained in the Second Progress Report (Wu, Yu, and LaBoube 1996). The shear lag effect does not control the strength calculation.

The tested ultimate loads of the 38 specimens with the IOF loading condition were compared with the calculated loads using the modified kC_1 factor, and the tested ultimate moments of the specimens obtained in the same loading condition were compared to the calculated moments using the yield strength reduction factor. The ratio of the tested ultimate moment to the calculated moment is plotted with respect to the ratio of the tested ultimate load to the calculated load for the 39 specimens tested in this program and for additional 36 specimens reported by Santaputra and Yu as shown in Fig. 5.2.1. The load and moment ratios are also listed in Table 5.2.1. The envelope for combined web crippling load-moment interaction as specified in Section 3.5 of the AISI Specifications is also shown in Fig. 5.2.1. It is noted in the figure that most of the tested data fall outside of the envelope, indicating the conservatism of using the modified kC_1 factor for predicting the web crippling strength of the specimens made of high-strength steels in the IOF loading condition.

5.3 EVALUATION OF TEST RESULTS WITH ETF LOADING CONDITION

Similar to the modified kC_3 factor used for predicting the web crippling strength for the EOF loading condition as discussed in Section 5.1, the modified kC_3 factor was also used for predicting the web crippling strength of the 36 specimens tested in this research program for the ETF loading condition.

The tested ultimate loads of the 36 specimens with the ETF loading condition were compared with the calculated loads using the modified kC_3 factor as discussed above. The ratio of the tested ultimate load to the calculated load is plotted with respect to the yield strength, F_y, for the 36 specimens tested in this program and 24 specimens reported by Santaputra and Yu as shown in Fig. 5.3.1. The load ratios are also listed in Table 5.3.1. It is noted in the figure that the ratio of the tested ultimate load to the calculated load has a tendency to

increase with increases in the yield strength of steel except for the yield strength of 165 ksi. The load ratios for the specimens tested in this program tend to be higher than those reported by Santaputra and Yu. It is apparent that all the load ratios are larger than 1.0 and range from 1.22 to 2.81, indicating that using the modified kC_3 for predicting the web crippling strength of the specimens made of high-strength steels is also conservative for the ETF loading condition.

The ratio of the tested ultimate load to the calculated load is also plotted with respect to the h/t ratio of the specimens as shown in Figure 5.3.2. It was noted that the h/t ratio does not seem to be a significant factor to affect the web crippling strength of the specimens on the basis of using the present factor (132-0.31(h/t)) in the AISI Specifications. Relatively large scatter of the data can be seen in Fig. 5.3.2 for the specimens with the h/t ratio less than 100. For the specimens with the h/t ratio larger than 100 and having the sloped webs, the bracing was also attached to the tension flanges of the specimen at a distance of 1/4" away from the edge of the end bearing plate to prevent the section from changing its shape.

5.4 EVALUATION OF TEST RESULTS WITH ITF LOADING CONDITION

Similar to the modified kC_1 factor used for predicting the web crippling strength for the IOF loading condition as discussed in Section 5.2, the modified kC_1 factor was also used for predicting the web crippling strength of the 35 specimens tested in this research program for the ITF loading condition.

The tested ultimate loads of the 35 specimens with the EOF loading condition were compared with the calculated loads using the modified kC_1 factor as discussed above. The ratio of the tested ultimate load to the calculated load is plotted with respect to the yield strength, F_y, for the 35 specimens tested in this program and for additional 24 specimens reported by Santaputra and Yu as shown in Fig. 5.4.1. The load ratios are also listed in Table 5.4.1. The figure indicates that the ratio of the tested ultimate load to the calculated load tends to increase with increases in the yield strength of steel, especially when the yield strength is larger than 80 ksi.

The load ratios range from 0.84 to 2.17. All load ratios with the yield strength larger than 80 ksi are greater than 1.0.

The ratio of the tested ultimate load to the calculated load is also plotted with respect to the h/t ratio of the specimens as shown in Figure 5.4.2. Once again, the h/t ratio does not appear to be a significant factor to affect the web crippling strength of the specimens on the basis of using the present factor (417-1.22(h/t)) in the AISI Specifications. Relatively large scatter of the data can be seen in Fig. 5.4.2 for the specimens with the h/t ratio less than 100. Several low load ratios, ranging from 0.84 to 0.91, correspond to the specimens with a thickness of 0.088 inches (the largest in this group) reported by Santaputra and Yu.

6. DEVELOPMENT OF MODIFIED kC_1 AND kC_3 FACTORS

The comparison between the tested ultimate web crippling loads to the calculated web crippling strength using the modified kC_1 and kC_3 factors and the AISI Specification, as discussed in Section 5, demonstrates that even with the largest kC_1 and kC_3 values that are allowed in the Specification for predicting web crippling strength, the tested ultimate loads tend to be higher than the calculated loads for most of the 262 specimens with the four basic loading conditions. Therefore, it may be necessary to develop new modified kC_1 and kC_3 factors for predicting the web crippling strength of the specimens made of high-strength steels. This section addresses this issue. Section 6.1 deals with the development of new modified kC_1 and kC_3 factors. Section 6.2 compares the tested ultimate loads with predicted loads using the new modified kC_1 and kC_3 factors.

6.1 DEVELOPMENT OF NEW MODIFIED kC_1 AND kC_3 FACTORS

As discussed in Section 5, the h/t ratios of the specimens included in this study do not appear to have a significant effect on the web crippling strength of the specimens for the four loading conditions. Even though these h/t ratios cover a wide range of values represented in practice, they are still within the limit specified in the AISI Specification. However, the only significant difference, in terms of parameters, as compared to the previous test results with which the present equations for predicting web crippling strength were developed is the yield strength of sheet steels. The yield strength used for developing the present equations for web crippling strength was usually less than 60 ksi, while the yield strength used for this study is more than 100 ksi. The effect of yield strength of a steel on the web crippling strength of structural members is reflected in the kC_1 and kC_3 factors in Section 3.4 of the AISI Specifications. These factors are written as:

For the IOF and ITF loading conditions,

$$k\,C_1 = \frac{F_y}{33}\left(1.22 - 0.22\,\frac{F_y}{33}\right) \qquad (6\text{-}1)$$

where $k=F_y/33$.

For the EOF and ETF loading conditions,

$$k\,C_3 = \frac{F_y}{33}\left(1.33 - 0.33\,\frac{F_y}{33}\right) \tag{6-2}$$

where $k=F_y/33$.

Therefore, our target is to only modify the existing kC_1 and kC_3 factors so that they can be used to predict the web crippling strength of the members made of high-strength steels. The test results presented in Section 5 also revealed the necessity for such modification.

The development of the new modified kC_1 and kC_3 factors requires three matters to be considered. First, it would be better to develop the factors on the basis of the present formats of the factors as stated in the AISI Specification without a significant change of the existing equations. The rationality behind this is that the present formats of the kC_1 and kC_3 factors are the results of extensive studies on the parameters that would affect the factors, and the factors were calibrated with a great number of test data with certain limitations on the ranges of various design parameters. At least the factors are suitable for those ranges of the parameters based on which the factors were developed. As a result, the new modified factors should reflect the parameters and the formats used in the present equations for the factors unless a complete theoretical approach is possible and does not lead to a complicated solution. Second, the new equations for the factors should be able to represent the part of the existing equations which have been valid in practice for many years. Third, it may be necessary to develop the new modified factors that can result in a lower bound solution (a relatively conservative solution if not too conservative).

In Section 2, a discussion was made on the kC_1 vs. F_y and kC_3 vs. F_y relationships as specified in Section 3.4 of the AISI Specification, and the kC_1 vs. F_y and kC_3 vs. F_y relationships are plotted as two curves shown in Fig. 2.1. Referring to this figure, it is found that the two curves are almost identical for the yield strength less than 40 ksi and the difference between the two curves is not significant with the yield strength between 40 to 60

ksi. As a result, it may be necessary for the new equations pass through, or at least near, the previous curves in these ranges of yield strength.

According to the above discussion, a new set of equations for the kC_1 and kC_3 factors were developed based on the available 262 web crippling tests that included the following parameters: the yield strength F_y ranged from 58.2 ksi to 165.1 ksi, h/t ratio from 25.99 to 208.19, R/t ratio from 1.496 to 5.696, N/t ratio from 22.70 to 88.24, N/h ratio from 0.17 to 2.02, thickness of steel sheets from 0.017 in. to 0.088 in, and the angle between plane of web and plane of bearing surface from 59.5 to 90 degree. The new modified kC_1 and kC_3 factors are expressed as follow:

For the IOF and ITF loading conditions,

$$k\,C_1 = \frac{F_y}{33}\left(1.13 - 0.13\,\frac{F_y}{33}\right) \tag{6-3}$$

where $k=F_y/33$ and $F_y \le 143.4$ ksi. At F_y equal to 143.4 ksi, the kC_1 reaches a peak value of 2.46 and remains as 2.46 for the yield strength larger than 143.4 ksi.

For the EOF and ETF loading conditions,

$$k\,C_3 = \frac{F_y}{33}\left(1.20 - 0.2\,\frac{F_y}{33}\right) \tag{6-4}$$

where $k=F_y/33$ and $F_y \le 99.0$ ksi. At F_y equal to 99.0 ksi, the kC_1 reaches a peak value of 1.80 and remains as 1.80 for the yield strength larger than 99.0 ksi.

The two equations have the same derivative at the yield strength of 16.5 ksi where the present kC_1 and kC_3 equations in the AISI Specifications also have the same derivative, that is, $d(kC_1 \text{ or } kC_3)/dF_y|F_y=16.5 \text{ ksi} = 0.0303$. The modified equations for the kC_1 and kC_3 factors are shown in Fig. 2.1 as compared to the present equations. The figure indicates that Equations 6-3 and 6-4 are almost identical to Equations 6-1 and 6-2 for the yield strength less than 40 ksi. The difference between Equations 6-3 and 6-4 and Equations 6-1 and 6-2 is also small for the yield strength between 40 and 60 ksi.. This allows the new modified factors also to be used

for predicting the web crippling strength of the members made of low-strength steels (less than 60 ksi). Thus, the predicted web crippling strength using the new equations is expected to be similar to that predict using the present equations for the member with the yield strength less than 60 ksi.

It is noted that for the IOF and ITF loading conditions, the peak value of the new modified kC_1 factor is about 1.45 times larger than the peak value of the present kC_1 factor, while for the EOF and ETF loading conditions, the peak value of the new modified kC_3 factor is about 1.34 times larger than the peak value of the present kC_3 factor. As a result, using the new modified factors can be more economical, leading to a relatively large amount of material savings as compared to using the present kC_1 and kC_3 factors.

6.2 COMPARISON OF TESTED ULTIMATE LOADS WITH PREDICTED LOADS USING THE NEW MODIFIED kC_1 AND kC_3 FACTORS

To evaluate the validity of the new modified kC_1 and kC_3 factors (Equations 6-3 and 6-4), the tested ultimate loads for the 148 specimens tested in this program and the 114 specimens reported by Santaputra and Yu (1986) were compared to the calculated loads using the new modified factors for the four loading conditions. The ratio of the tested ultimate load to the calculated load is plotted with respect to F_y for the EOF, ETF, and ITF loading conditions as shown in Figures 6.2.1, 6.2.4, and 6.2.6., respectively. The ratio of the tested ultimate load to the calculated load is also plotted with respect to the h/t ratio for the EOF, ETF, and ITF loading conditions as shown in Figures 6.2.2, 6.2.5, and 6.2.7., respectively. The comparison for the combined moment and web crippling load is illustrated in Fig. 6.2.3 for the IOF loading condition. The results of the comparisons are listed in Tables 6.2.1 through 6.2.4.

For the specimens tested in the EOF and ETF loading conditions, the ratio of the tested ultimate load to the calculated load using the new modified kC_3 factor still tends to be larger than 1.0. The load ratio ranges from 0.93 to 2.17 for the specimens with the EOF loading condition and from 0.96 to 2.09 for the specimens with

the ETF loading condition. The use of the new modified kC_3 factor leads to be a conservative solution, but considerable improvement has been made on predicting the web crippling strength.

For the specimens tested in the IOF loading condition, a large number of tested data still fall outside of the web crippling load-moment interaction envelope, indicating a conservative yet reasonable agreement between the tested data and the calculated values using the new modified kC_1 factor and the yield strength reduction factor.

For the specimens tested in the ITF loading condition, the ratio of the tested ultimate load to the calculated load using the new modified kC_1 factor tends to be larger than 1.0 for the specimens tested in this program, but the ratio is relatively lower for some specimens tested by Santaputra and Yu. The load ratio ranges from 0.72 to 1.56 with an average of 1.11. Reasonable agreement between the tested ultimate loads and the calculated loads is achieved.

Finally, if a simple and conservative solution is needed, it is recommended that the present kC_1 in Section 3.4 of the AISI Specification can be used for all the IOF, ITF, EOF, and ETF loading conditions. If this approach is used, the lowest load ratios of some of the specimens with the ITF loading condition as resulted from using the new modified kC_1 will be increased from 0.72 to 0.84.

7. SUMMARY

A total of 148 web crippling tests have been completed using the Structural Grade 80 of ASTM A653 steel at the Department of Civil Engineering of University of Missouri-Rolla. The test results have been evaluated along with an additional 114 web crippling tests which were reported by Santaputra and Yu (1986) as part of a project on the Design of Automotive Components Using High-Strength Sheet Steels. The preliminary research findings and the evaluation of the results are summarized as follows:

(1) The kC_1 and kC_3 factors, as stated in Section 3.4 of the AISI Specifications (AISI, 1986 and 1991) for predicting the web crippling strength of structural members, represent two parabolic curves with respect to yield strength of steel, F_y. The values of the factors reach a peak at the F_y equal to 91.5 ksi for kC_1 and 66.5 ksi for kC_3 and then decrease with further increases in yield strength. It is not rational to use the descending branch of the curves for predicting web crippling strength with higher yield strength of steels since the factors were mainly developed based on the materials with yield strength less than 60 ksi (lay on the ascending branch of the curves).

(2) The web crippling tests conducted in this program and those reported in 1986 indicated that the tested ultimate loads for the four loading conditions were higher than the predicted loads using the AISI Specifications with the modified kC_1 and kC_3 factors (1.691 for kC_1 when F_y exceeds 91.5 ksi and 1.34 for kC_3 when F_y exceeds 66.5 ksi) and the high yield strength of the steels (exceeding 80 ksi). The ratio of the tested ultimate load to the calculated load tends to increase with further increase in the yield strength of the steel beyond 80 ksi. Therefore, it is conservative to use the kC_1 and kC_3 factors in Section 3.4 of the AISI Specifications for predicting web crippling strength of structural members with yield strength exceeding 80 ksi.

(3) The test data indicated that the low ductility of the Structural Grade 80 steel does not affect the web crippling strength of the members made of such a steel.

(4) New modified kC_1 and kC_3 factors were developed based on the 262 web crippling tests, which included the following parameters: the yield strength F_y ranged from 58.2 ksi to 165.1 ksi, h/t ratio from 25.99 to 208.19, R/t ratio from 1.496 to 5.696, N/t ratio from 22.70 to 88.24, N/h ratio from 0.17 to 2.02, thickness of steel sheets from 0.017" to 0.088", and the angle between plane of web and plane of bearing surface from 59.5 to 90 degree. Reasonable agreement was found between the tested ultimate loads and the predicted loads using the new modified kC_1 and kC_3 factors. The solutions tend to be conservative.

(5) In order to simplify designs, the current kC_1 in Section 3.4 of the AISI Specification can be used for all the IOF, ITF, EOF, and ETF loading conditions, resulting in a simple but conservative solution.

8. FUTURE RESEARCH WORK

The research work reported herein is a part of an overall research project on Strength of Flexural Members Using Structural Grade 80 of A653 and Grade E of A611 Steels, sponsored by the American Iron and Steel Institute. Future research work of the project will include a preliminary study on screwed and welded connections using the Structural Grade 80 steel. Results of the connection tests will be evaluated and reported in the Fourth Progress Report.

ACKNOWLEDGEMENTS

The research work reported herein was conducted in the Department of Civil Engineering at the University of Missouri-Rolla under the sponsorship of the American Iron and Steel Institute. Drs. Wei-Wen Yu and R.A. LaBoube are the directors of the project.

The financial assistance granted by the Institute and the technical guidance provided by members of the Subcommittee 24 - Flexural Members of the AISI Committee on the Specification for the Design of Cold-Formed Steel Structural Members and the AISI staff (D.F. Boring, R.B. Haws, H. Chen, K.C. Slaughter, and S.P. Bridgewater) are gratefully acknowledged. The Subcommittee members are: J.N. Nunnery (Chairman), R.E. Albrecht, R.L. Brockenbrough, R.E. Brown, C.R. Clauer, D.S. Ellifritt, S.J. Errera, J.M. Fisher, T.V. Galambos, M. Golovin, G.J. Hancock, A.J. Harrold, R.B. Haws, R.B. Heagler, D.L. Johnson, W.E. Kile, R.A. LaBoube, M.R. Loseke, R. Madsen, T.H. Miller, T.M. Murray, T.B. Pekoz, D.C. Perry, R.M. Schuster, P.A. Seaburg, W.L. Shoemaker, T. Sputo, T.W. Trestain, and W.W. Yu.

All steels used for forming the specimens were kindly donated by Inland Steel Company and National Steel Company. Thanks are also due to J. Bradshaw, J. McCracken, and S. Gabel, staff of the Department of Civil Engineering, for their technical support.

REFERENCES

American Iron and Steel Institute. (1991). "Load and Resistance Factor Design Specification for Cold-Formed Steel Structural Members," March 16, 1991 Edition.

American Iron and Steel Institute. (1986). "Specification for the Design of Cold-Formed Steel structural Members," August 19, 1986 Edition with December 11, 1989 Addendum.

ASTM A446. "Standard Specification for Steel Sheet, Zinc-Coated (Galvanized) by the Hot-Dip Process, Physical (Structural Quality)," Annual Book of ASTM Standards.

Dhalla, A.K., and Winter, G. (1971). "Influence of Ductility on the Structural Behavior of Cold-Formed Steel Members," Report No. 336, Cornell University, June.

Glauz, R.S. (1990). "Cold-Formed Steel Design Program, User's Manual,"

Hetrakul, N. and Yu, W.W. (1978). "Structural Behavior of Beam Webs Subjected to Web Crippling and a Combination of Web Crippling and Bending," Final Report, Civil Engineering Study 78-4, Department of Civil Engineering, University of Missouri-Rolla, Rolla, MO.

Pan, L.C. (1987). "Effective Design Widths of High Strength Cold-Formed Steel Members." Ph.D. Dissertation, Department of Civil Engineering, University of Missouri-Rolla, Rolla, MO.

Santaputra, C. and Yu, W.W. (1986). "Design of Automotive Structural Components Using High Strength Sheet Steels, Web Crippling of Cold-Formed Steel Beams," Eighth Progress Report, Civil Engineering Study, 86-1, Department of Civil Engineering, University of Missouri-Rolla, Rolla, MO.

Steel Deck Institute (SDI). (1992). "Steel Deck Institute Design Manual for Composite Decks, Form Decks, Roof Decks, and Cellular Metal Floor Deck with Electrical Distribution." Steel Deck Institute, Publication No. 28.

United Steel Deck (USD). (1994). "Steel Decks for Floors and Roofs, Design Manual and Catalog of Products." Nicholas J. Bouras, Inc.

Wu, S., Yu, W.W., and LaBoube, R.A. (1995). "Strength of Flexural Members Using Structural Grade 80 of A653 and Grade E of A611 Steels." First Progress Report, Civil Engineering Study 95-5, Department of Civil Engineering, University of Missouri-Rolla, Rolla, MO.

Wu, S., Yu, W.W., and LaBoube, R.A. (1996). "Strength of Flexural Members Using Structural Grade 80 of A653 Steel (Deck Penal Tests)." Second Progress Report, Civil Engineering Study 96-4, Department of Civil Engineering, University of Missouri-Rolla, Rolla, MO.

Yu, Wei-Wen. (1991). "Cold-Formed Steel Design," Second Edition, John Wiley & Sons. Inc..

APPENDIX

NOTATIONS

The following symbols are used in this report:

E = modulus of elasticity, 29500 ksi.

F_y = specified yield strength of sheet steel.

F_u = specified tensile strength of sheet steel.

H = flat width of web

$k = F_y/33$

R = inside bend radius

t = thickness of sheet steel

w = flat width of compression flange

θ = angle between planes of the web and bearing surface

Table 3.1.1 h/t and w/t Ratios Used for the *Design* of Specimens with Sloped and Vertical Webs

t (gage#) (inches)	w (inches)								
	1	2	2	3	3	3	2	3	4.5
0.017 (26) Sloped Web	58.82	117.65	--	--	--	--	--	--	--
0.029 (22) Sloped Web	34.48	68.97	68.97	103.45	103.45	103.45	--	--	--
0.029 (22) Vertical Web	--	--	--	--	--	--	68.97	103.45	155.17
t (gage #) (inches)	h (inches)								
	0.75	1.5	2	3	4.5	6	1.5	3	4.5
0.017 (26) Sloped Web	44.12	88.24	--	--	--	--	--	--	--
0.029 (22) Sloped Web	25.86	51.72	68.97	103.45	155.17	206.90	--	--	--
0.029 (22) Vertical Web	--	--	--	--	--	--	51.72	103.45	155.27
R (in.)	1/8, 1/16	1/8, 1/16	1/8, 1/16	1/8, 1/16	1/8, 1/16	1/8, 1/16	1/8	1/8	1/8
# of Ribs	2	2	2	1	1	1	1	1	1

Note: see Figure 3.1.1 for the measurement of w and h. 1 inch = 25.4 mm.

Table 3.1.2 Material Properties of 22, 24, 26, and 28 Gage Steel Sheets

Direction	Gage	Thickness (in.)	0.2% Offset Yield Strength F_y (ksi)	Tensile Strength F_u (ksi)	Tensile-to-Yield Ratio F_u/F_y	Local Elongation in 1/2-in. Gage Length (%)	Uniform Elongation Outside Fracture (%)	Elongation in 2-in. Gage Length (%)
Parallel to Rolling Direction	22	0.029	103.9	107.7	1.04	11.98	1.29	3.67
	24	0.024	110.1	116.4	1.06	9.33	1.23	2.69
	26	0.017	112.5	115.9	1.03	9.13	0.77	2.40
	28	0.015	111.0	116.1	1.05	7.89	1.04	2.77
Perpendicular to Rolling Direction	22	0.029	119.6	121.2	1.02	7.29	0.41	1.99
	24	0.024	126.0	128.5	1.02	6.40	0.35	1.78
	26	0.017	129.7	132.6	1.02	3.78	0.43	1.32
	28	0.015	127.3	130.1	1.02	3.78	0.43	1.38

Note: All the steel sheets were made of the Structural Grade 80 of ASTM A653 Steel. 1 inch = 25.4 mm. 1 ksi = 6.895 MPa.

Table 3.2.1 Measured Dimensions of Specimens

Type of Specimen (#)	$L_{1,2}$ (in.)	$L_{2,3}$ (in.) ($\theta_{2,3}$ in degree)	$L_{3,4}$ (in.)	$L_{4,5}$ (in.) ($\theta_{4,5}$ in degree)	$L_{5,6}$ (in.)	$L_{6,7}$ (in.) ($\theta_{6,7}$ in degree)	$L_{7,8}$ (in.)	$L_{8,9}$ (in.) ($\theta_{8,9}$ in degree)	$L_{9,10}$ (in.)
t26h0.75R3/32θ60 (1)	1.060	0.910 (61,62)	1.200	0.901 (61.5,60)	2.193	0.908 (61.5,60.5)	1.184	0.912 (60.5,61)	1.075
t26h0.75R3/64θ60 (2)	1.029	0.850 (61,61.5)	1.110	0.853 (61.5,60)	2.109	0.840 (62,60.5)	1.104	0.838 (60.5,61)	1.027
t26h1.5R3/32θ60 (3)	1.065	1.670 (60,60)	2.184	1.658 (61,60)	2.201	1.651 (61,61)	2.200	1.648 (61,63)	1.076
t26h1.5R3/64θ60 (4)	1.035	1.591 (60,60)	2.110	1.581 (60,60)	2.125	1.594 (60.5,60)	2.118	1.583 (59.5,61)	1.046
t22h0.75R5/64θ60 (5)	1.089	0.929 (60,61.5)	1.195	0.934 (61.5,58.5)	2.183	0.951 (60,60)	1.188	0.935 (60,62)	1.080
t22h0.75R1/16θ60 (6)	1.064	0.851 (60,61)	1.128	0.873 (61.5,61)	2.105	0.852 (60.5,60)	1.130	0.867 (60,61)	1.054
t22h1.5R5/64θ60 (7)	1.071	1.696 (58.5,60.5)	2.204	1.673 (61,58)	2.171	1.677 (59.5,60)	2.207	1.667 (60,61)	1.094
t22h1.5R1/16θ60 (8)	1.030	1.612 (59.5,60)	2.105	1.619 (60.5,59)	2.142	1.619 (60,60)	2.128	1.613 (60,61)	1.044
t22h2R5/64θ60 (9)	1.066	2.184 (60.5,61.5)	2.192	2.165 (62.5,60)	2.165	2.183 (60,60.5)	2.204	2.156 (60,63)	1.104
t22h2R1/16θ60 (10)	1.030	2.105 (59,60)	2.120	2.094 (60.5,60)	2.172	2.117 (59.5,60)	2.117	2.102 (60,60.5)	1.055

Note: See Figure 3.2.1 for dimensions. 1 inch = 25.4 mm.

Table 3.2.1 Measured Dimensions of Specimens (Continued)

Type of Specimen (#)	$L_{1,2}$ (in.)	$L_{2,3}$ (in.) ($\theta_{2,3}$ in degree)	$L_{3,4}$ (in.)	$L_{4,5}$ (in.) ($\theta_{4,5}$ in degree)	$L_{5,6}$ (in.)	$L_{6,7}$ (in.) ($\theta_{6,7}$ in degree)	$L_{7,8}$ (in.)	$L_{8,9}$ (in.) ($\theta_{8,9}$ in degree)	$L_{9,10}$ (in.)
t22h3R5/64θ60 (11)	1.082	3.201 (59,61.5)	3.190	3.188 (60,61)	1.103				
t22h3R1/16θ60 (12)	1.050	3.100 (60,61)	3.150	3.113 (60,61)	1.047				
t22h4.5R5/64θ60 (13)	1.077	4.681 (61,62.5)	3.183	4.676 (61,62)	1.102				
t22h4.5R1/16θ60 (14)	1.040	4.619 (61,61)	3.108	4.617 (60.5,61.5)	1.057				
t22h6R5/64θ60 (15)	1.083	6.174 (63,63)	3.177	6.162 (61,64)	1.107				
t22h6R1/16θ60 (16)	1.045	6.118 (61,61)	3.126	6.088 (60,62)	1.050				
t22h1.5R1/8θ90 (17)	1.142	1.793 (90,90)	2.324	1.780 (89,90)	1.126				
t22h3R1/8θ90 (18)	1.132	3.327 (90,91)	3.282	3.302 (90,90)	1.154				
t22h4.5R1/8θ90 (19)	1.124	4.817 (89.5,91)	4.833	4.805 (90,90.5)	1.140				

Note: See Figure 3.2.1 for dimensions. 1 inch = 25.4 mm.

Table 3.2.2 Properties of the Specimens

Specimen	Thickness (in.)	F_y (ksi)	Average h/t	Average w/t	Average R/t	Average θ (degree)
t26h0.75R3/32θ60	0.017	112.5	45.72	62.44	5.51	61
t26h0.75R3/64θ60	0.017	112.5	45.29	60.69	2.76	61
t26h1.5R3/32θ60	0.017	112.5	89.78	121.27	5.51	61
t26h1.5R3/64θ60	0.017	112.5	89.02	120.01	2.76	60.1
t22h0.75R5/64θ60	0.029	103.9	28.02	36.79	2.69	60.4
t22h0.75R1/16θ60	0.029	103.9	25.99	35.24	2.16	60.6
t22h1.5R5/64θ60	0.029	103.9	53.60	71.81	2.69	59.8
t22h1.5R1/16θ60	0.029	103.9	52.07	69.34	2.16	60
t22h2R5/64θ60	0.029	103.9	70.55	71.44	2.69	61
t22h2R1/16θ60	0.029	103.9	68.93	69.42	2.16	59.9
t22h3R5/64θ60	0.029	103.9	105.86	105.70	2.69	60.4
t22h3R1/16θ60	0.029	103.9	103.44	104.94	2.16	60.5
t22h4.5R5/64θ60	0.029	103.9	156.93	105.35	2.69	61.6
t22h4.5R1/16θ60	0.029	103.9	155.53	103.46	2.16	61
t22h6R5/64θ60	0.029	103.9	208.19	105.05	2.69	62.8
t22h6R1/16θ60	0.029	103.9	206.73	104.08	2.16	61
t22h1.5R1/8θ90	0.029	103.9	50.97	69.52	4.31	90
t22h3R1/8θ90	0.029	103.9	103.67	102.55	4.31	90
t22h4.5R1/8θ90	0.029	103.9	155.28	156.03	4.31	90

Note: 1 inch = 25.4 mm. 1 ksi= 6.895 MPa.

Table 5.1.1 Tested Ultimate Load, Calculated Load, and Comparison between the Tested Ultimate Load and the Calculated Load for EOF Loading Condition

Specimen	F_y (ksi)	Average h/t	P_{test} (kips)			$P_{calc,old\ KC3}$ (kips)	$P_{test}/P_{calc,old\ KC3}$		
			Test 1	Test 2	Test 3		Test 1	Test 2	Test 3
t26h0.75R3/32θ60	112.5	45.72	0.654	0.655		0.261	2.51	2.51	
t26h0.75R3/64θ60	112.5	45.29	0.707	0.659	0.668	0.385	1.84	1.71	1.74
t26h1.5R3/32θ60	112.5	89.78	0.440	0.439		0.241	1.83	1.82	
t26h1.5R3/64θ60	112.5	89.02	0.497	0.479		0.354	1.40	1.35	
t22h0.75R5/64θ60	103.9	28.02	1.909	1.836		0.987	1.93	1.86	
t22h0.75R1/16θ60	103.9	25.99	1.924	1.963		1.099	1.75	1.79	
t22h1.5R5/64θ60	103.9	53.60	1.652	1.644		0.941	1.76	1.75	
t22h1.5R1/16θ60	103.9	52.07	1.850	1.865		1.047	1.77	1.78	
t22h2R5/64θ60	103.9	70.55	1.203	1.306		0.918	1.31	1.42	
t22h2R1/16θ60	103.9	68.93	1.272	1.330		1.015	1.25	1.31	
t22h3R5/64θ60	103.9	105.86	0.875	0.852		0.353	2.48	2.41	
t22h3R1/16θ60	103.9	103.44	0.948	0.908		0.393	2.41	2.31	
t22h4.5R5/64θ60	103.9	156.93	0.659	0.687		0.329	2.00	2.09	
t22h4.5R1/16θ60	103.9	155.53	0.728	0.744		0.364	2.00	2.04	
t22h6R5/64θ60	103.9	208.19	0.549	0.558		0.303	1.81	1.84	
t22h6R1/16θ60	103.9	206.73	0.603	0.592		0.334	1.80	1.77	
t22h1.5R1/8θ90	103.9	50.97	0.819	0.848		0.309	2.65	2.74	
t22h3R1/8θ90	103.9	103.67	0.627	0.621		0.286	2.19	2.17	
t22h4.5R1/8θ90	103.9	155.28	0.498	0.495		0.265	1.88	1.87	
Mean								1.92	
COV								0.196	

Note: 1 kip = 4.448 kN.

Table 5.1.1 Tested Ultimate Load, Calculated Load, and Comparison of the Tested Ultimate Load with the Calculated Load for EOF Loading Condition (Continued)

Specimen	Thickness (in.)	F_y (ksi)	h/t	P_{test} (kips)	$P_{calculated\ kC_t}$ (kips)	$P_{test}/P_{calculated\ kC_t}$
1-HEOF-A11	0.048	58.2	62.0	0.719	0.472	1.52
1-HEOF-A12	0.048	58.2	62.0	0.700	0.472	1.48
1-HEOF-A21	0.048	58.2	79.9	0.694	0.460	1.51
1-HEOF-A22	0.048	58.2	80.3	0.688	0.460	1.50
1-HEOF-A31	0.048	58.2	100.5	0.669	0.447	1.50
1-HEOF-A32	0.048	58.2	100.3	0.643	0.447	1.44
2-HEOF-A11	0.085	88.3	31.9	2.919	1.828	1.60
2-HEOF-A12	0.085	88.3	32.0	2.981	1.896	1.57
2-HEOF-A21	0.085	88.3	43.5	2.994	1.832	1.63
2-HEOF-A22	0.085	88.3	43.5	3.125	1.901	1.64
2-HEOF-A31	0.085	88.3	55.8	2.713	1.803	1.50
2-HEOF-A32	0.085	88.3	55.5	2.825	1.837	1.54
3-HEOF-A11	0.065	113.1	42.6	2.050	1.032	1.99
3-HEOF-A12	0.065	113.1	42.8	2.106	1.114	1.89
3-HEOF-A21	0.065	113.1	58.2	2.006	1.064	1.89
3-HEOF-A22	0.065	113.1	57.8	2.075	1.064	1.95
3-HEOF-A31	0.065	113.1	73.7	1.894	1.015	1.87
3-HEOF-A32	0.065	113.1	73.7	1.869	0.963	1.94
4-HEOF-A11	0.047	141.2	64.2	1.313	0.650	2.02
4-HEOF-A12	0.047	141.2	61.6	1.300	0.548	2.37
4-HEOF-A21	0.047	141.2	83.3	1.219	0.511	2.39
4-HEOF-A22	0.047	141.2	82.9	1.125	0.471	2.39
4-HEOF-A31	0.047	141.2	105.7	1.088	0.534	2.04
4-HEOF-A32	0.047	141.2	105.4	1.063	0.613	1.73
5-HEOF-A11	0.046	165.1	63.9	1.293	0.445	2.91
5-HEOF-A12	0.046	165.1	63.4	1.285	0.445	2.89
5-HEOF-A21	0.046	165.1	86.0	1.200	0.431	2.78
5-HEOF-A11	0.046	165.1	85.4	1.178	0.431	2.73
5-HEOF-A11	0.046	165.1	108.2	1.050	0.417	2.52
5-HEOF-A11	0.046	165.1	107.3	1.035	0.418	2.48
Mean						1.97
COV						0.239

Note: 1 kip = 4.448 kN. 1 ksi = 6.895 MPa. The above test data are from Santaputra and Yu (1986). P_{test} = tested load per web. $P_{calculated\ kC_t}$ = Calculated load per web using the present kC_t in Section 3.4 of the AISI Specification.

Table 5.2.1 Tested Load and Moment, Calculated Load and Moment, Comparison of Tested Load and Moment with Calculated Load and Moment for IOF Loading Condition

Specimen	F_y (ksi)	Average h/t	P_{test} (kips)		M_{test}		$P_{calc,old\ KCI}$ (kips)	$M_{calc,ted\ by}$ (kip-in_	$P_{test}/P_{calc,old\ KCI}$		$M_{test}/M_{calc,ted\ by}$	
			Test 1	Test 2	Test 1	Test 2			Test 1	Test 2	Test 1	Test 2
t26h0.75R3/32θ60	112.5	45.72	1.057	1.071	2.246	2.276	1.037	2.65	1.02	1.03	0.85	0.86
t26h0.75R3/64θ60	112.5	45.29	1.228	1.240	2.610	2.635	1.273	2.36	0.96	0.97	1.11	1.12
t26h1.5R3/32θ60	112.5	89.78	1.351	1.319	3.378	3.298	0.97	5.44	1.39	1.36	0.62	0.61
t26h1.5R3/64θ60	112.5	89.02	1.382	1.361	3.455	3.403	1.185	4.81	1.17	1.15	0.72	0.71
t22h0.75R5/64θ60	103.9	28.02	3.328	3.386	6.656	6.772	3.01	5.51	1.11	1.12	1.21	1.23
t22h0.75R1/16θ60	103.9	25.99	3.179	3.255	6.358	6.510	3.13	4.86	1.02	1.04	1.31	1.34
t22h1.5R5/64θ60	103.9	53.60	3.735	3.599	9.338	8.998	2.89	12.52	1.29	1.25	0.75	0.72
t22h1.5R1/16θ60	103.9	52.07	3.830	3.778	9.575	9.445	3.004	11.83	1.27	1.26	0.81	0.80
t22h2R5/64θ60	103.9	70.55	3.538	3.501	10.172	10.065	2.835	18.93	1.25	1.23	0.54	0.53
t22h2R1/16θ60	103.9	68.93	3.710	3.799	10.666	10.922	2.928	17.17	1.27	1.30	0.62	0.64
t22h3R5/64θ60	103.9	105.86	1.831	1.773	6.866	6.649	1.337	14.02	1.37	1.33	0.49	0.47
t22h3R1/16θ60	103.9	103.44	1.816	1.869	6.810	7.009	1.391	13.51	1.31	1.34	0.50	0.52
t22h4.5R5/64θ60	103.9	156.93	1.648	1.645	8.034	8.019	1.235	20.56	1.33	1.33	0.69	0.39
t22h4.5R1/16θ60	103.9	155.53	1.693	1.694	8.253	8.258	1.279	19.9	1.32	1.32	0.41	0.41
t22h6R5/64θ60	103.9	208.19	1.523	1.545	8.948	9.077	1.131	27.36	1.35	1.37	0.33	0.33
t22h6R1/16θ60	103.9	206.73	1.645	1.685	9.664	9.899	1.164	26.25	1.41	1.45	0.37	0.38
t22h1.5R1/8θ90	103.9	50.97	1.686	1.693	4.426	4.444	1.554	8.13	1.08	1.09	0.54	0.55
t22h3R1/8θ90	103.9	103.67	1.793	1.837	6.500	6.659	1.433	18.16	1.25	1.28	0.36	0.37
t22h4.5R1/8θ90	103.9	155.28	1.818	1.698	8.863	8.278	1.315	25.95	1.38	1.29	0.34	0.32

Note: 1 kip = 4.448 kN, 1 inch = 25.4 mm.

Table 5.2.1 Tested Ultimate Load, Calculated Load, and Comparison of the Tested Load and Moment with the Calculated Load and Moment for IOF Loading Condition (Continued)

Specimen	Thickness (in.)	F_y (ksi)	h/t	P_{test} (kips)	M_{test} (k-in.)	$P_{calc,old\ kC_1}$ (kips)	$M_{cal,test\ Fy}$ (k-in.)	$P_{test}/P_{calc,old\ kC_1}$	$M_{test}/M_{cal,test\ Fy}$
1-HIOF-A11	0.048	58.2	63.6	1.425	13.54	1.645	27.24	0.87	0.50
1-HIOF-A12	0.048	58.2	63.4	1.400	13.3	1.646	27.06	0.85	0.49
1-HIOF-A21	0.048	58.2	83.0	1.465	16.12	1.557	41.90	0.94	0.39
1-HIOF-A22	0.048	58.2	82.8	1.465	16.12	1.496	41.85	0.98	0.39
1-HIOF-A31	0.048	58.2	102.0	1.450	18.13	1.531	58.49	0.95	0.31
1-HIOF-A32	0.048	58.2	102.2	1.500	18.75	1.510	58.67	0.99	0.32
2-HIOF-A11	0.082	88.3	35.1	5.400	51.30	6.210	69.90	0.87	0.73
2-HIOF-A12	0.082	88.3	35.4	5.365	5097	6.090	70.94	0.88	0.72
2-HIOF-A21	0.082	88.3	47.4	5.740	63.14	5.985	109.94	0.96	0.57
2-HIOF-A22	0.082	88.3	47.5	5.700	62.70	5.984	110.26	0.95	0.57
2-HIOF-A31	0.082	88.3	59.7	6.265	78.31	5.914	155.02	1.06	0.51
2-HIOF-A32	0.082	88.3	59.8	6.375	79.69	5.913	155.52	1.08	0.51
3-HIOF-A11	0.062	113.1	47.7	4.290	40.76	3.492	57.87	1.23	0.70
3-HIOF-A12	0.062	113.1	47.8	4.300	40.85	3.612	57.56	1.19	0.71
3-HIOF-A21	0.062	113.1	63.2	4.290	47.19	3.531	87.93	1.21	0.54
3-HIOF-A22	0.062	113.1	63.3	4.265	46.92	3.560	88.27	1.20	0.53
3-HIOF-A31	0.062	113.1	79.3	4.325	54.06	3.561	122.22	1.21	0.44
3-HIOF-A32	0.062	113.1	78.8	4.350	54.38	3.419	123.89	1.27	0.44
4-HIOF-A11	0.047	141.2	64.2	2.720	25.84	2.262	45.69	1.20	0.57
4-HIOF-A12	0.047	141.2	64.6	2.600	24.70	2.308	45.82	1.13	0.54
4-HIOF-A21	0.047	141.2	86.5	2.725	29.98	2.048	66.25	1.33	0.45
4-HIOF-A22	0.047	141.2	87.1	2.740	30.14	2.069	66.24	1.32	0.46
4-HIOF-A31	0.047	141.2	107.8	2.700	33.75	2.091	79.14	1.29	0.43
4-HIOF-A32	0.047	141.2	107.8	2.630	32.88	2.069	79.64	1.27	0.41
4-HIOF-A13	0.047	141.2	61.0	2.490	23.66	1.772	44.38	1.41	0.53
4-HIOF-A14	0.047	141.2	61.0	2.475	23.51	1.772	44.35	1.40	0.53
4-HIOF-A23	0.047	141.2	82.3	2.625	27.56	1.715	68.83	1.53	0.40
4-HIOF-A24	0.047	141.2	82.5	2.665	27.98	1.715	69.05	1.55	0.41
4-HIOF-A33	0.047	141.2	102.9	2.575	32.19	1.660	85.65	1.55	0.38
4-HIOF-A34	0.047	141.2	102.9	2.610	32.63	1.660	86.69	1.57	0.38
5-HIOF-A11	0.046	165.1	63.2	2.365	22.47	1.684	49.60	1.40	0.45
5-HIOF-A12	0.046	165.1	63.2	2.325	22.09	1.685	49.44	1.38	0.45
5-HIOF-A21	0.046	165.1	85.4	2.500	27.50	1.628	73.41	1.54	0.38
5-HIOF-A22	0.046	165.1	85.0	2.535	27.89	1.629	72.93	1.56	0.38
5-HIOF-A31	0.046	165.1	106.5	2.465	30.81	1.574	91.14	1.57	0.34
5-HIOF-A32	0.046	165.1	107.1	2.435	30.44	1.573	91.76	1.55	0.33

Note: 1 kip = 4.448 kN. 1 ksi = 6.895 MPa. The above test data are from Santaputra and Yu (1986). P_{test} = tested load per web. $P_{cal,old\ kC_1}$ = Calculated load per web using the present kC_1 in Section 3.4 of the AISI Specification. M_{test}=Tested Moment for entire section. $M_{cal,test\ Fy}$=Calculated moment using the yield strength reduction factor for entire section.

Table 5.3.1 Tested Ultimate Load, Calculated Load, and Comparison of the Tested Ultimate Load with the Calculated Load for ETF Loading Condition

Specimen	F_y (ksi)	Average h/t	P_{test} (kips)			$P_{calc,old\ KC3}$ (kips)	$P_{test}/P_{calc,old\ KC3}$		
			Test 1	Test 2	Test 3		Test 1	Test 2	Test 3
t26h0.75R3/32θ60	112.5	45.72	0.611	0.590		0.225	2.72	2.62	
t26h0.75R3/64θ60	112.5	45.29	0.676	0.673		0.331	2.04	2.03	
t26h1.5R3/32θ60	112.5	89.78	0.498	0.559	0.511	0.199	2.50	2.81	2.57
t26h1.5R3/64θ60	112.5	89.02	0.571	0.567		0.292	1.96	1.94	
t22h0.75R5/64θ60	103.9	28.02	1.979	2.064	2.014	0.862	2.30	2.39	2.34
t22h0.75R1/16θ60	103.9	25.99	1.999	2.072		0.961	2.08	2.16	
t22h1.5R5/64θ60	103.9	53.60	1.553	1.614		0.804	1.93	2.01	
t22h1.5R1/16θ60	103.9	52.07	1.854	1.729		0.895	2.07	1.93	
t22h2R5/64θ60	103.9	70.55	1.306	1.426		0.772	1.69	1.85	
t22h2R1/16θ60	103.9	68.93	1.450	1.561		0.855	1.70	1.83	
t22h3R5/64θ60	103.9	105.86	0.593	0.639		0.346	1.71	1.85	
t22h3R1/16θ60	103.9	103.44	0.618	0.622		0.387	1.60	1.61	
t22h4.5R5/64θ60	103.9	156.93	0.444	0.467		0.293	1.52	1.59	
t22h4.5R1/16θ60	103.9	155.53	0.592	0.466	0.452	0.325	1.82	1.43	1.39
t22h6R5/64θ60	103.9	208.19	0.376	0.369		0.239	1.57	1.54	
t22h6R1/16θ60	103.9	206.73	0.478	0.376	0.366	0.264	1.81	1.42	1.39
Mean							1.94		
COV							0.201		

Note: 1 kip = 4.448 kN.

Table 5.3.1 Tested Ultimate Load, Calculated Load, and Comparison of the Tested Ultimate Load with the Calculated Load for ETF Loading Condition (Continued)

Specimen	Thickness (in.)	F_y (ksi)	h/t	P_{test} (kips)	$P_{cal,old\ kC_3}$ (kips)	$P_{test}/P_{cal,old\ kC_3}$
1-HETF-A11	0.047	58.2	62.5	0.725	0.476	1.52
1-HETF-A12	0.047	58.2	62.9	0.713	0.476	1.50
1-HETF-A21	0.047	58.2	83.7	0.725	0.448	1.62
1-HETF-A22	0.047	58.2	84.2	0.725	0.448	1.62
1-HETF-A31	0.047	58.2	105.0	0.650	0.420	1.55
1-HETF-A32	0.047	58.2	105.0	0.662	0.420	1.57
2-HETF-A11	0.088	77.1	32.1	0.825	2.082	1.36
2-HETF-A12	0.088	77.1	32.1	2.787	2.082	1.34
2-HETF-A21	0.088	77.1	43.5	2.700	2.022	1.34
2-HETF-A22	0.088	77.1	43.5	2.650	2.022	1.31
2-HETF-A31	0.088	77.1	55.2	2.425	1.960	1.24
2-HETF-A32	0.088	77.1	55.0	2.400	1.960	1.22
3-HETF-A11	0.065	116.9	44.5	1.525	0.928	1.64
3-HETF-A12	0.065	116.9	44.6	1.600	0.928	1.72
3-HETF-A21	0.065	116.9	60.0	1.413	0.890	1.59
3-HETF-A22	0.065	116.9	59.8	1.487	0.891	1.67
3-HETF-A31	0.065	116.9	76.2	1.300	0.851	1.53
3-HETF-A32	0.065	116.9	75.8	1.312	0.852	1.54
5-HETF-A11	0.046	165.1	63.9	0.750	0.464	1.61
5-HETF-A12	0.046	165.1	63.7	0.762	0.465	1.64
5-HETF-A21	0.046	165.1	86.0	0.675	0.436	1.55
5-HETF-A22	0.046	165.1	86.0	0.700	0.436	1.61
5-HETF-A31	0.046	165.1	106.9	0.612	0.409	1.50
5-HETF-A32	0.046	165.1	106.7	0.600	0.410	1.47
Mean						1.51
COV						0.092

Note: 1 kip = 4.448 kN. 1 ksi = 6.895 MPa. The above test data are from Santaputra and Yu (1986). P_{test} = tested load per web. $P_{cal,old\ kC_3}$ = Calculated load per web using the present kC_3 in Section 3.4 of the AISI Specification.

Table 5.4.1 Tested Ultimate Load, Calculated Load, and Comparison of the Tested Ultimate Load with the Calculated Load for ITF Loading Condition

Specimen	F_y (ksi)	Average h/t	P_{test} (kips)				$P_{calc,old\ KCI}$ (kips)	$P_{test}/P_{calc,old\ KCI}$			
			Test 1	Test 2	Test 3	Test 4		Test 1	Test 2	Test 3	Test 4
t26h0.75R3/32θ60	112.5	45.72	1.642	1.927	1.870	1.869	0.89	1.84	2.17	2.10	2.10
t26h0.75R3/64θ60	112.5	45.29	2.179	2.154			1.093	1.99	1.97		
t26h1.5R3/32θ60	112.5	89.78	1.386	1.406			0.757	1.83	1.86		
t26h1.5R3/64θ60	112.5	89.02	1.496	1.500			0.927	1.61	1.62		
t22h0.75R5/64θ60	103.9	28.02	5.928	5.468	5.590		3.226	1.84	1.69	1.73	
t22h0.75R1/16θ60	103.9	25.99	5.858	5.688			3.367	1.74	1.69		
t22h1.5R5/64θ60	103.9	53.60	4.488	4.719			2.954	1.52	1.60		
t22h1.5R1/16θ60	103.9	52.07	4.483	4.445			3.079	1.46	1.44		
t22h2R5/64θ60	103.9	70.55	3.900	4.188			2.798	1.39	1.50		
t22h2R1/16θ60	103.9	68.93	4.366	4.224			2.899	1.51	1.46		
t22h3R5/64θ60	103.9	105.86	1.769	1.743			1.213	1.46	1.44		
t22h3R1/16θ60	103.9	103.44	1.871	1.886			1.27	1.47	1.49		
t22h4.5R5/64θ60	103.9	156.93	1.500	1.561			0.957	1.57	1.63		
t22h4.5R1/16θ60	103.9	155.53	1.569	1.451			0.995	1.58	1.46		
t22h6R5/64θ60	103.9	208.19	1.295	1.236			0.696	1.86	1.78		
t22h6R1/16θ60	103.9	206.73	1.204	1.156			0.722	1.67	1.60		
Mean								1.68			
COV								0.124			

Note: 1 kip = 4.448 kN. 1 ksi = 6.895 MPa.

Table 5.4.1 Tested Ultimate Load, Calculated Load, and Comparison of the Tested Ultimate Load with the Calculated Load for ITF Loading Condition (Continued)

Specimen	Thickness (in.)	F_y (ksi)	h/t	P_{test} (kips)	$P_{calc,old\ kC_1}$ (kips)	$P_{test}/P_{calc,old\ kC_1}$
1-HITF-A11	0.047	58.2	61.8	1.650	1.772	0.93
1-HITF-A12	0.047	58.2	61.8	1.625	1.772	0.92
1-HITF-A21	0.047	58.2	83.1	1.650	1.638	1.01
1-HITF-A22	0.047	58.2	83.3	1.625	1.636	0.99
1-HITF-A31	0.047	58.2	105.7	1.600	1.495	1.07
1-HITF-A32	0.047	58.2	105.4	1.625	1.496	1.09
2-HITF-A11	0.088	77.1	32.1	6.875	8.177	0.84
2-HITF-A12	0.088	77.1	32.1	6.900	8.177	0.84
2-HITF-A21	0.088	77.1	43.6	6.875	7.874	0.87
2-HITF-A22	0.088	77.1	43.8	6.800	7.868	0.86
2-HITF-A31	0.088	77.1	55.5	6.875	7.559	0.91
2-HITF-A32	0.088	77.1	55.4	6.900	7.562	0.91
3-HITF-A11	0.065	116.9	44.9	5.050	4.129	1.22
3-HITF-A12	0.065	116.9	44.5	5.150	4.136	1.25
3-HITF-A21	0.065	116.9	59.5	4.850	3.926	1.24
3-HITF-A22	0.065	116.9	59.5	4.800	3.926	1.22
3-HITF-A31	0.065	116.9	75.4	4.800	3.706	1.30
3-HITF-A32	0.065	116.9	75.4	4.700	3.706	1.27
5-HITF-A11	0.046	165.1	64.3	2.950	1.942	1.52
5-HITF-A12	0.046	165.1	64.3	3.000	1.942	1.54
5-HITF-A21	0.046	165.1	84.5	2.775	1.800	1.54
5-HITF-A22	0.046	165.1	85.0	2.750	1.797	1.53
5-HITF-A31	0.046	165.1	108.2	2.625	1.635	1.61
5-HITF-A32	0.046	165.1	108.7	2.613	1.632	1.60
Mean						1.17
COV						0.231

Note: 1 kip = 4.448 kN. 1 ksi = 6.895 MPa. The above test data are from Santaputra and Yu (1986). P_{test} = tested load per web. $P_{cal,old\ kC_1}$ = Calculated load per web using the present kC_1 in Section 3.4 of the AISI Specification.

Table 6.2.1 Tested Ultimate Load, Calculated Load, and Comparison of the Tested Ultimate Load with the Calculated Load for EOF Loading Condition

Specimen	F_y (ksi)	Average h/t	P_{test} (kips)			$P_{calc,new\ kC3}$ (kips)	$P_{test}/P_{calc,new\ kC3}$		
			Test 1	Test 2	Test 3		Test 1	Test 2	Test 3
t26h0.75R3/32θ60	112.5	45.72	0.654	0.655		0.351	1.87	1.87	
t26h0.75R3/64θ60	112.5	45.29	0.707	0.659	0.668	0.517	1.37	1.27	1.29
t26h1.5R3/32θ60	112.5	89.78	0.440	0.439		0.324	1.36	1.35	
t26h1.5R3/64θ60	112.5	89.02	0.497	0.479		0.476	1.04	1.01	
t22h0.75R5/64θ60	103.9	28.02	1.909	1.836		1.326	1.44	1.38	
t22h0.75R1/16θ60	103.9	25.99	1.924	1.963		1.476	1.30	1.33	
t22h1.5R5/64θ60	103.9	53.60	1.652	1.644		1.264	1.31	1.30	
t22h1.5R1/16θ60	103.9	52.07	1.850	1.865		1.406	1.32	1.33	
t22h2R5/64θ60	103.9	70.55	1.203	1.306		1.233	0.98	1.06	
t22h2R1/16θ60	103.9	68.93	1.272	1.330		1.363	0.93	0.98	
t22h3R5/64θ60	103.9	105.86	0.875	0.852		0.474	1.85	1.80	
t22h3R1/16θ60	103.9	103.44	0.948	0.908		0.528	1.79	1.72	
t22h4.5R5/64θ60	103.9	156.93	0.659	0.687		0.442	1.49	1.55	
t22h4.5R1/16θ60	103.9	155.53	0.728	0.744		0.489	1.49	1.52	
t22h6R5/64θ60	103.9	208.19	0.549	0.558		0.407	1.35	1.37	
t22h6R1/16θ60	103.9	206.73	0.603	0.592		0.449	1.34	1.32	
t22h1.5R1/8θ90	103.9	50.97	0.819	0.848		0.415	1.97	2.04	
t22h3R1/8θ90	103.9	103.67	0.627	0.621		0.384	1.63	1.62	
t22h4.5R1/8θ90	103.9	155.28	0.498	0.495		0.356	1.40	1.39	
Mean								1.43	
COV								0.196	

Note: 1 kip = 4.448 kN.

Table 6.2.1 Tested Ultimate Load, Calculated Load, and Comparison of the Tested Ultimate Load with the Calculated Load for EOF Loading Condition (Continued)

Specimen	Thickness (in.)	F_y (ksi)	h/t	P_{test} (kips)	$P_{cal,new\ kC_t}$ (kips)	$P_{test}/P_{cal,new\ kC_t}$
1-HEOF-A11	0.048	58.2	62.0	0.719	0.535	1.34
1-HEOF-A12	0.048	58.2	62.0	0.700	0.535	1.31
1-HEOF-A21	0.048	58.2	79.9	0.694	0.521	1.33
1-HEOF-A22	0.048	58.2	80.3	0.688	0.521	1.32
1-HEOF-A31	0.048	58.2	100.5	0.669	0.506	1.32
1-HEOF-A32	0.048	58.2	100.3	0.643	0.506	1.27
2-HEOF-A11	0.085	88.3	31.9	2.919	2.427	1.20
2-HEOF-A12	0.085	88.3	32.0	2.981	2.517	1.18
2-HEOF-A21	0.085	88.3	43.5	2.994	2.435	1.23
2-HEOF-A22	0.085	88.3	43.5	3.125	2.524	1.24
2-HEOF-A31	0.085	88.3	55.8	2.713	2.394	1.13
2-HEOF-A32	0.085	88.3	55.5	2.825	2.439	1.16
3-HEOF-A11	0.065	113.1	42.6	2.050	1.386	1.48
3-HEOF-A12	0.065	113.1	42.8	2.106	1.496	1.41
3-HEOF-A21	0.065	113.1	58.2	2.006	1.429	1.40
3-HEOF-A22	0.065	113.1	57.8	2.075	1.429	1.45
3-HEOF-A31	0.065	113.1	73.7	1.894	1.363	1.39
3-HEOF-A32	0.065	113.1	73.7	1.869	1.294	1.44
4-HEOF-A11	0.047	141.2	64.2	1.313	0.873	1.50
4-HEOF-A12	0.047	141.2	61.6	1.300	0.736	1.77
4-HEOF-A21	0.047	141.2	83.3	1.219	0.686	1.78
4-HEOF-A22	0.047	141.2	82.9	1.125	0.633	1.78
4-HEOF-A31	0.047	141.2	105.7	1.088	0.717	1.52
4-HEOF-A32	0.047	141.2	105.4	1.063	0.823	1.29
5-HEOF-A11	0.046	165.1	63.9	1.293	0.598	2.17
5-HEOF-A12	0.046	165.1	63.4	1.285	0.598	2.15
5-HEOF-A21	0.046	165.1	86.0	1.200	0.579	2.07
5-HEOF-A11	0.046	165.1	85.4	1.178	0.579	2.03
5-HEOF-A11	0.046	165.1	108.2	1.050	0.560	1.87
5-HEOF-A11	0.046	165.1	107.3	1.035	0.561	1.84
Mean						1.51
COV						0.207

Note: 1 kip = 4.448 kN. 1 ksi = 6.895 MPa. The above test data are from Santaputra and Yu (1986). P_{test} = tested load per web. $P_{cal,new\ kC_t}$ = Calculated load per web using the new modified kC_t.

Table 6.2.2 Tested Load and Moment, Calculated Load and Moment, Comparison of Tested Load and Moment with Calculated Load and Moment for IOF Loading Condition

Specimen	F_y (ksi)	Average h/t	P_{test} (kips)		M_{test}		$P_{calc,new\ KCI}$ (kips)	$M_{calc,ted\ Fy}$ (kip-in)	$P_{test}/P_{calc,new\ KCI}$		$M_{test}/M_{calc,ted\ Fy}$	
			Test 1	Test 2	Test 1	Test 2			Test 1	Test 2	Test 1	Test 2
t26h0.75R3/32θ60	112.5	45.72	1.057	1.071	2.246	2.276	1.436	2.65	0.74	0.75	0.85	0.86
t26h0.75R3/64θ60	112.5	45.29	1.228	1.240	2.610	2.635	1.763	2.36	0.70	0.70	1.11	1.12
t26h1.5R3/32θ60	112.5	89.78	1.351	1.319	3.378	3.298	1.343	5.44	1.01	0.98	0.62	0.61
t26h1.5R3/64θ60	112.5	89.02	1.382	1.361	3.455	3.403	1.641	4.81	0.84	0.83	0.72	0.71
t22h0.75R5/64θ60	103.9	28.02	3.328	3.386	6.656	6.772	4.039	5.51	0.82	0.84	1.21	1.23
t22h0.75R1/16θ60	103.9	25.99	3.179	3.255	6.358	6.510	4.200	4.86	0.76	0.77	1.31	1.34
t22h1.5R5/64θ60	103.9	53.60	3.735	3.599	9.338	8.998	3.878	12.52	0.96	0.93	0.75	0.72
t22h1.5R1/16θ60	103.9	52.07	3.830	3.778	9.575	9.445	4.031	11.83	0.95	0.94	0.81	0.80
t22h2R5/64θ60	103.9	70.55	3.538	3.501	10.172	10.065	3.804	18.93	0.93	0.92	0.54	0.53
t22h2R1/16θ60	103.9	68.93	3.710	3.799	10.666	10.922	3.929	17.17	0.94	0.97	0.62	0.64
t22h3R5/64θ60	103.9	105.86	1.831	1.773	6.866	6.649	1.794	14.02	1.02	0.99	0.49	0.47
t22h3R1/16θ60	103.9	103.44	1.816	1.869	6.810	7.009	1.867	13.51	0.97	1.00	0.50	0.52
t22h4.5R5/64θ60	103.9	156.93	1.648	1.645	8.034	8.019	1.657	20.56	0.99	0.99	0.69	0.39
t22h4.5R1/16θ60	103.9	155.53	1.693	1.694	8.253	8.258	1.716	19.9	0.99	0.99	0.41	0.41
t22h6R5/64θ60	103.9	208.19	1.523	1.545	8.948	9.077	1.516	27.36	1.00	1.02	0.33	0.33
t22h6R1/16θ60	103.9	206.73	1.645	1.685	9.664	9.899	1.562	26.25	1.05	1.08	0.37	0.38
t22h1.5R1/8θ90	103.9	50.97	1.686	1.693	4.426	4.444	2.085	8.13	0.81	0.81	0.54	0.55
t22h3R1/8θ90	103.9	103.67	1.793	1.837	6.500	6.659	1.923	18.16	0.93	0.96	0.36	0.37
t22h4.5R1/8θ90	103.9	155.28	1.818	1.698	8.863	8.278	1.765	25.95	1.03	0.96	0.34	0.32

Note: 1 kip = 4.448 kN, 1 inch = 25.4 mm.

Table 6.2.2 Tested Ultimate Load, Calculated Load and Moment, and Comparison of the Tested Load and Moment with the Calculated Load and Moment for IOF Loading Condition (Continued)

Specimen	Thickness (in.)	F_y (ksi)	h/t	P_{test} (kips)	M_{test} (k-in.)	$P_{calc,new\ kC_1}$ (kips)	$M_{calcted\ Fy}$ (k-in.)	$P_{test}/P_{calc,new\ kC_1}$	$M_{test}/M_{calcted\ Fy}$
1-HIOF-A11	0.048	58.2	63.6	1.425	13.54	1.781	27.24	0.80	0.50
1-HIOF-A12	0.048	58.2	63.4	1.400	13.3	1.782	27.06	0.79	0.49
1-HIOF-A21	0.048	58.2	83.0	1.465	16.12	1.686	41.90	0.87	0.39
1-HIOF-A22	0.048	58.2	82.8	1.465	16.12	1.620	41.85	0.90	0.39
1-HIOF-A31	0.048	58.2	102.0	1.450	18.13	1.658	58.49	0.87	0.31
1-HIOF-A32	0.048	58.2	102.2	1.500	18.75	1.635	58.67	0.92	0.32
2-HIOF-A11	0.082	88.3	35.1	5.400	51.30	7.695	69.90	0.70	0.73
2-HIOF-A12	0.082	88.3	35.4	5.365	5097	7.546	70.94	0.71	0.72
2-HIOF-A21	0.082	88.3	47.4	5.740	63.14	7.416	109.94	0.77	0.57
2-HIOF-A22	0.082	88.3	47.5	5.700	62.70	7.415	110.26	0.77	0.57
2-HIOF-A31	0.082	88.3	59.7	6.265	78.31	7.328	155.02	0.85	0.51
2-HIOF-A32	0.082	88.3	59.8	6.375	79.69	7.327	155.52	0.87	0.51
3-HIOF-A11	0.062	113.1	47.7	4.290	40.76	4.844	57.87	0.89	0.70
3-HIOF-A12	0.062	113.1	47.8	4.300	40.85	5.011	57.56	0.86	0.71
3-HIOF-A21	0.062	113.1	63.2	4.290	47.19	4.898	87.93	0.88	0.54
3-HIOF-A22	0.062	113.1	63.3	4.265	46.92	4.939	88.27	0.86	0.53
3-HIOF-A31	0.062	113.1	79.3	4.325	54.06	4.940	122.22	0.88	0.44
3-HIOF-A32	0.062	113.1	78.8	4.350	54.38	4.743	123.89	0.92	0.44
4-HIOF-A11	0.047	141.2	64.2	2.720	25.84	3.284	45.69	0.83	0.57
4-HIOF-A12	0.047	141.2	64.6	2.600	24.70	3.351	45.82	0.78	0.54
4-HIOF-A21	0.047	141.2	86.5	2.725	29.98	2.973	66.25	0.92	0.45
4-HIOF-A22	0.047	141.2	87.1	2.740	30.14	3.004	66.24	0.91	0.46
4-HIOF-A31	0.047	141.2	107.8	2.700	33.75	3.036	79.14	0.89	0.43
4-HIOF-A32	0.047	141.2	107.8	2.630	32.88	3.004	79.64	0.88	0.41
4-HIOF-A13	0.047	141.2	61.0	2.490	23.66	2.573	44.38	0.97	0.53
4-HIOF-A14	0.047	141.2	61.0	2.475	23.51	2.573	44.35	0.96	0.53
4-HIOF-A23	0.047	141.2	82.3	2.625	27.56	2.490	68.83	1.05	0.40
4-HIOF-A24	0.047	141.2	82.5	2.665	27.98	2.490	69.05	1.07	0.41
4-HIOF-A33	0.047	141.2	102.9	2.575	32.19	2.410	85.65	1.07	0.38
4-HIOF-A34	0.047	141.2	102.9	2.610	32.63	2.410	86.69	1.08	0.38
5-HIOF-A11	0.046	165.1	63.2	2.365	22.47	2.393	49.60	0.99	0.45
5-HIOF-A12	0.046	165.1	63.2	2.325	22.09	2.395	49.44	0.97	0.45
5-HIOF-A21	0.046	165.1	85.4	2.500	27.50	2.265	73.41	1.10	0.38
5-HIOF-A22	0.046	165.1	85.0	2.535	27.89	2.176	72.93	1.16	0.38
5-HIOF-A31	0.046	165.1	106.5	2.465	30.81	2.227	91.14	1.11	0.34
5-HIOF-A32	0.046	165.1	107.1	2.435	30.44	2.197	91.76	1.11	0.33

Note: 1 kip = 4.448 kN. 1 ksi = 6.895 MPa. The above test data are from Santaputra and Yu (1986). P_{test} = tested load per web. $P_{calc,new\ kC_1}$ = Calculated load per web using the new modified kC_1. M_{test}=Tested Moment for entire section. $M_{calcted\ Fy}$=Calculated moment using the yield strength reduction factor for entire section.

Table 6.2.3 Tested Ultimate Load, Calculated Load, and Comparison of the Tested Ultimate Load with the Calculated Load for ETF Loading Condition

Specimen	F_y (ksi)	Average h/t	P_{test} (kips)			$P_{calc,new\ KC3}$ (kips)	$P_{test}/P_{calc,new\ KC3}$		
			Test 1	Test 2	Test 3		Test 1	Test 2	Test 3
t26h0.75R3/32θ60	112.5	45.72	0.611	0.590		0.302	2.02	1.95	
t26h0.75R3/64θ60	112.5	45.29	0.676	0.673		0.445	1.52	1.51	
t26h1.5R3/32θ60	112.5	89.78	0.498	0.559	0.511	0.267	1.86	2.09	1.91
t26h1.5R3/64θ60	112.5	89.02	0.571	0.567		0.392	1.46	1.45	
t22h0.75R5/64θ60	103.9	28.02	1.979	2.064	2.014	1.158	1.71	1.78	1.74
t22h0.75R1/16θ60	103.9	25.99	1.999	2.072		1.291	1.55	1.61	
t22h1.5R5/64θ60	103.9	53.60	1.553	1.614		1.080	1.44	1.49	
t22h1.5R1/16θ60	103.9	52.07	1.854	1.729		1.202	1.54	1.44	
t22h2R5/64θ60	103.9	70.55	1.306	1.426		1.037	1.26	1.38	
t22h2R1/16θ60	103.9	68.93	1.450	1.561		1.149	1.26	1.36	
t22h3R5/64θ60	103.9	105.86	0.593	0.639		0.465	1.28	1.37	
t22h3R1/16θ60	103.9	103.44	0.618	0.622		0.520	1.19	1.20	
t22h4.5R5/64θ60	103.9	156.93	0.444	0.467		0.394	1.13	1.19	
t22h4.5R1/16θ60	103.9	155.53	0.592	0.466	0.452	0.437	1.36	1.07	1.04
t22h6R5/64θ60	103.9	208.19	0.376	0.369		0.321	1.17	1.15	
t22h6R1/16θ60	103.9	206.73	0.478	0.376	0.366	0.355	1.35	1.06	1.03
Mean							1.45		
COV							0.196		

Note: 1 kip = 4.448 kN. 1 ksi = 6.895 MPa.

Table 6.2.3 Tested Ultimate Load, Calculated Load, and Comparison of the Tested Ultimate Load with the Calculated Load for ETF Loading Condition (Continued)

Specimen	Thickness (in.)	F_y (ksi)	h/t	P_{test} (kips)	$P_{cal,new\ kC_3}$ (kips)	$P_{test}/P_{cal,new\ kC_3}$
1-HETF-A11	0.047	58.2	62.5	0.725	0.539	1.34
1-HETF-A12	0.047	58.2	62.9	0.713	0.539	1.32
1-HETF-A21	0.047	58.2	83.7	0.725	0.508	1.43
1-HETF-A22	0.047	58.2	84.2	0.725	0.508	1.43
1-HETF-A31	0.047	58.2	105.0	0.650	0.476	1.37
1-HETF-A32	0.047	58.2	105.0	0.662	0.476	1.39
2-HETF-A11	0.088	77.1	32.1	0.825	2.660	1.06
2-HETF-A12	0.088	77.1	32.1	2.787	2.660	1.05
2-HETF-A21	0.088	77.1	43.5	2.700	2.583	1.05
2-HETF-A22	0.088	77.1	43.5	2.650	2.583	1.05
2-HETF-A31	0.088	77.1	55.2	2.425	2.504	0.97
2-HETF-A32	0.088	77.1	55.0	2.400	2.504	0.96
3-HETF-A11	0.065	116.9	44.5	1.525	1.247	1.22
3-HETF-A12	0.065	116.9	44.6	1.600	1.247	1.28
3-HETF-A21	0.065	116.9	60.0	1.413	1.196	1.18
3-HETF-A22	0.065	116.9	59.8	1.487	1.197	1.24
3-HETF-A31	0.065	116.9	76.2	1.300	1.143	1.14
3-HETF-A32	0.065	116.9	75.8	1.312	1.144	1.15
5-HETF-A11	0.046	165.1	63.9	0.750	0.623	1.20
5-HETF-A12	0.046	165.1	63.7	0.762	0.625	1.22
5-HETF-A21	0.046	165.1	86.0	0.675	0.586	1.15
5-HETF-A22	0.046	165.1	86.0	0.700	0.586	1.20
5-HETF-A31	0.046	165.1	106.9	0.612	0.549	1.11
5-HETF-A32	0.046	165.1	106.7	0.600	0.551	1.09
Mean						1.19
COV						0.116

Note: 1 kip = 4.448 kN. 1 ksi = 6.895 MPa. The above test data are from Santaputra and Yu (1986). P_{test} = tested load per web. $P_{cal,new\ kC_3}$ = Calculated load per web using the new modified kC_3.

Table 6.2.4 Tested Ultimate Load, Calculated Load, and Comparison of the Tested Ultimate Load with the Calculated Load for ITF Loading Condition

Specimen	F_y (ksi)	Average h/t	P_{test} (kips)				$P_{calc,new\ KCI}$ (kips)	$P_{test}/P_{calc,new\ KCI}$			
			Test 1	Test 2	Test 3	Test 4		Test 1	Test 2	Test 3	Test 4
t26h0.75R3/32θ60	112.5	45.72	1.642	1.927	1.870	1.869	1.232	1.33	1.56	1.52	1.52
t26h0.75R3/64θ60	112.5	45.29	2.179	2.154			1.513	1.44	1.42		
t26h1.5R3/32θ60	112.5	89.78	1.386	1.406			1.048	1.32	1.34		
t26h1.5R3/64θ60	112.5	89.02	1.496	1.500			1.284	1.17	1.17		
t22h0.75R5/64θ60	103.9	28.02	5.928	5.468	5.590		4.329	1.37	1.26	1.29	
t22h0.75R1/16θ60	103.9	25.99	5.858	5.688			4.518	1.30	1.26		
t22h1.5R5/64θ60	103.9	53.60	4.488	4.719			3.964	1.13	1.19		
t22h1.5R1/16θ60	103.9	52.07	4.483	4.445			4.132	1.09	1.08		
t22h2R5/64θ60	103.9	70.55	3.900	4.188			3.755	1.04	1.12		
t22h2R1/16θ60	103.9	68.93	4.366	4.224			3.890	1.12	1.09		
t22h3R5/64θ60	103.9	105.86	1.769	1.743			1.628	1.09	1.07		
t22h3R1/16θ60	103.9	103.44	1.871	1.886			1.704	1.10	1.11		
t22h4.5R5/64θ60	103.9	156.93	1.500	1.561			1.284	1.17	1.22		
t22h4.5R1/16θ60	103.9	155.53	1.569	1.451			1.335	1.18	1.09		
t22h6R5/64θ60	103.9	208.19	1.295	1.236			0.934	1.39	1.32		
t22h6R1/16θ60	103.9	206.73	1.204	1.156			0.969	1.24	1.19		
Mean COV								1.24 0.115			

Note: 1 kip = 4.448 kN. 1 ksi = 6.895 MPa.

Table 6.2.4 Tested Ultimate Load, Calculated Load, and Comparison of the Tested Ultimate Load with the Calculated Load for ITF Loading Condition (Continued)

Specimen	Thickness (in.)	F_y (ksi)	h/t	P_{test} (kips)	$P_{cal,new\ kC_t}$ (kips)	$P_{test}/P_{cal,new\ kC_t}$
1-HITF-A11	0.047	58.2	61.8	1.650	1.919	0.86
1-HITF-A12	0.047	58.2	61.8	1.625	1.919	0.85
1-HITF-A21	0.047	58.2	83.1	1.650	1.774	0.93
1-HITF-A22	0.047	58.2	83.3	1.625	1.772	0.92
1-HITF-A31	0.047	58.2	105.7	1.600	1.619	0.99
1-HITF-A32	0.047	58.2	105.4	1.625	1.620	1.00
2-HITF-A11	0.088	77.1	32.1	6.875	9.567	0.72
2-HITF-A12	0.088	77.1	32.1	6.900	9.567	0.72
2-HITF-A21	0.088	77.1	43.6	6.875	9.212	0.75
2-HITF-A22	0.088	77.1	43.8	6.800	9.205	0.74
2-HITF-A31	0.088	77.1	55.5	6.875	8.844	0.78
2-HITF-A32	0.088	77.1	55.4	6.900	8.847	0.78
3-HITF-A11	0.065	116.9	44.9	5.050	5.791	0.87
3-HITF-A12	0.065	116.9	44.5	5.150	5.801	0.89
3-HITF-A21	0.065	116.9	59.5	4.850	5.506	0.88
3-HITF-A22	0.065	116.9	59.5	4.800	5.506	0.87
3-HITF-A31	0.065	116.9	75.4	4.800	5.198	0.92
3-HITF-A32	0.065	116.9	75.4	4.700	5.198	0.90
5-HITF-A11	0.046	165.1	64.3	2.950	2.825	1.04
5-HITF-A12	0.046	165.1	64.3	3.000	2.825	1.06
5-HITF-A21	0.046	165.1	84.5	2.775	2.619	1.06
5-HITF-A22	0.046	165.1	85.0	2.750	2.614	1.05
5-HITF-A31	0.046	165.1	108.2	2.625	2.379	1.10
5-HITF-A32	0.046	165.1	108.7	2.613	2.374	1.10
Mean						1.11
COV						0.187

Note: 1 kip = 4.448 kN. 1 ksi = 6.895 MPa. The above test data are from Santaputra and Yu (1986). P_{test} = tested load per web. $P_{cal,new\ kC_t}$ = Calculated load per web using the new modified kC_t.

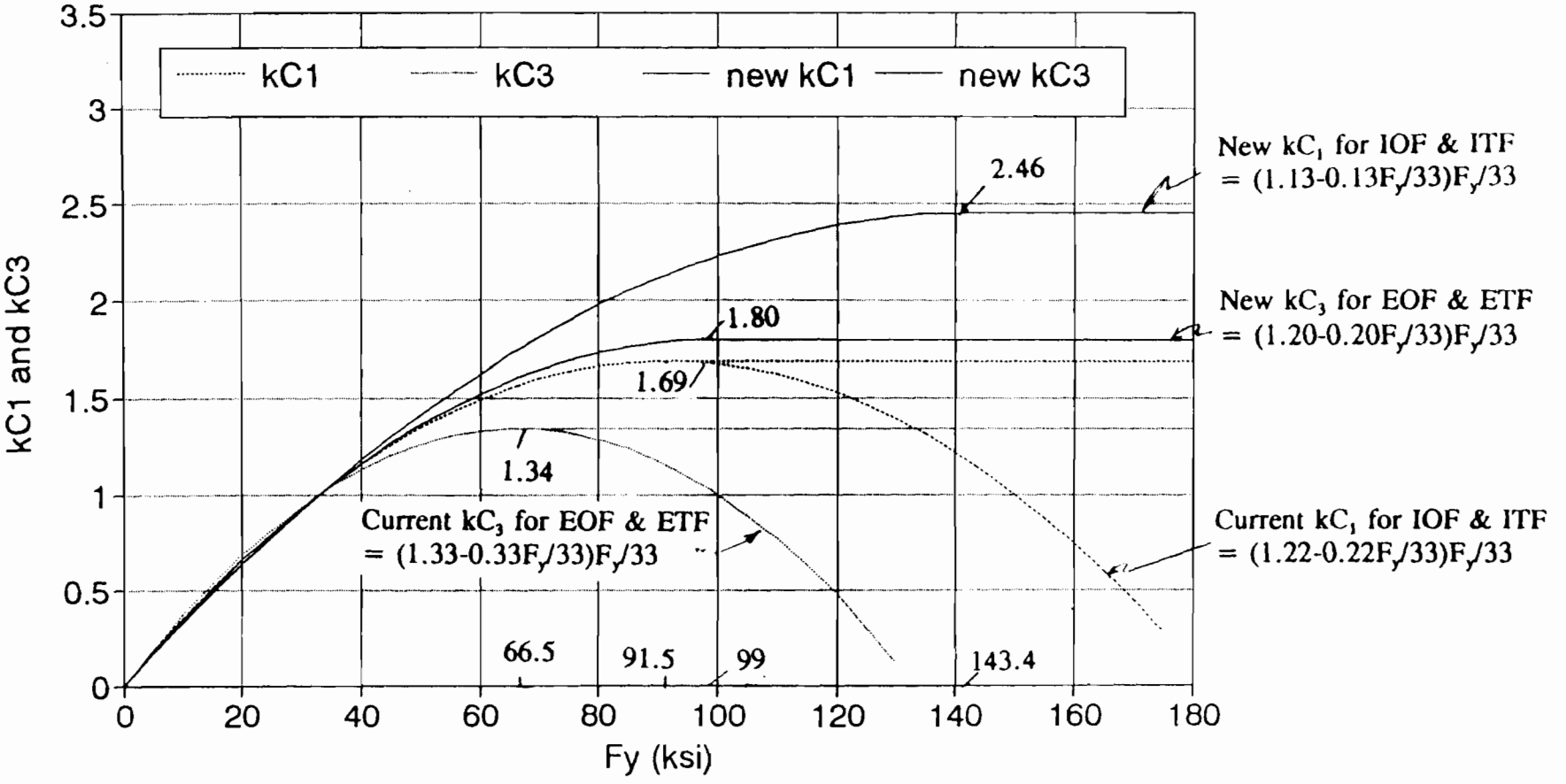

Fig. 2.1 kC_1 and kC_3 Factors vs. F_y

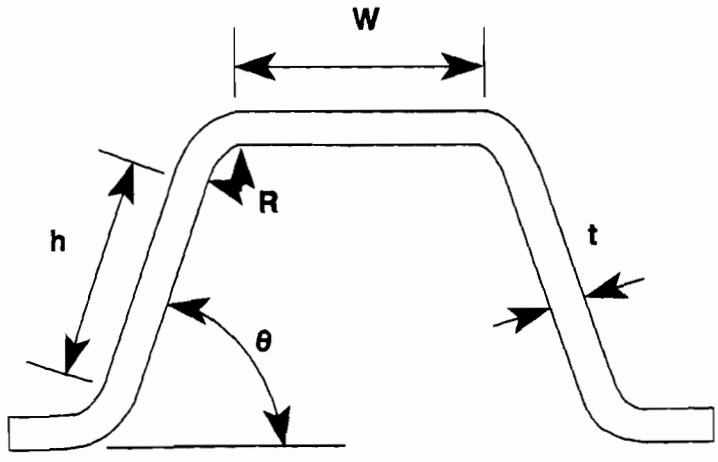

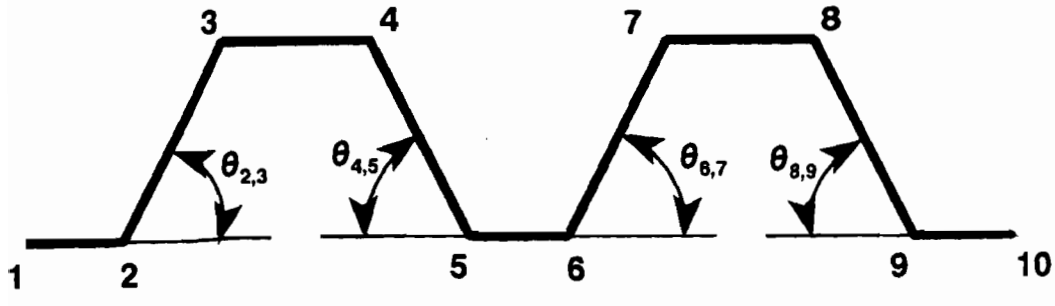

Fig. 3.1.1 Cross Section of Test Specimen

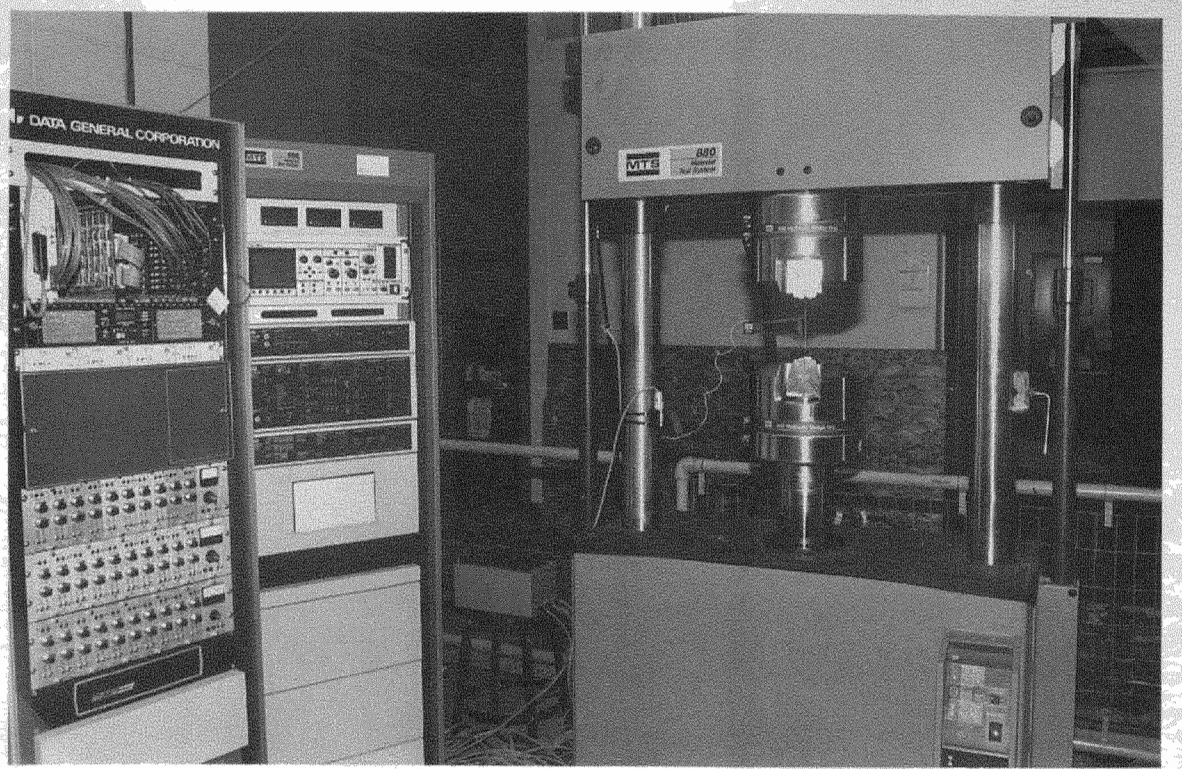

Fig. 4.1.1 MTS Test System

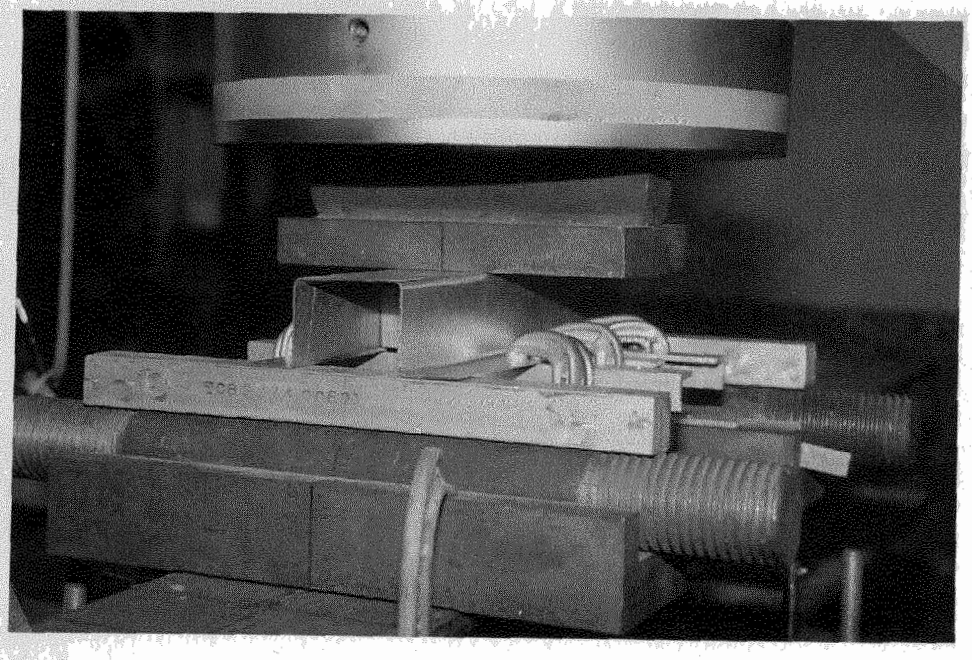

Fig. 4.1.2 Test Setup for EOF Condition

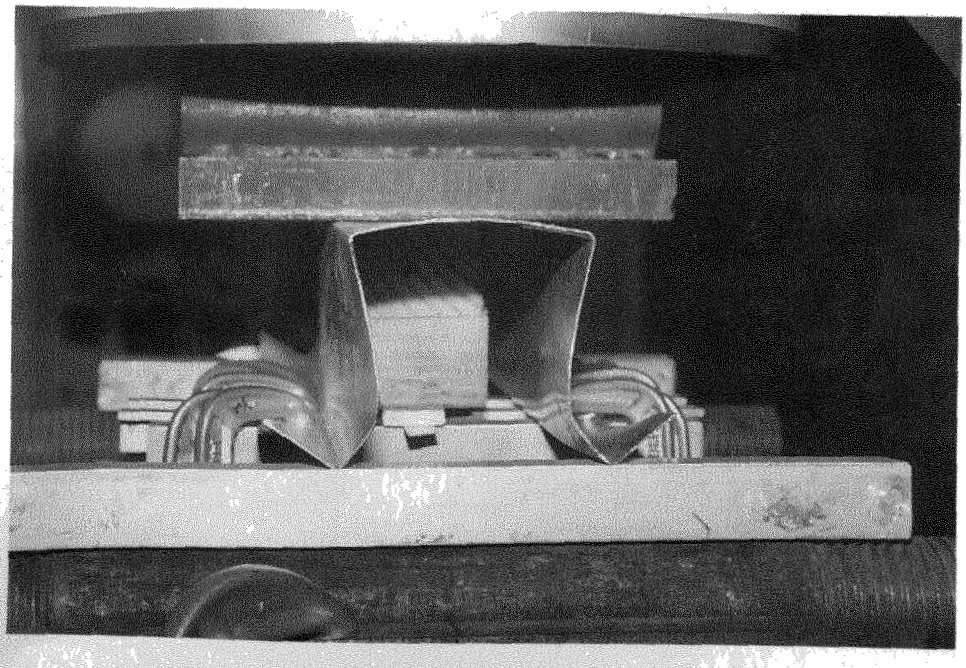

Fig. 4.1.3 Use of Wooden Blocks in EOF Condition

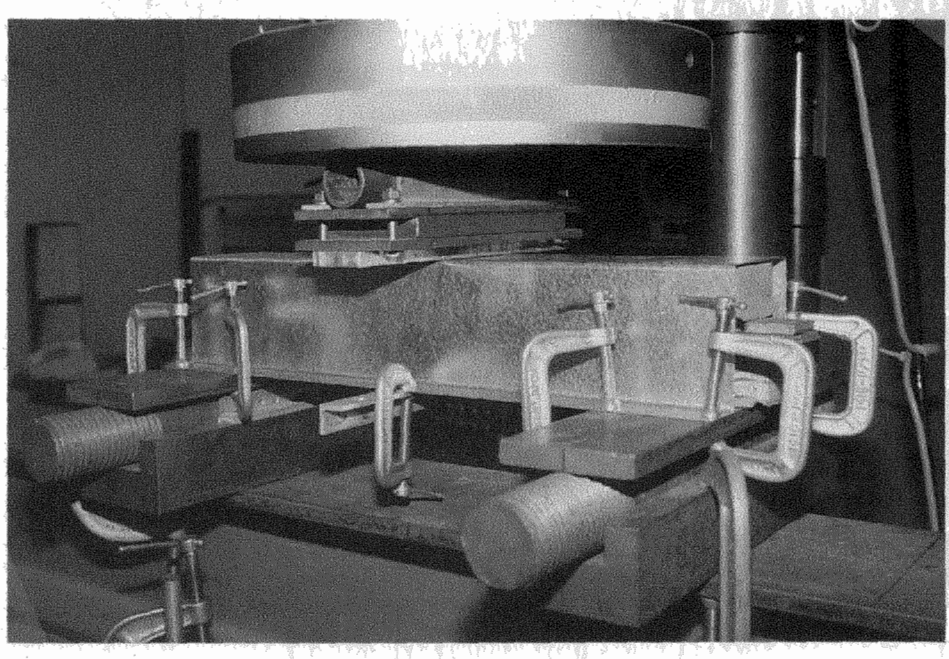

Fig. 4.1.4 Test Setup for IOF Condition

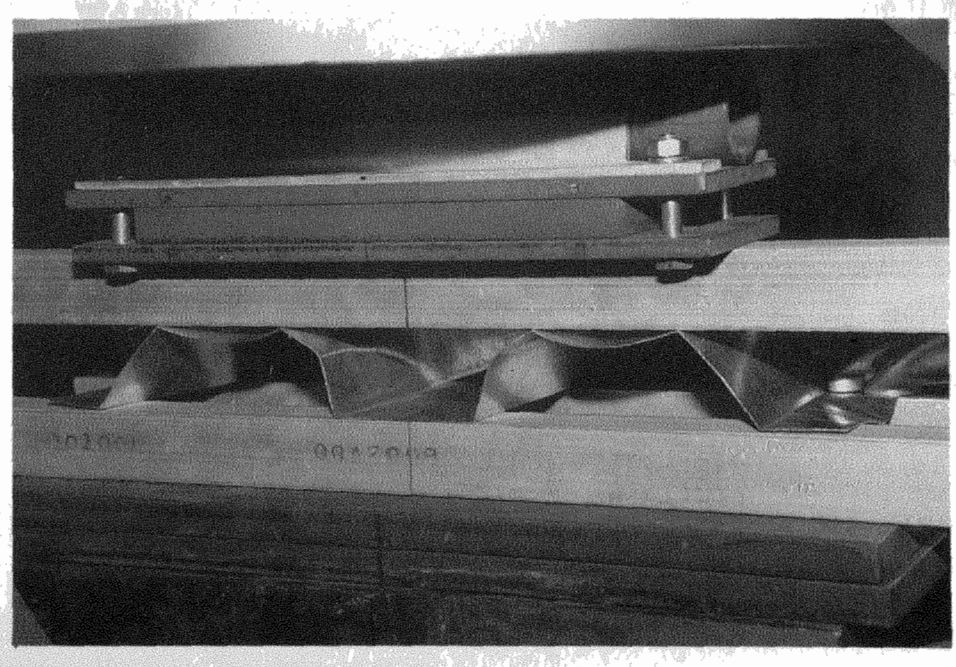

Fig. 4.1.5 Test Setup for ETF Condition (Specimens with Two Ribs)

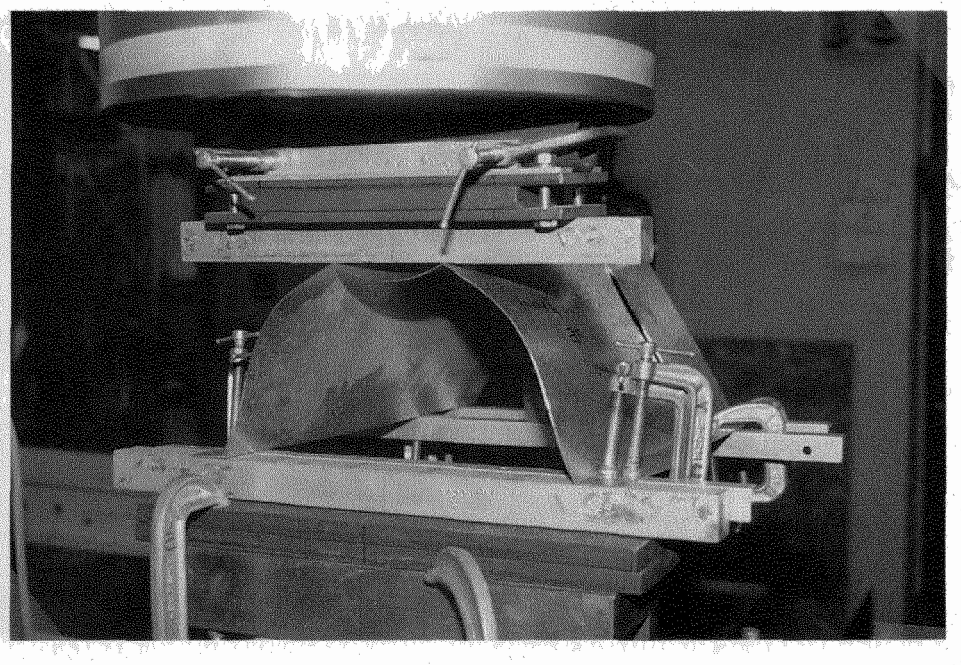

Fig. 4.1.6 Test Setup for ETF Condition (Specimens with One Rib)

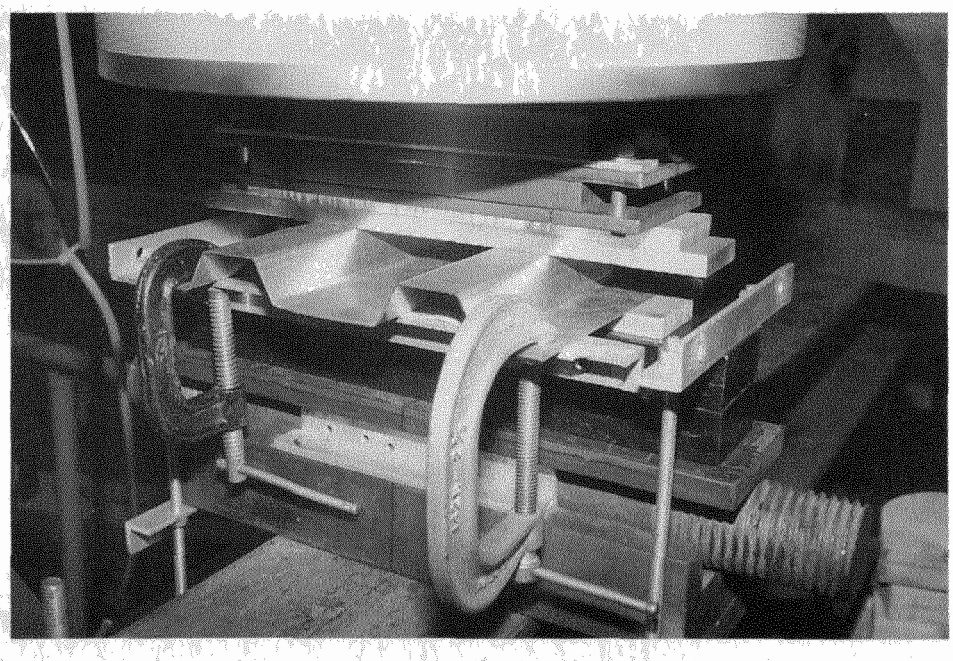

Fig. 4.1.7 Test Setup for ITF Condition

Fig. 4.3.1 Bottom Flange Deformation at End Bearing Plate in EOF Condition

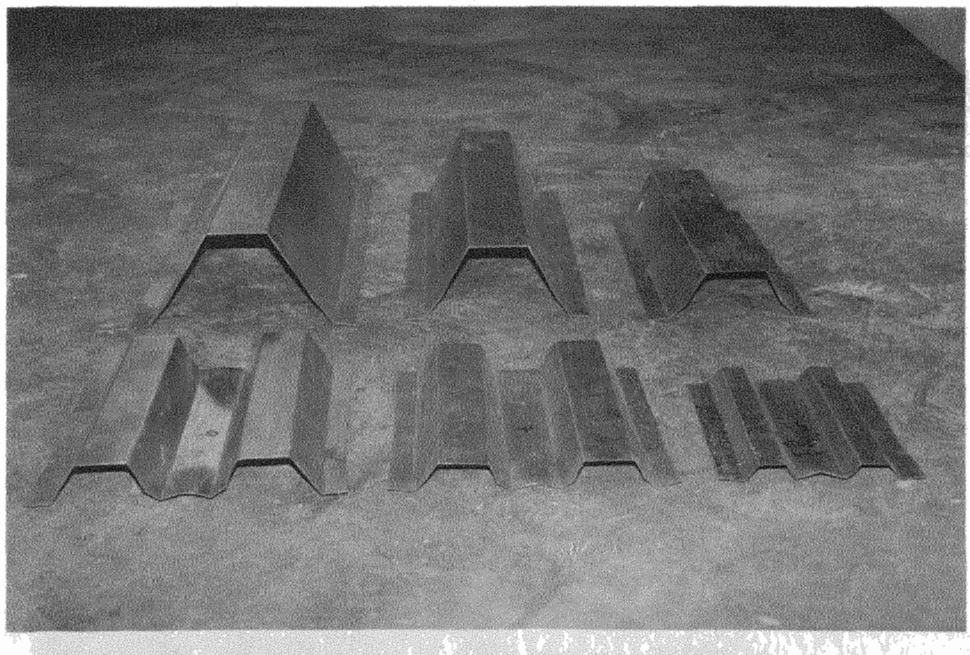

Fig. 4.3.2 Failure of Specimens after Tests in EOF Condition

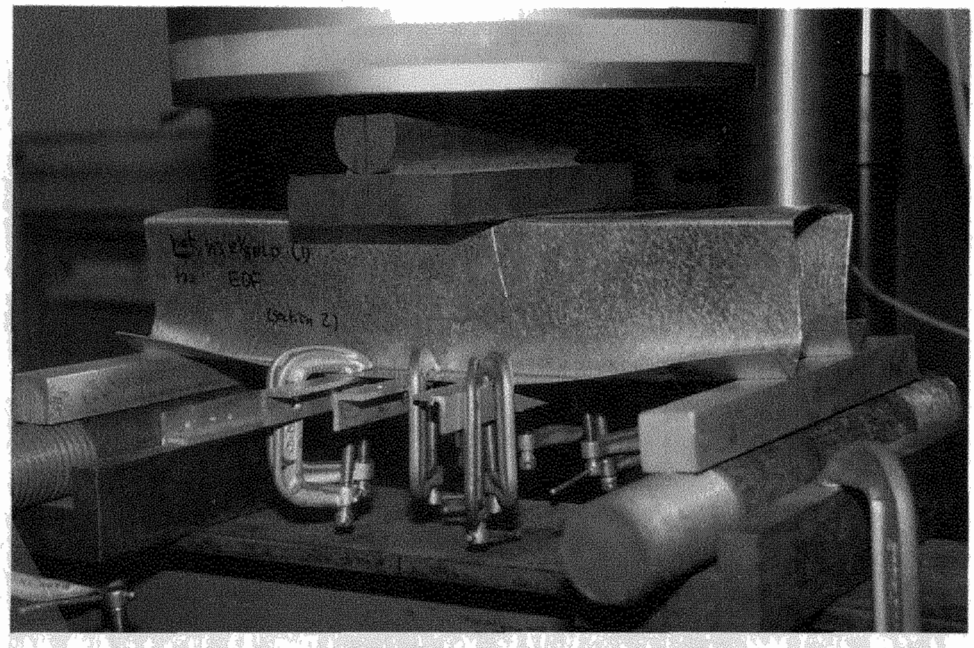

Fig. 4.3.3 Bottom Flange Deformation at End Bearing Plate for Specimen with Vertical Webs in EOF Condition

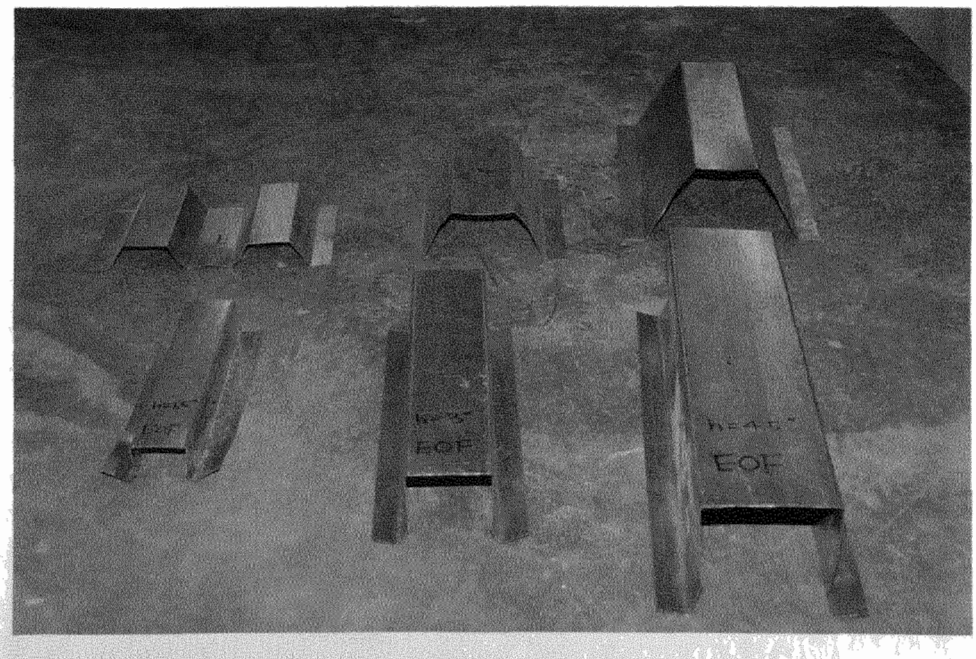

Fig. 4.3.4 Failure of Specimens with Vertical Webs after Tests in EOF Condition

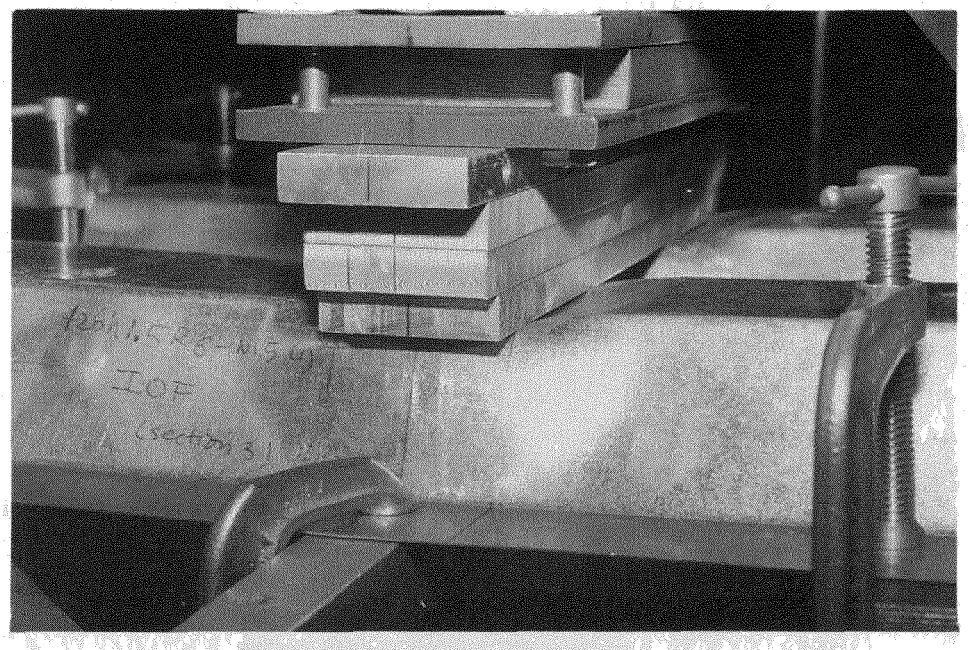

Fig. 4.4.1 Local Deformation at Applied Load for Specimen in IOF Condition

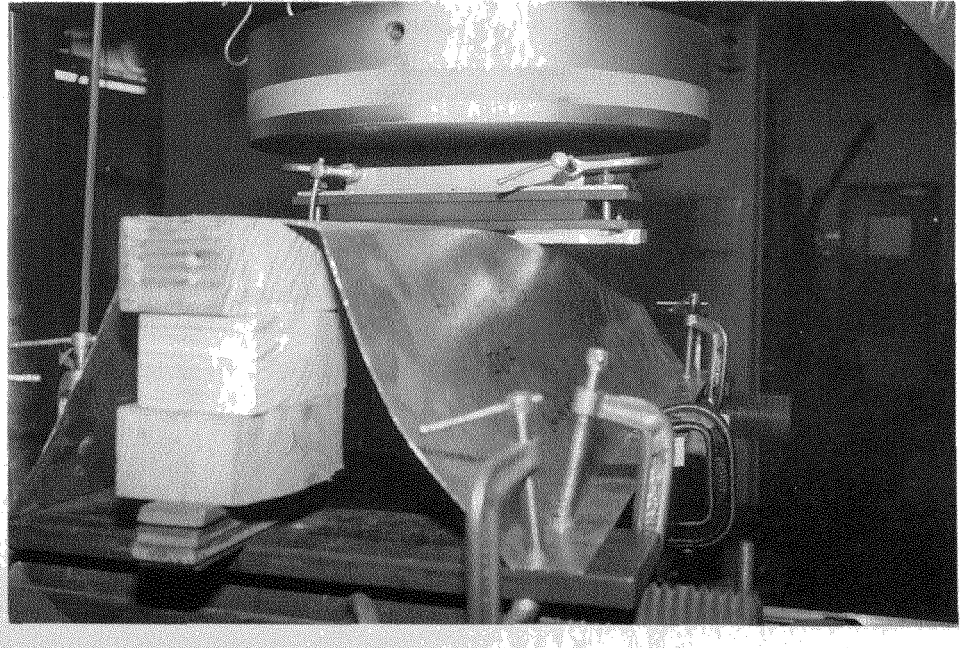

Fig. 4.4.2 Deformation of Specimen in IOF Condition

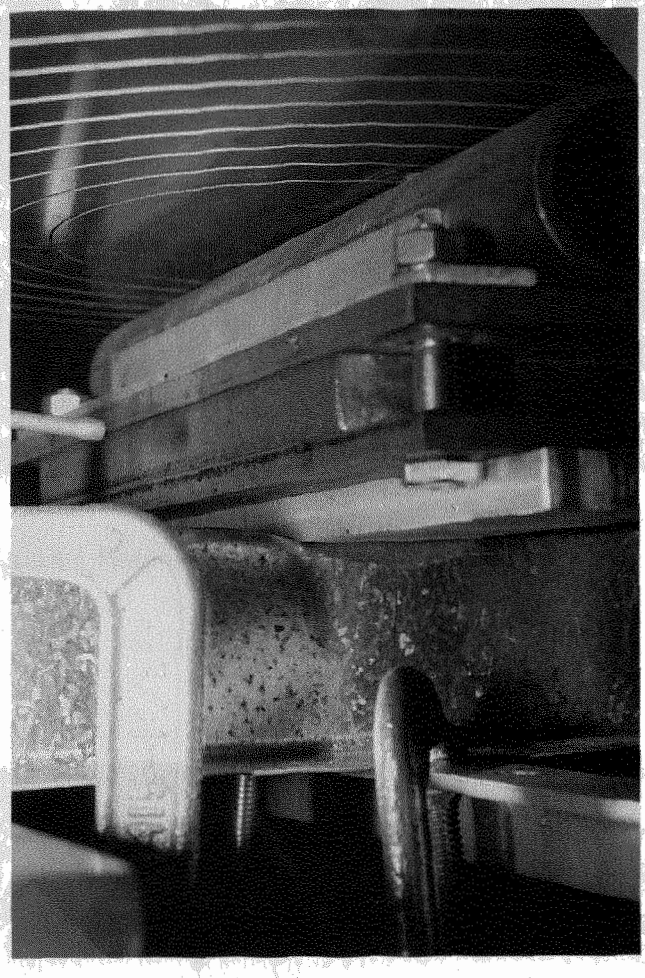

Fig. 4.4.3 Local Web Failure underneath Central Bearing Plate in IOF Condition

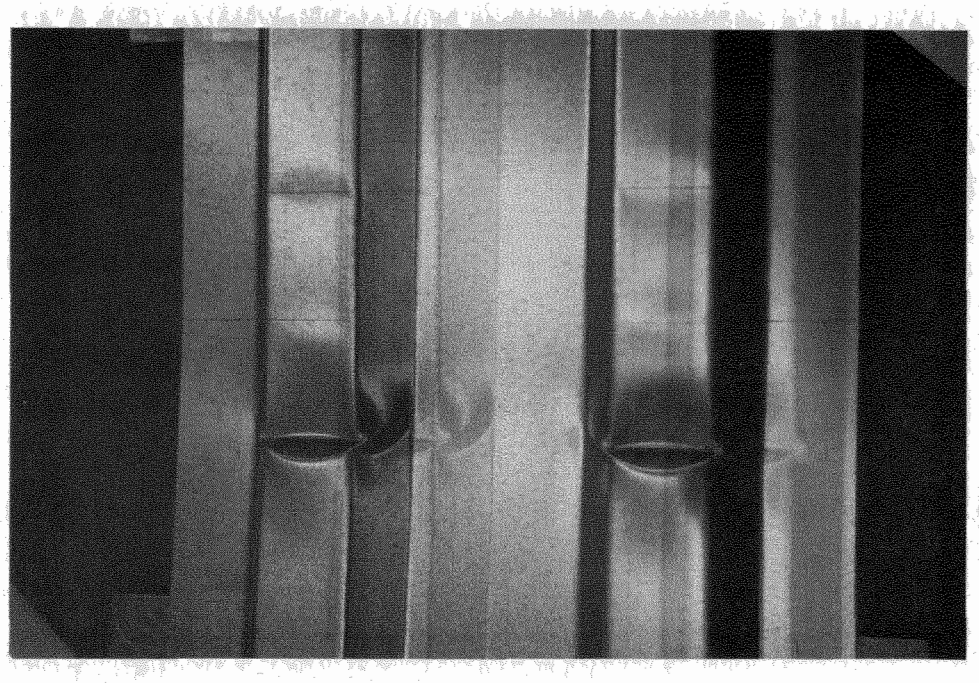

Fig. 4.4.4 Failure of Specimen after Test in IOF Condition

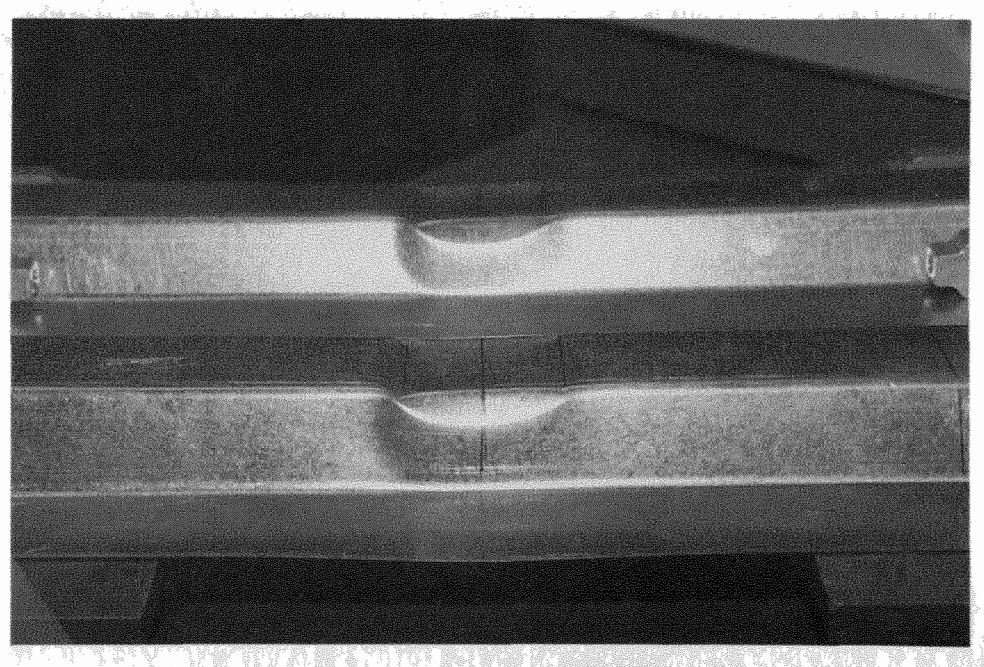

Fig. 4.4.5 Local Failure of Specimen after Test in IOF Condition

Fig. 4.4.6 Failure of Specimens after Tests in IOF Condition

Fig. 4.4.7 Comparison of Failure between Specimens with Vertical Webs and Sloped Webs

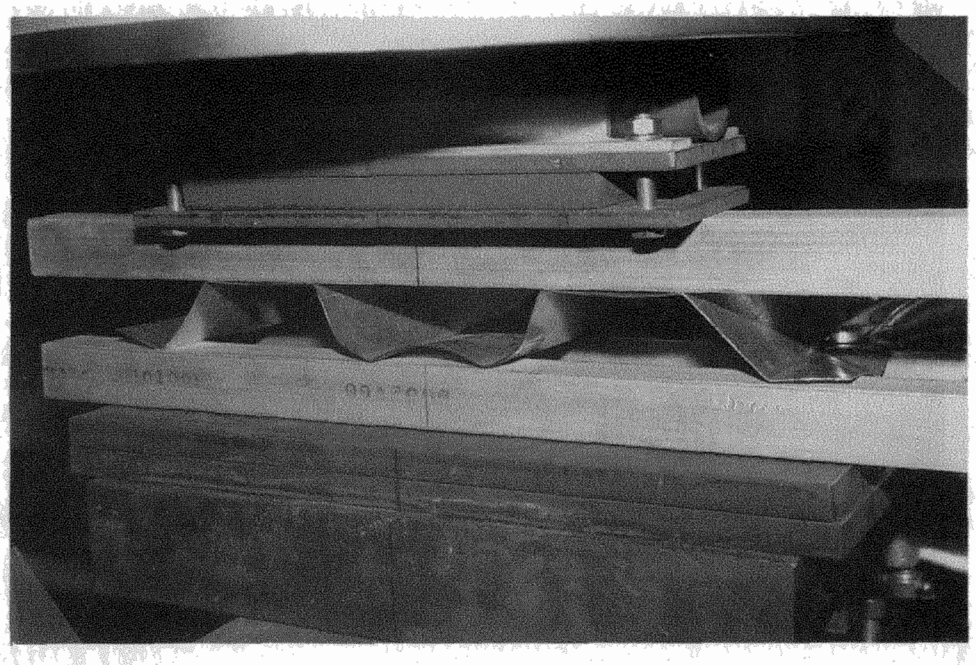

Fig. 4.5.1 Flange Deformation at End Bearing Plate in ETF Condition

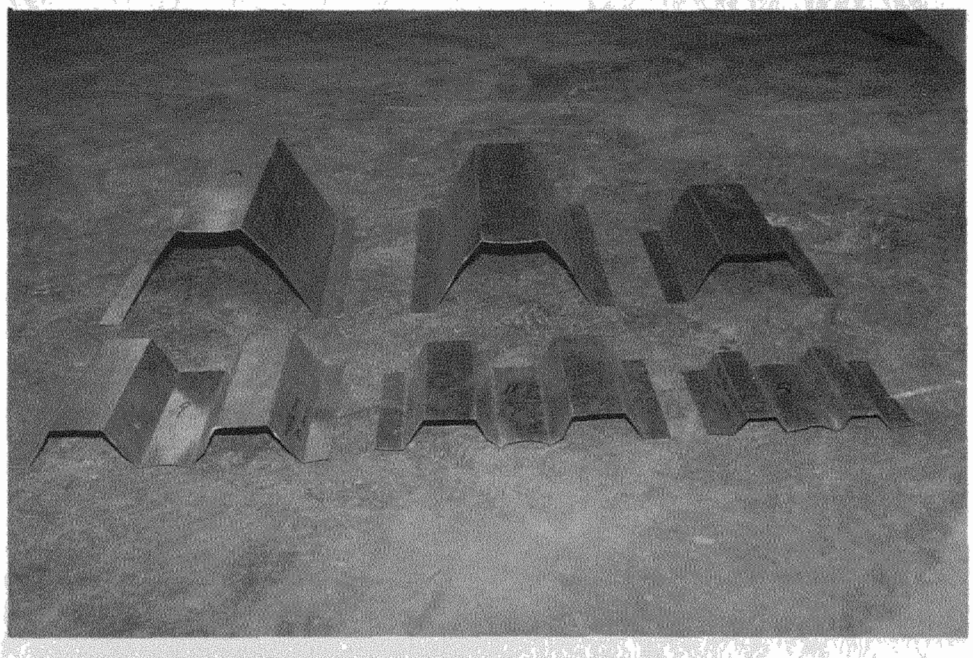

Fig. 4.5.2 Failure of Specimens after Tests in ETF Condition

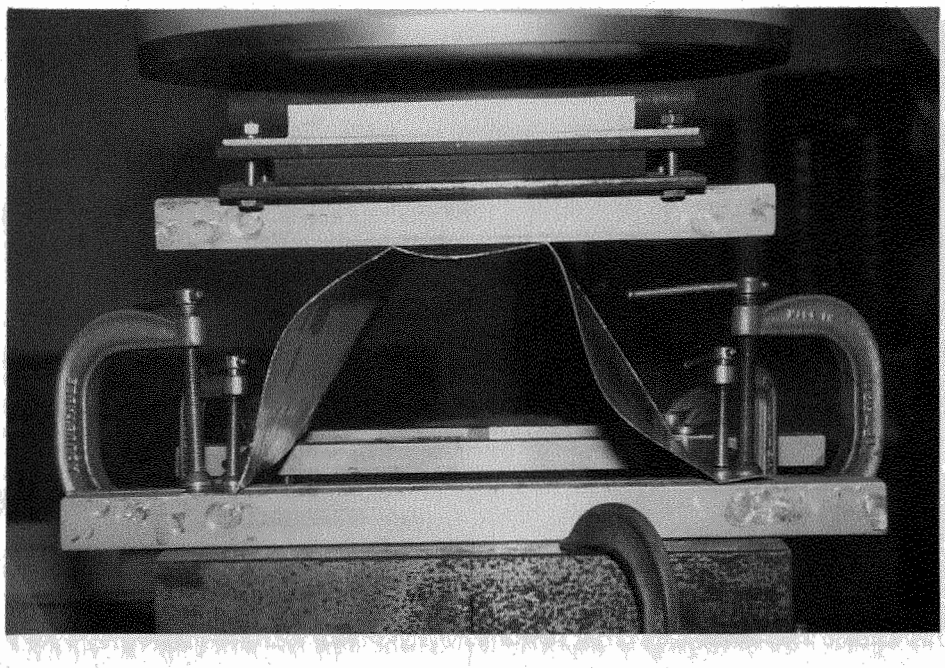

Fig. 4.5.3 Asymmetric Deformation of Webs in ETF Condition

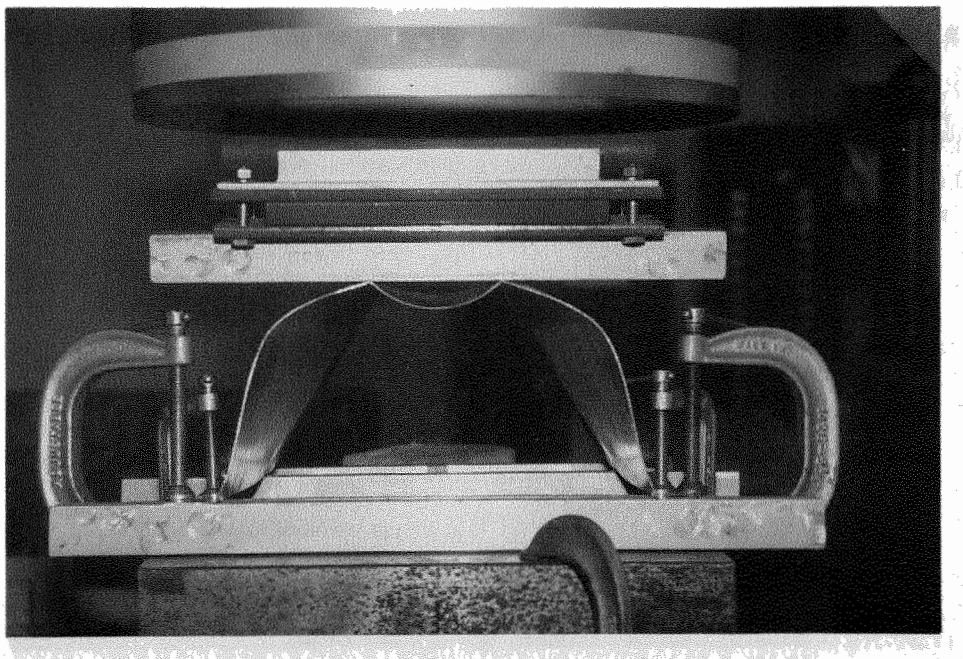

Fig. 4.5.4 Symmetric Deformation of Webs in ETF Condition

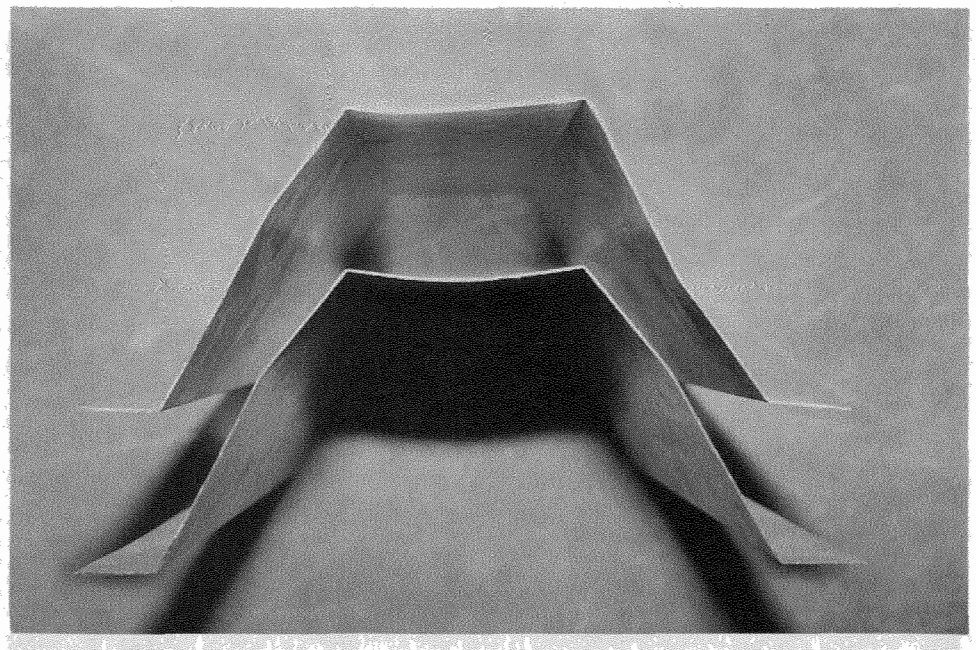

g. 4.5.5 Failure of Specimens with Asymmetric and Symmetric Web Deformations after Tests in ETF Condition

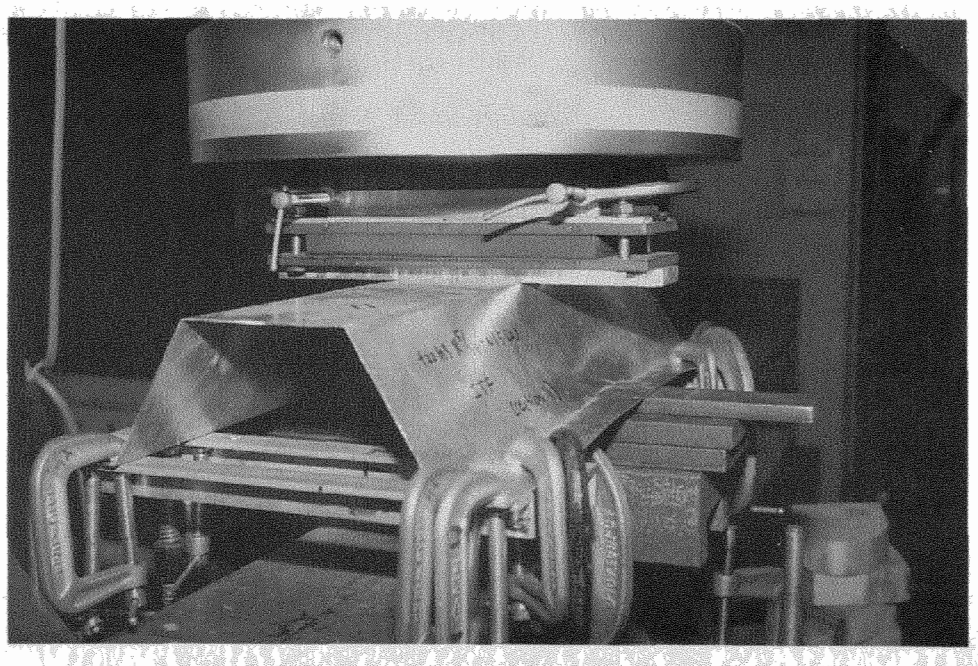

Fig. 4.6.1 Local Deformation of Webs at Bearing Plate in ITF Condition

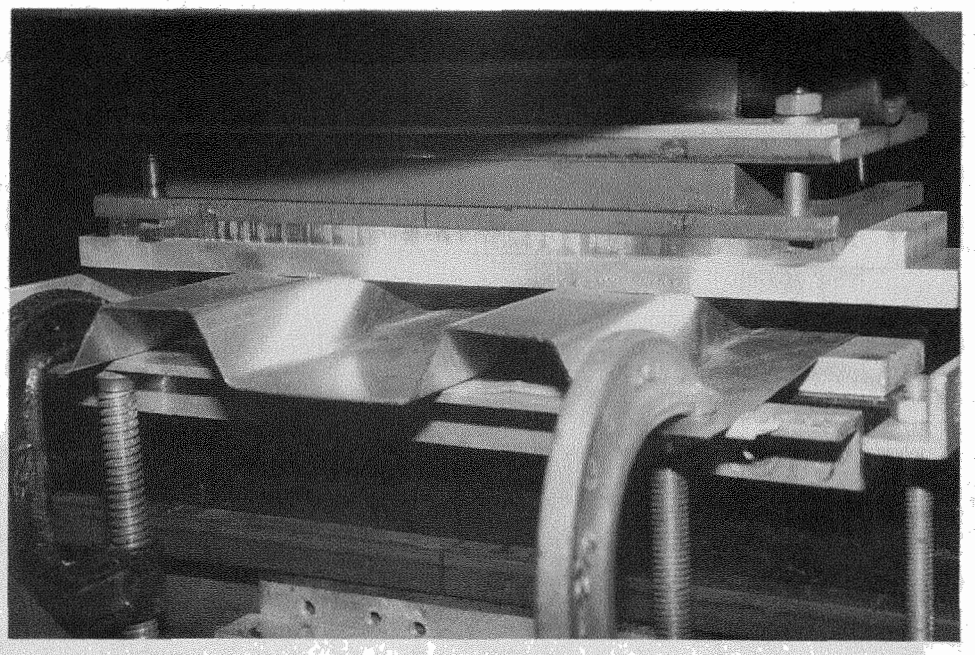

Fig. 4.6.2 Local Deformation of Webs at Bearing Plate in ITF Condition

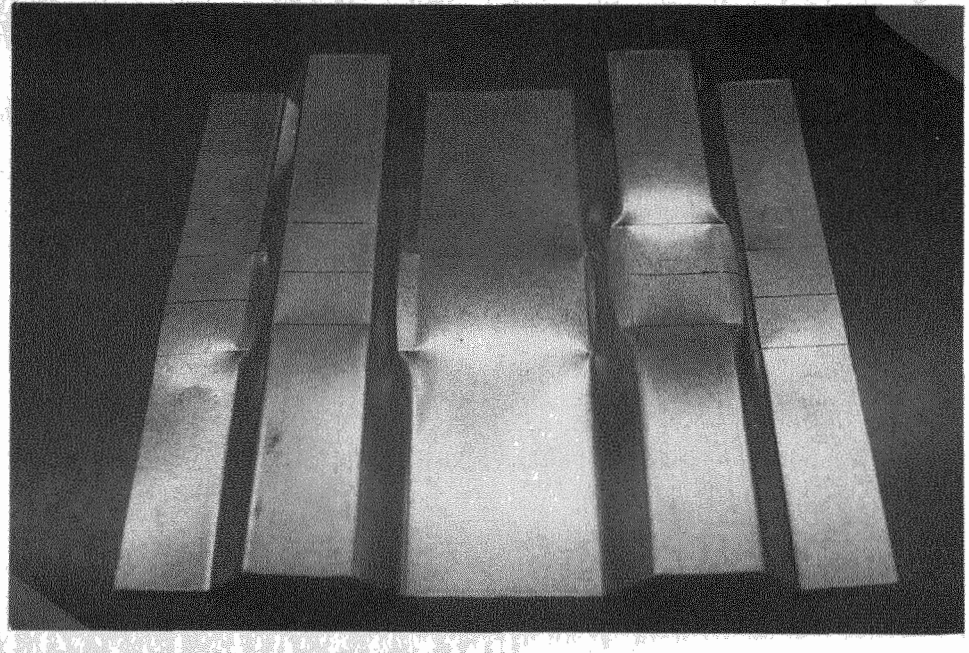

Fig. 4.6.3 Failure of Specimen after Test in ITF Condition

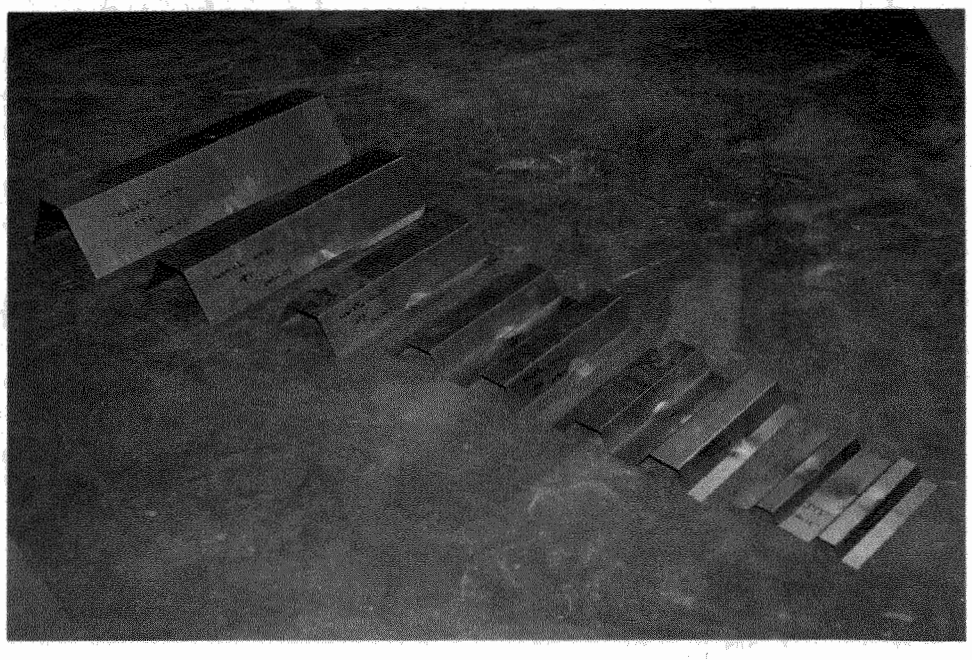

Fig. 4.6.4 Failure of Specimens after Tests in ITF Condition

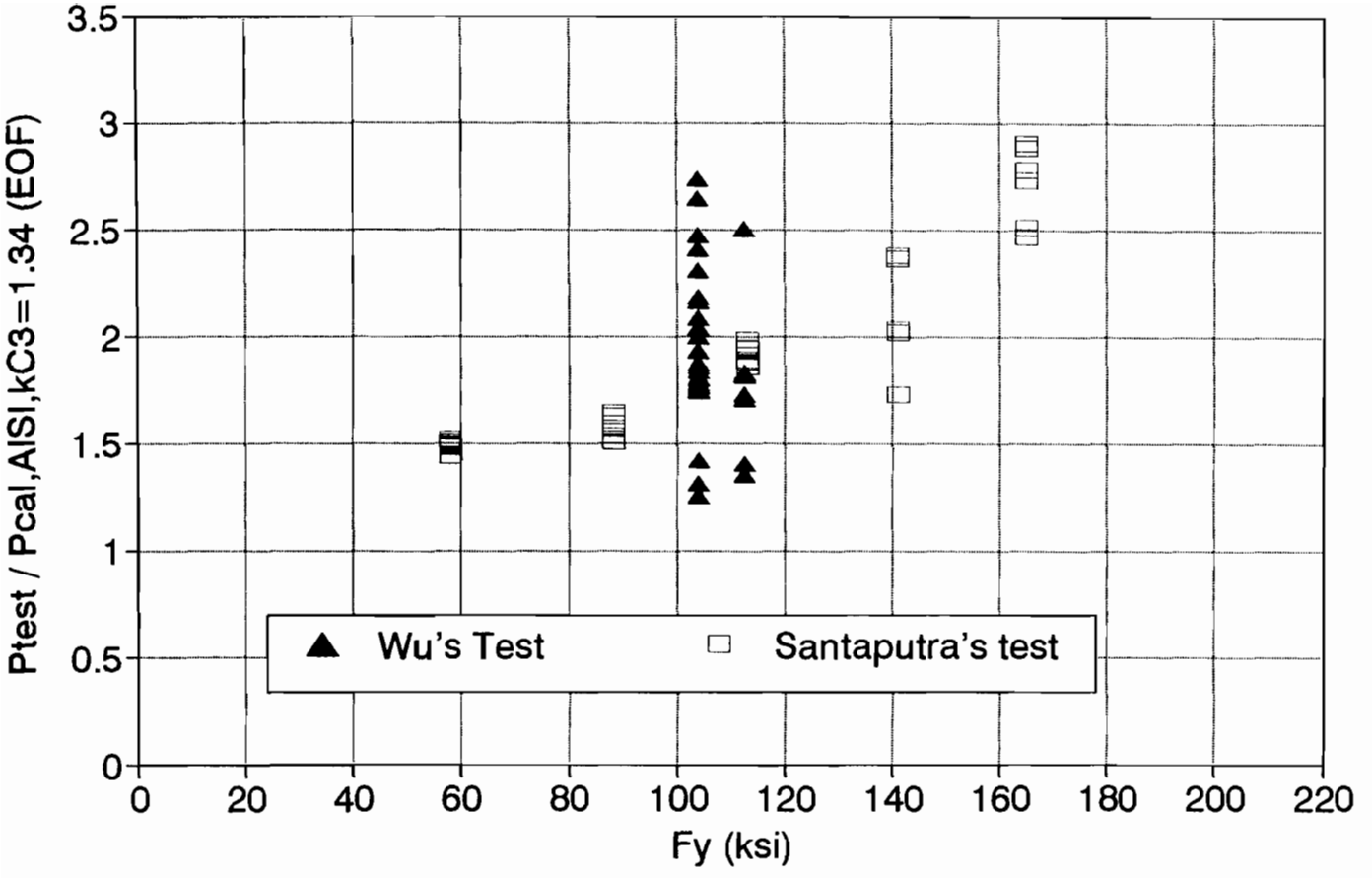

Fig. 5.1.1 Ratio of Tested Load to Calculated Load Using AISI Specification vs. F_y for EOF Condition

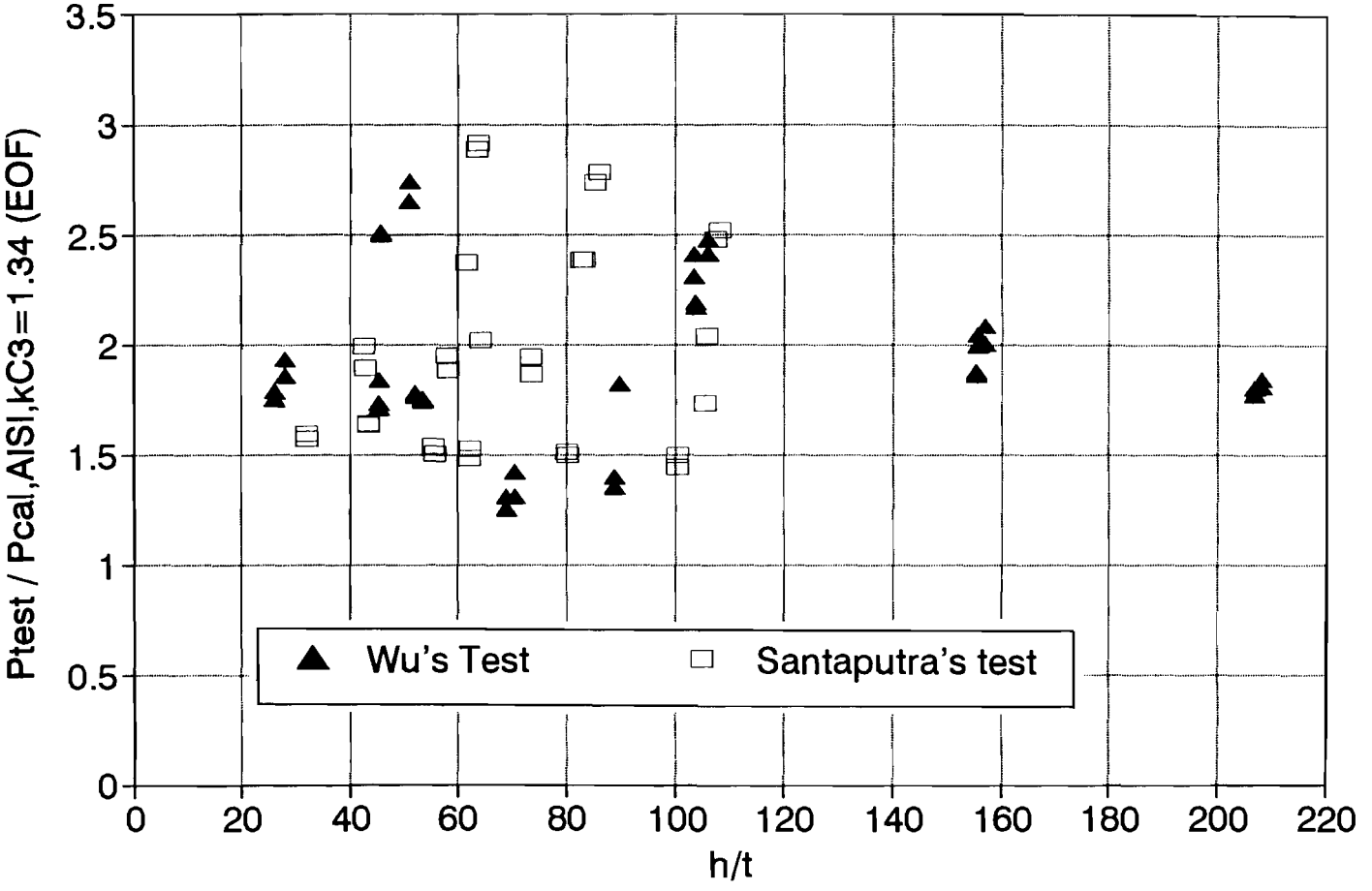

Fig. 5.1.2 Ratio of Tested Load to Calculated Load Using AISI Specification vs. h/t Ratio for EOF Condition

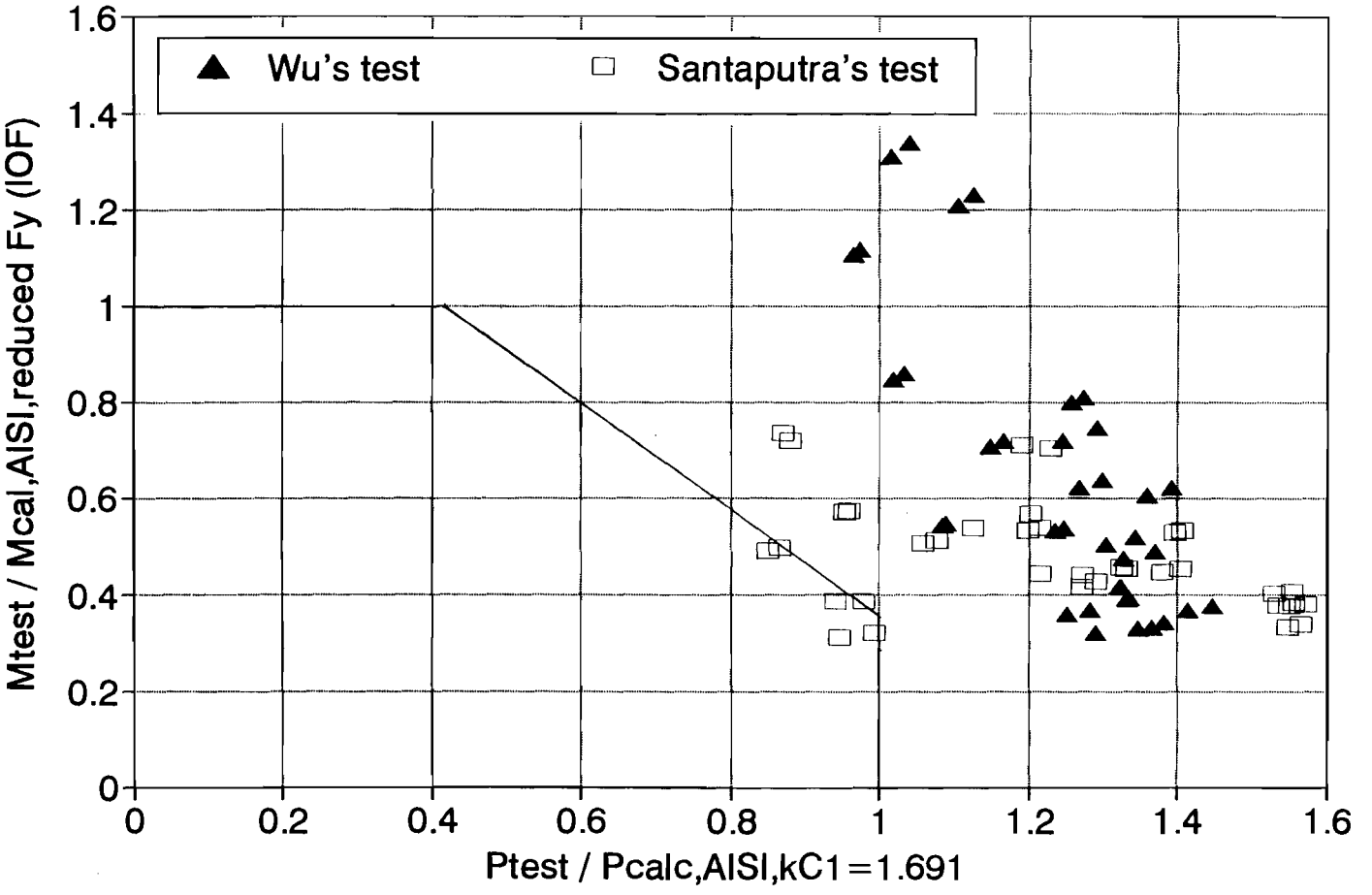

Fig. 5.2.1 Web Crippling and Moment Interaction for IOF Condition (Using Reduced F_y for Calculated Moment)

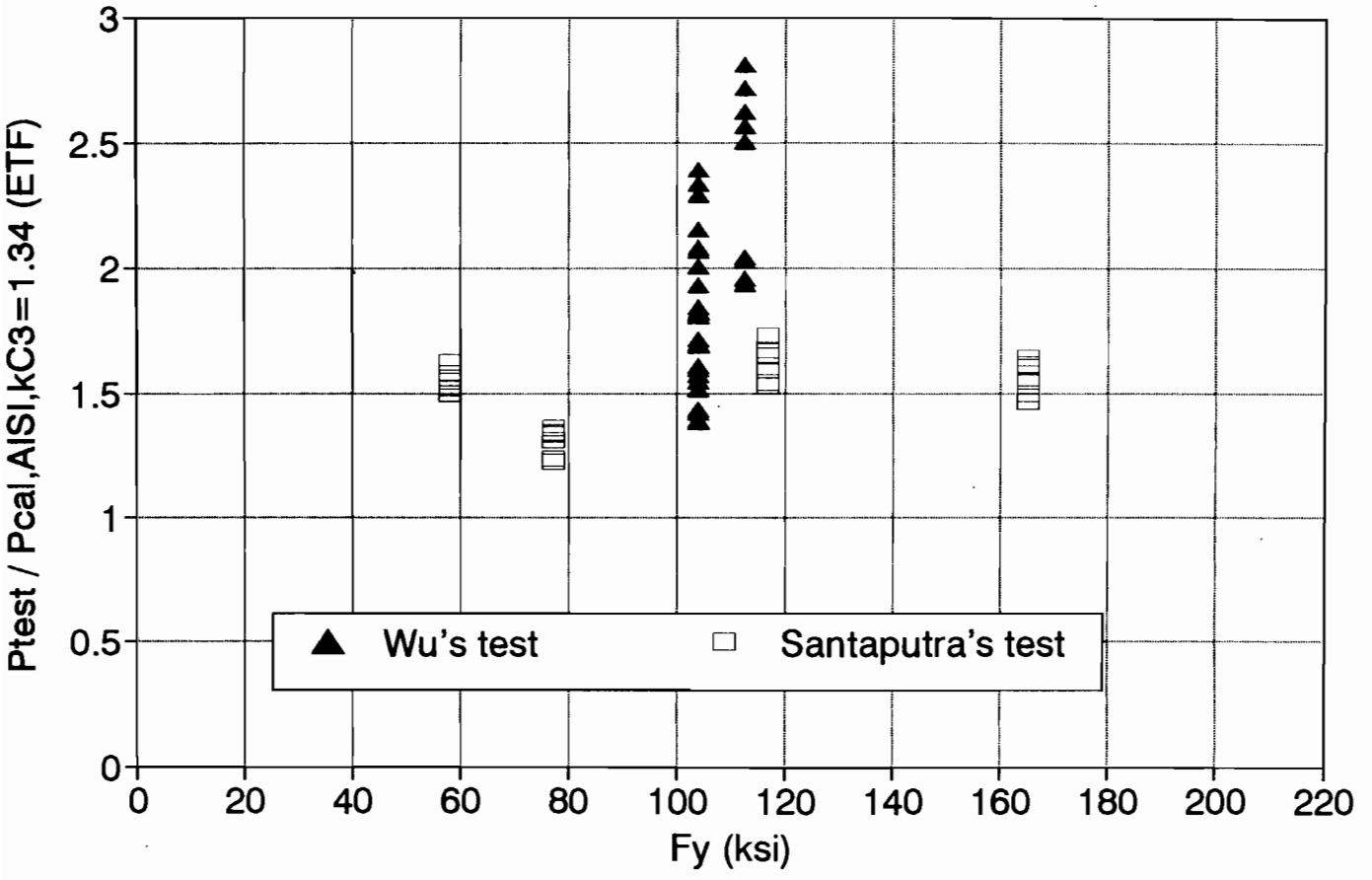

Fig. 5.3.1 Ratio of Tested Load to Calculated Load Using AISI Specification vs. F_y for ETF Condition

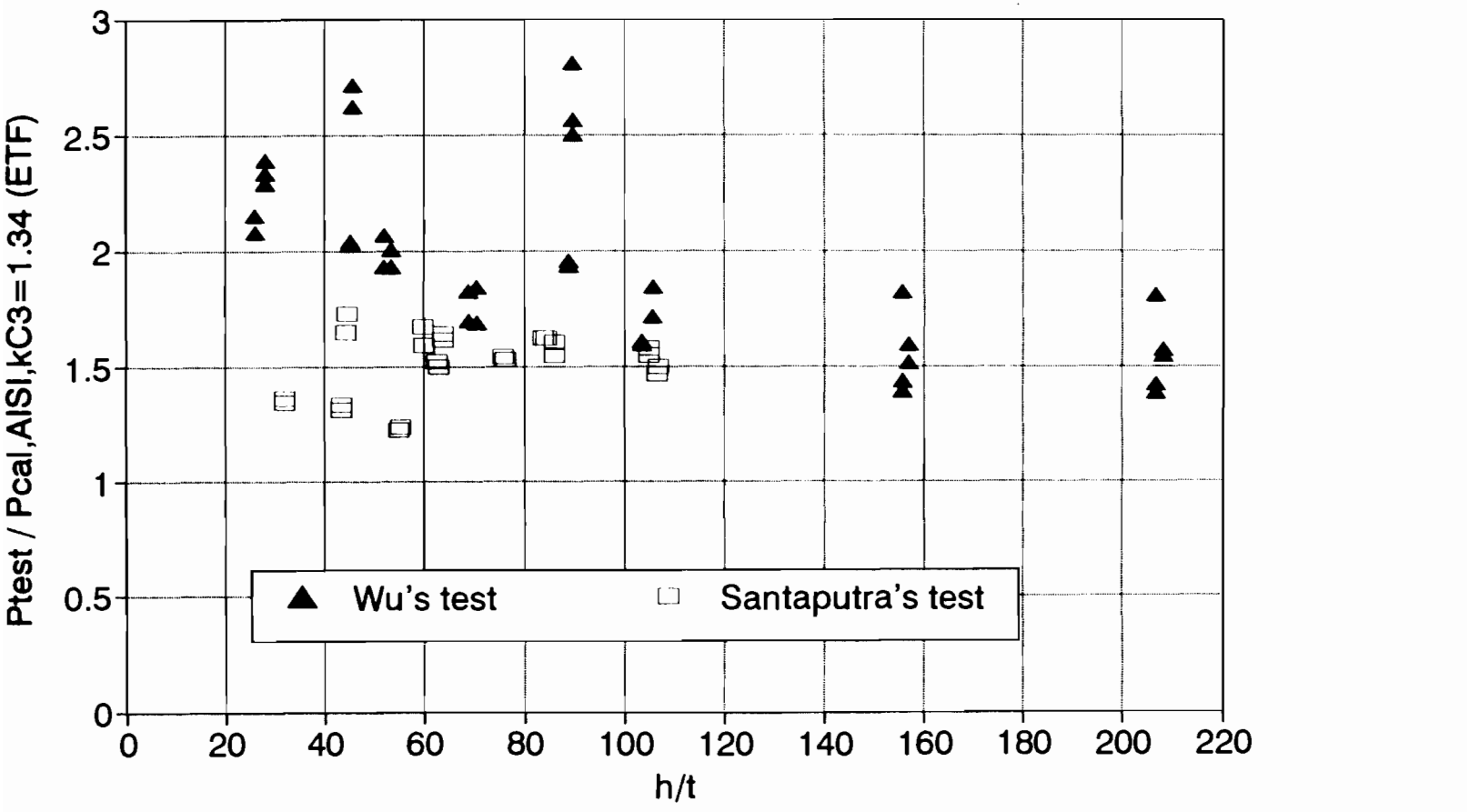

Fig. 5.3.2 Ratio of Tested Load to Calculated Load Using AISI Specification vs. h/t Ratio for ETF Condition

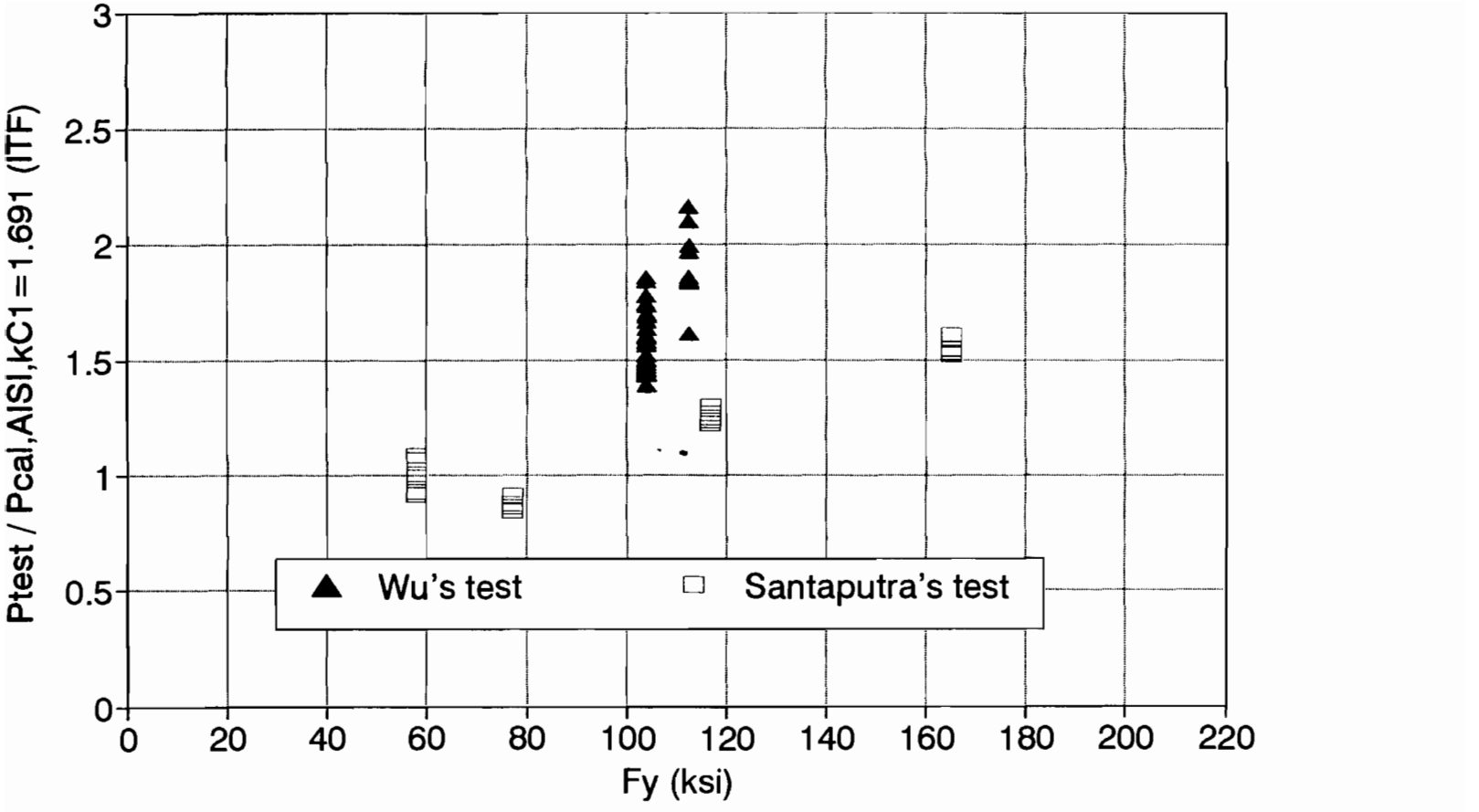

Fig. 5.4.1 Ratio of Tested Load to Calculated Load Using AISI Specification vs. F_y for ITF Condition

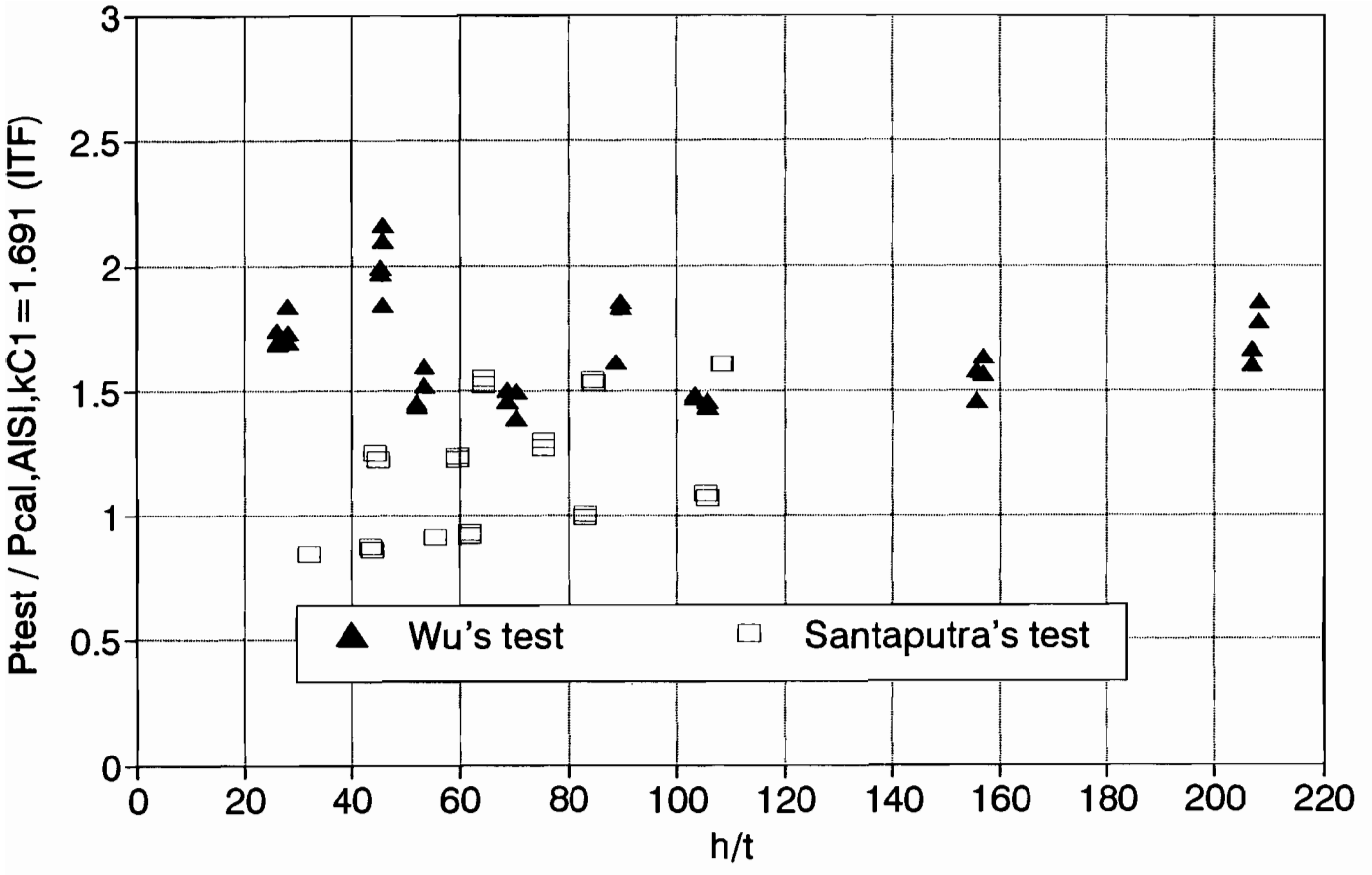

Fig. 5.4.2 Ratio of Tested Load to Calculated Load Using AISI Specification vs. h/t Ratio for ITF Condition

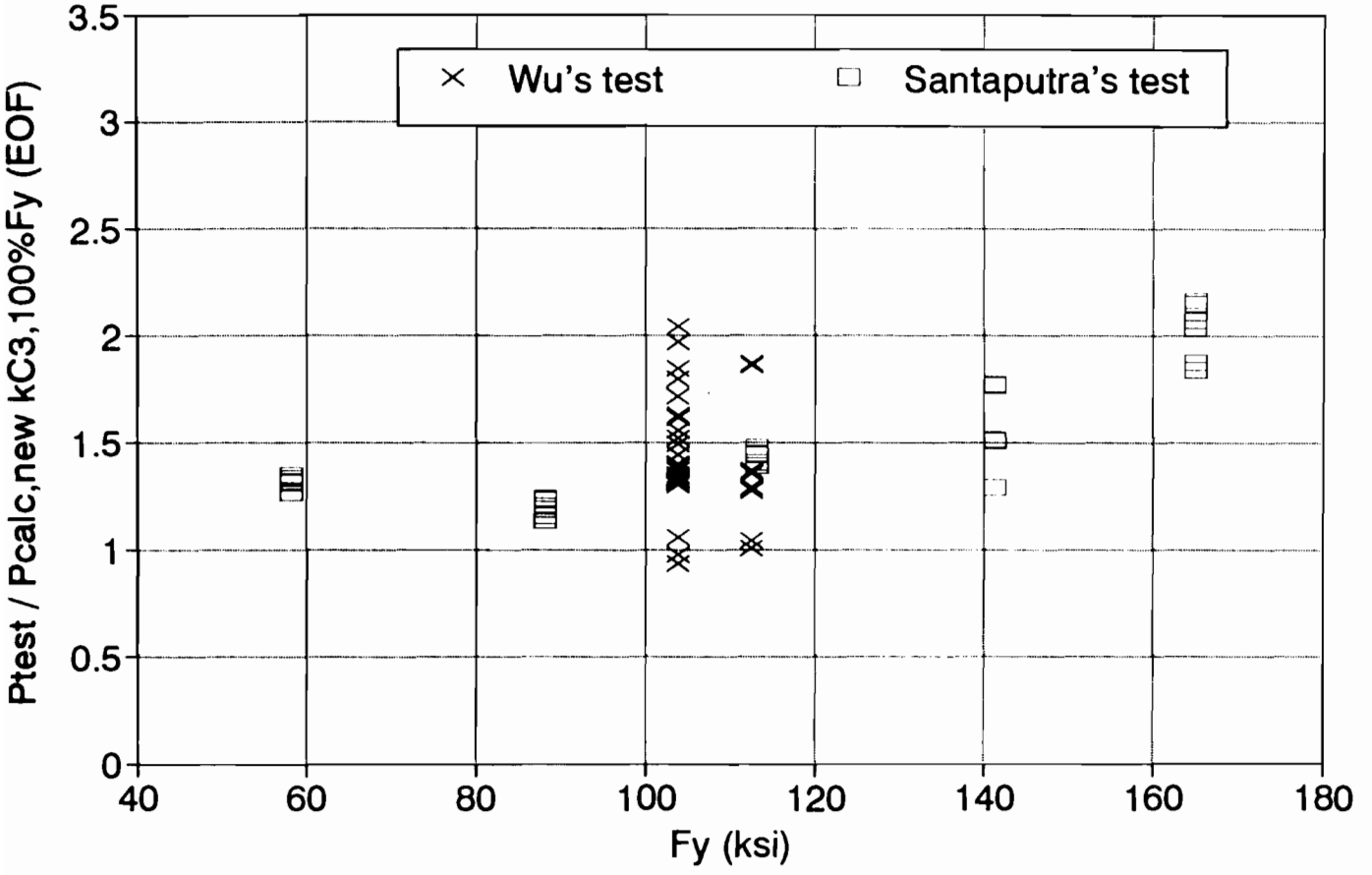

Fig. 6.2.1 Ratio of Tested Load to Calculated Load Using New kC_3 and Actual Yield Strength vs. F_y for EOF Condition

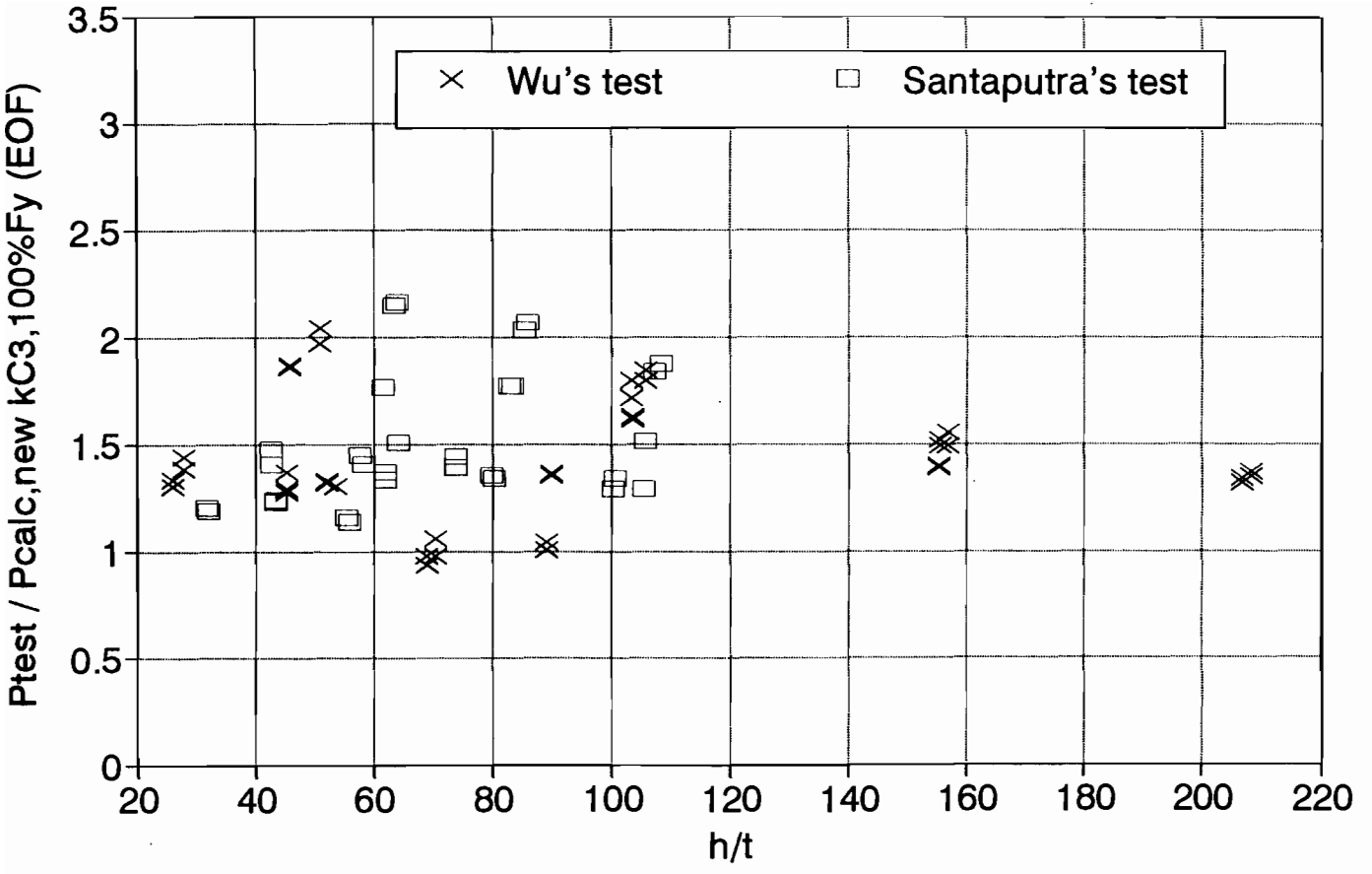

Fig. 6.2.2 Ratio of Tested Load to Calculated Load Using New kC_3 and Actual Yield Strength vs. h/t Ratio for EOF Condition

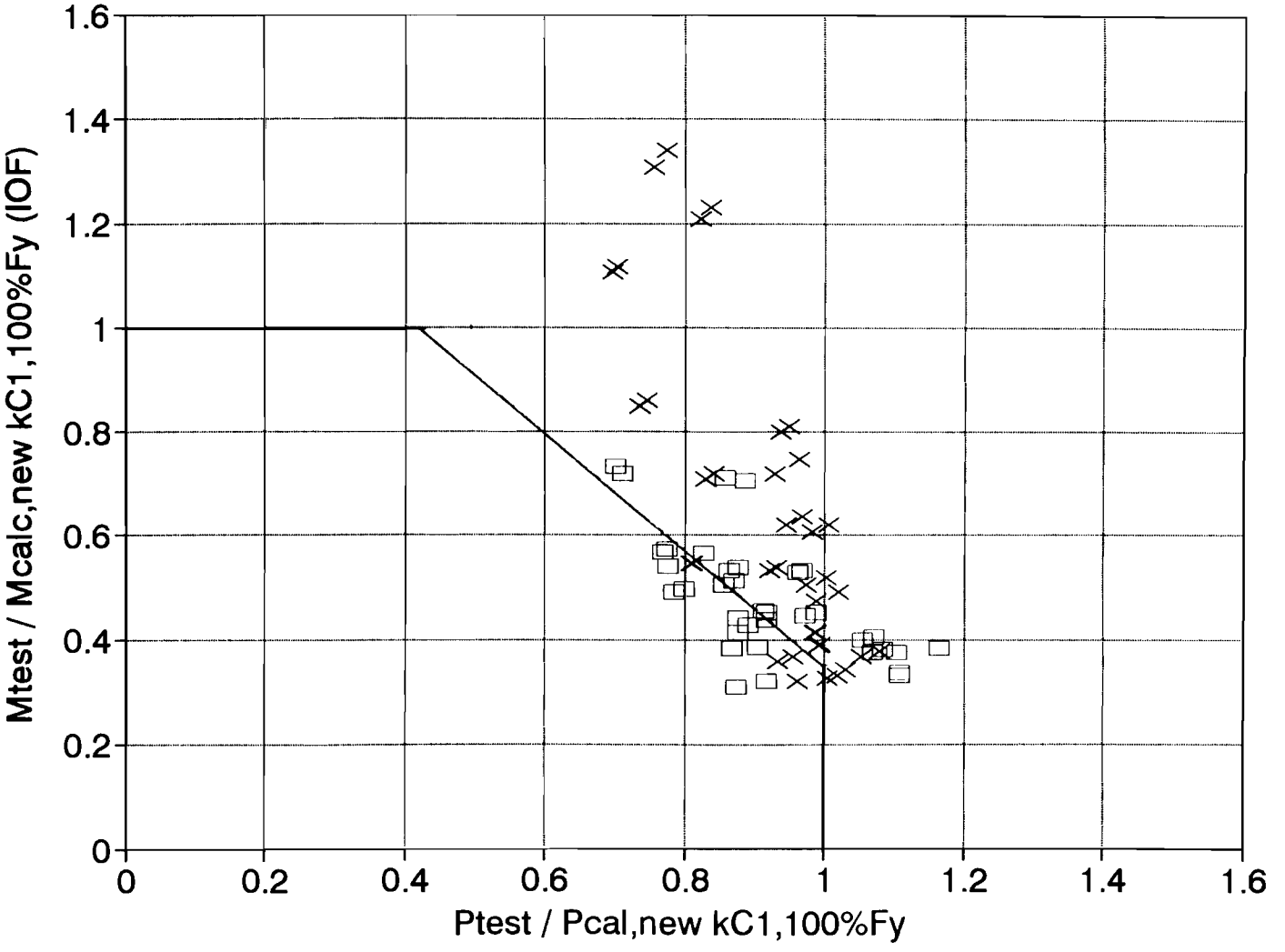

Fig. 6.2.3 Web Crippling and Moment Interaction for IOF Condition and Using New kC_1 and Actual Yield Strength

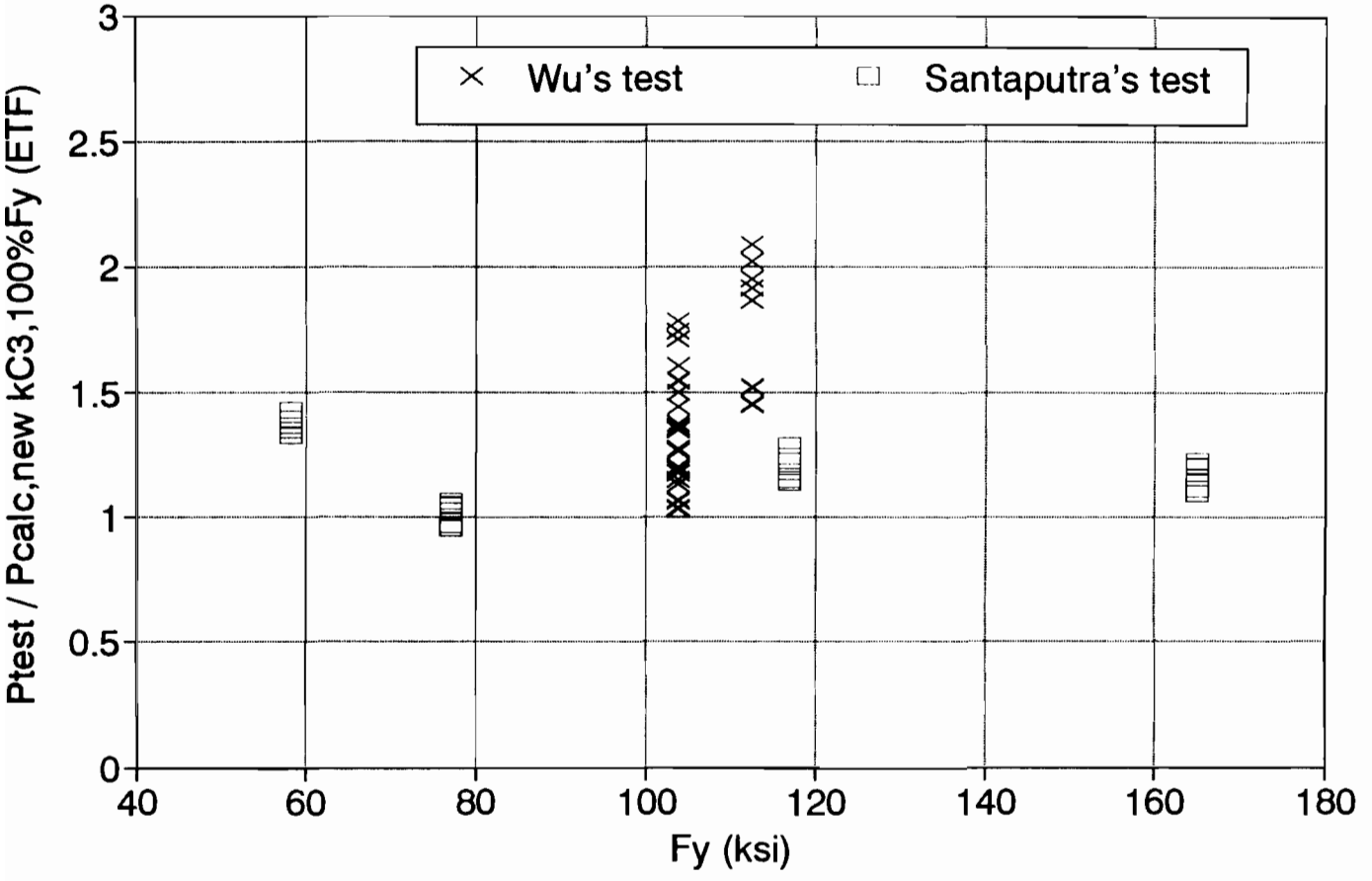

Fig. 6.2.4 Ratio of Tested Load to Calculated Load Using New kC_3 and Actual Yield Strength vs. F_y for ETF Condition

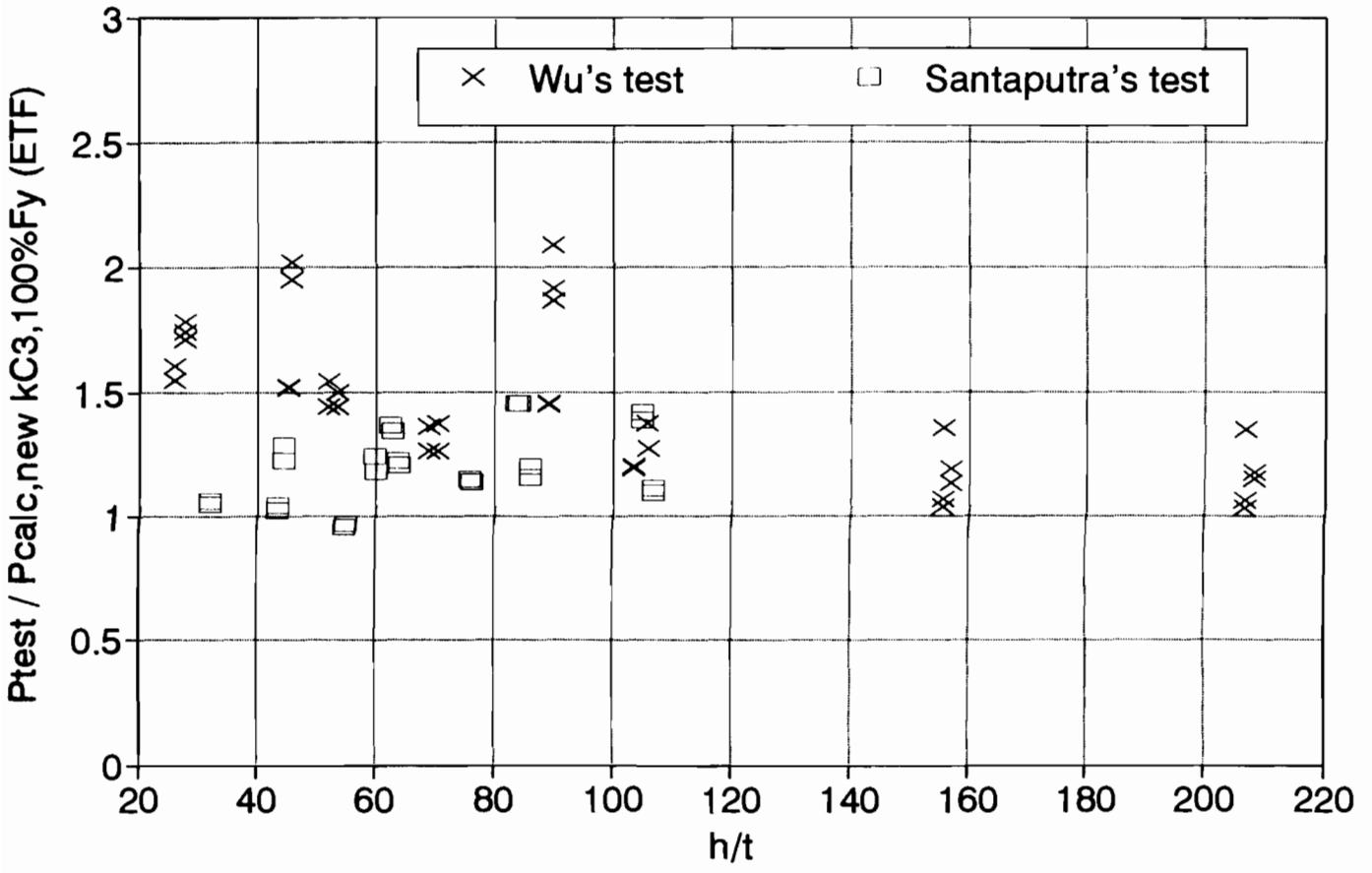

Fig. 6.2.5 Ratio of Tested Load to Calculated Load Using New kC_3 and Actual Yield Strength vs. h/t Ratio for ETF Condition

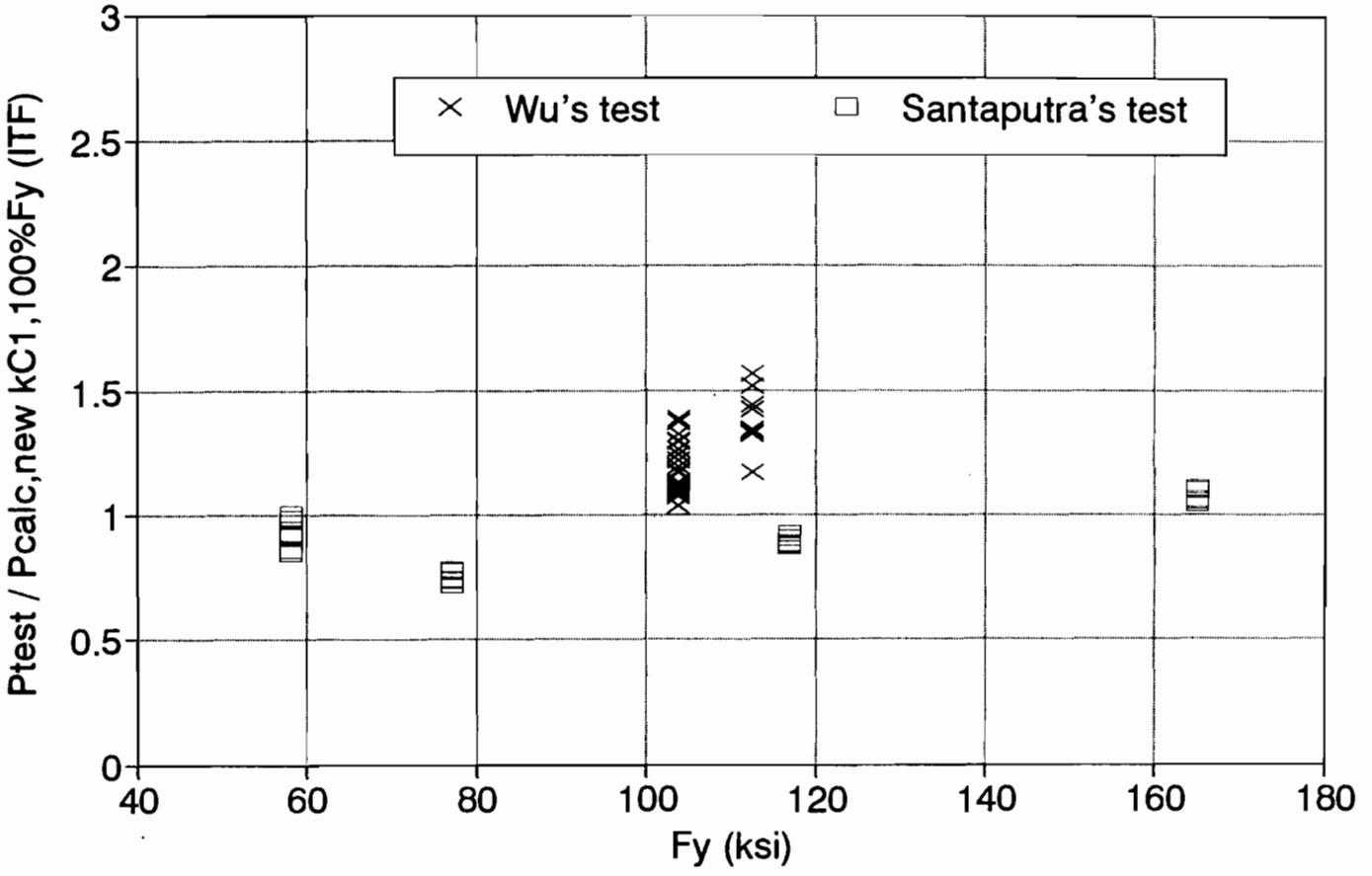

Fig. 6.2.6 Ratio of Tested Load to Calculated Load Using New kC_1 and Actual Yield Strength vs. F_y for ITF Condition

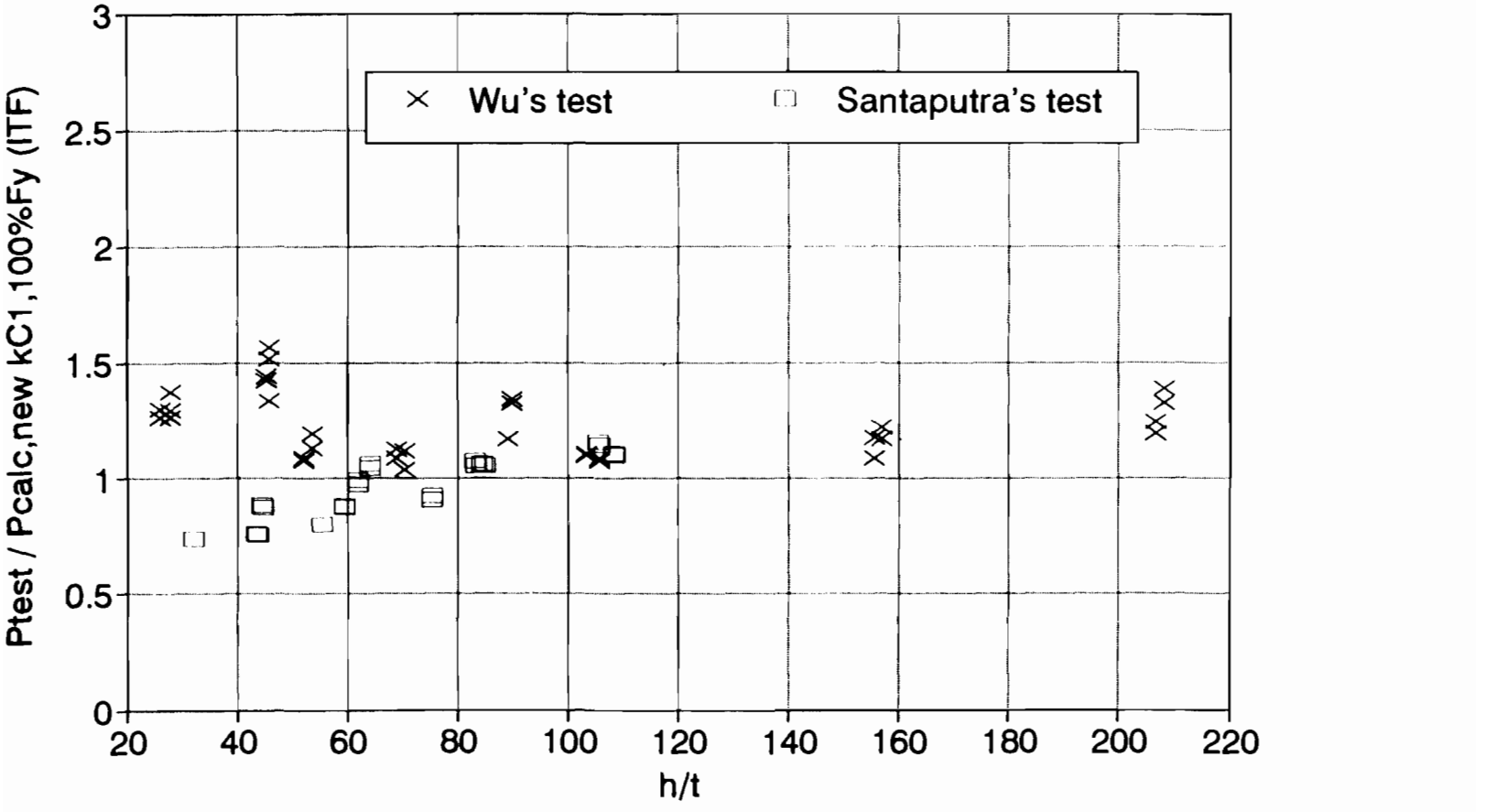

Fig. 6.2.7 Ratio of Tested Load to Calculated Load Using New kC_1 and Actual Yield Strength vs. h/t Ratio for ITF Condition